Transfer films and their effect on signal errors for helical scan data tape recording systems

CHRISTOPHER W SKIDMORE

Master of Philosophy

THE UNIVERSITY OF ASTON IN BIRMINGHAM

September 2001

THE UNIVERSITY OF ASTON IN BIRMINGHAM

Transfer films and their effect on signal errors for helical scan data tape recording systems

CHRISTOPHER W SKIDMORE

Master of Philosophy

September 2001

Thesis summary

'Transfer deposits' or '*staining*' on a magnetic recording heads causes spacing losses at very high recording densities, resulting in signal degradation when reading or writing of data from a magnetic tape.

The aims of this project, which is funded by Hewlett Packard, are to understand and establish the mechanism of head stain and to determine the physical/chemical changes that occur at the head-tape interface of a helical scan DDS Digital Data Storage system. AES results show head stain mainly consist of magnetic particles in the form of gamma iron oxide (γ-Fe_2O_3), which are transferred from the surface of the tape to the surface of the head. Further tape cycling showed at 25°C/35%RH (high water vapour content) stain was deposited on the glass region only of the read head. Whereas at 40°C/10%RH (lower water vapour content) stain was deposited on both the glass and ferrite regions of the read head and the stain thickness increase on the glass and ferrite regions of the read head as the tape was cycled. The results indicate that the error rate is approximately directly proportional to the average stain thickness at 25°C/35%RH and 40°C/10%RH. In addition it was found that the thickness of the stain is dependant on the humidity, temperature, the number of tape cycles and abrasivity of the tape (tape roughness). The average head wear (= tape roughness) for 25°C/35%RH and 40°C/10%RH is directly proportional to the power of number of tape cycles, where the average head wear rate is a function of the number of tape cycles, humidity and temperature. The results presented show that the surface roughness of DDS tape decreases that is the tape becomes smoother as the tape was cycled and the surface roughness after 5000 tape cycles are independent to the humidity and temperature for 25°C/35%RH and 40°C/10%RH. The results indicate that the tape smoothing correlates with the reduction in the head wear rate as the tape was cycled.

Further research work would include expanding the humidity and temperature combination such as 5°C/35%RH, 5°C/10%RH, 25°C/80%RH, 40°C/35%RH, 40°C/80%RH and 10°C/10%RH; develop a method of measuring the areal coverage of the stain; devise a technique of measuring the surface adhesion forces of the stain, at ferrite and glass regions of the inductive head and tape.

Key Words: Tribology, Stain, Surface Roughness, Helical Scan, Inductive Head

The acknowledgements

For the help and guidance from Professor J.L Sullivan, Drs P.H. Clifton and S. Saied, EECS, Aston University, Aston Triangle, Birmingham B4 7ET, UK in producing this thesis and Hewlett-Packard Ltd., Computer Peripherals Bristol, Filton Road, Stoke Gifford, Bristol, BS12 6QR, UK for funding this research project.

The Table of Contents

List of Figures and Tables

Page

The figures

The figures

Table 14 showing the XPS survey of all elements detected and average percentage atomic concentrations [AT%] at the surface of virgin DDS-2 (M120), and DDS-3 (M125 and F125) tapes. 109

Table 15 showing the carbon synthesis calculated in average percentage atomic concentrations [AT%] of virgin DDS-2 (M120) tape, DDS-3 (M125 and F125) tape. CAR is Carboxyl O=C-O molecule which originates from the binder, whereas C-Cl and C-N is from the binder. C total is the total amount of Carbon C detected in XPS survey. The ratio Fe/N is the iron (magnetic particles)/binder ratio and C-C is the total amount of carbon, which is independent to the rest of the tape system. C Total – (C-C) is the carbon difference, which is distributed between the binder and lubricant. TOA is the take off angle that is the angle where the auger electrons are collected relative to the normal to the sample surface. 110

Chapter 1 The Literature Review

1.0 Introduction

There is a growing requirement from business and home users requiring greater data tape densities to backup more data onto a smaller convenient package. To achieve this direct contact between the magnetic recording head and data tape and the use of smaller magnetic particles and thinner magnetic coating for the tape are required. Using smaller the magnetic particles increases the data recording density (bytes/m^3). Intimate contact between the surface of the head and tape interface introduces many tribological problems, such as the deposition of a thin *transfer deposit* on the heads, and friction and wear of the magnetic tape and head. These problems become a significant limiting factor in designing magnetic data tape recording systems.

A *transfer deposit* is commonly referred to as head '*stain*' mainly consists of iron oxide particles and polymer from the tape surface. This head 'stain' can cause problems at very high data densities such as spacing between the head and tape resulting in loss of data when reading or writing of data from the magnetic tape. The development of *transfer deposit* on ferrite inductive heads is not fully understood. An investigation is needed to:

(1) Understand and establish the mechanisms involved in the development of transfer deposits or head staining

(2) Identify the physical adhesion forces involved

(3) Understand the chemical changes at the head and tape interface

(4) Understand how humidity and temperature affects head staining

(5) To develop a relationship between stain thickness and tape abrasivity versus humidity and temperature, and stain thickness versus error rates and stain areal coverage

(6) Finally, to develop a predictive model based on the above relationship.

The Computer Peripherals Bristol division of Hewlett Packard HP, who is sponsoring this project are particular interested in understanding the mechanism of staining on DDS

drives. Primarily experiments performed at HP have shown that in HP Digital Data Storage (DDS) helical scan tape system; a progressive increase in their uncorrected error rate develops when operated at low humidity. Thus, Hewlett Packard would like to understand this phenomenon of a '*staining*' on ferrite recording heads, so that the problem could be reduced to a minimum.

In this chapter, a background in the early history of magnetic storage from the early days of magnetic recording to the present including the Helical Scan Digital Data Storage DDS system are presented. This chapter is followed with an introducing the reader to the structure of a tape, friction and wear between the head-tape interface and the present knowledge on staining. In addition, the structure of a read/write head and the principles of magnetic recording and playback are included.

1.1 The history of magnetic recording, the need for mass storage, and the technology

In the early days of computing, where a computer occupied a large room, a typical computer was programmed by an array of punch cards to support the main memory. A typical example of a punch card is where holes represent a '0' and a filled hole represents a '1'. The hole and filled is considered as an off and on which represents a binary code. With the advent of plastic such as PVC, an alternative means of storing large amounts of data (1's and 0's) was invented in a form of a very thin plastic flexible tape with magnetic particles embedded into the tape.

The basic idea on how this type of storage medium works is as follows. When a magnetic fringe field generated from an electromagnetic source is placed close to the moving media, the local acicular magnetic particle very close to the source acquires a magnet flux moment. The orientation of these magnetic moments can be adjusted by changing the direction of the external magnetic field. The orientation is dependent on the magnetic nature of the magnetic particle. Most common orientations of the magnetic moments are one orientation is directly opposite and lie parallel to each other. This condition can be referred to as *longitude* recording. Each of these orientations can be represented as either a '1' or '0' respectively.

These days magnetic recording tape is used in audio, video (moving pictures) and data storage. An example of the use of this tape is in the world's first analogue video recorder, which was called the Ampex VR1000 and was built in 1956 by a company Ampex. This early type of video recorder weighed in at around 100 pounds and held several hundred

vacuum tubes. The video was recorded as an analogue signal from a rotating drum onto a reel-to-reel flexible magnetic tape.

Further down the evolutionary path of magnetic flexible tape, Digital Audio Tape (DAT for short) format developed by Hewlett Packard and Sony was introduced into the general market. This type of technology has the capacity to store 1.3 Gigabytes of data on a magnetic tape of length 120 m and 4 mm wide and the tape was contained in a small removable cartridge of roughly the size of a credit card. At that time this data capacity exceeded the largest of the hard drives in use. A helical scan recording system as shown in figures 1(a) and (b) are used to record and read data from the DAT tape. Two companies Hewlett Packard and Sony who developed the initial DAT format took this further by introducing the DDS format (Digital Data Storage). This format uses the digital audio tape and drive technology in combination with logic and software to deliver low error rates- less than 1 error in 10^{15} bits of data. Thus making the DDS system a reliable means of storing computer data. The main functions of this system are (1) to serve as a data backup system for hard drives used in workstation and mainframe computers; (2) data interchange, where computers not connected electronically can transfer data from one computer to another; and (3) fast file retrieval.

A helical scan recorder is a system where the DDS tape is wrapped around a rotating drum (at 2500-RPM as in DDS-1). The rotating drum has four protruding heads- two read and two write each at 90 degrees from each other. The drum is set at an angle of 6 degrees from the horizontal and the flexible tape (DDS tape) passes by the drum. A track of data of width 9.1 μm (DDS-2 and 3 format) is scanned diagonally across the tape representing a helical pattern. A typical DDS layout is shown below in figure 1 and a commercial DDS drive is shown in figure 2.

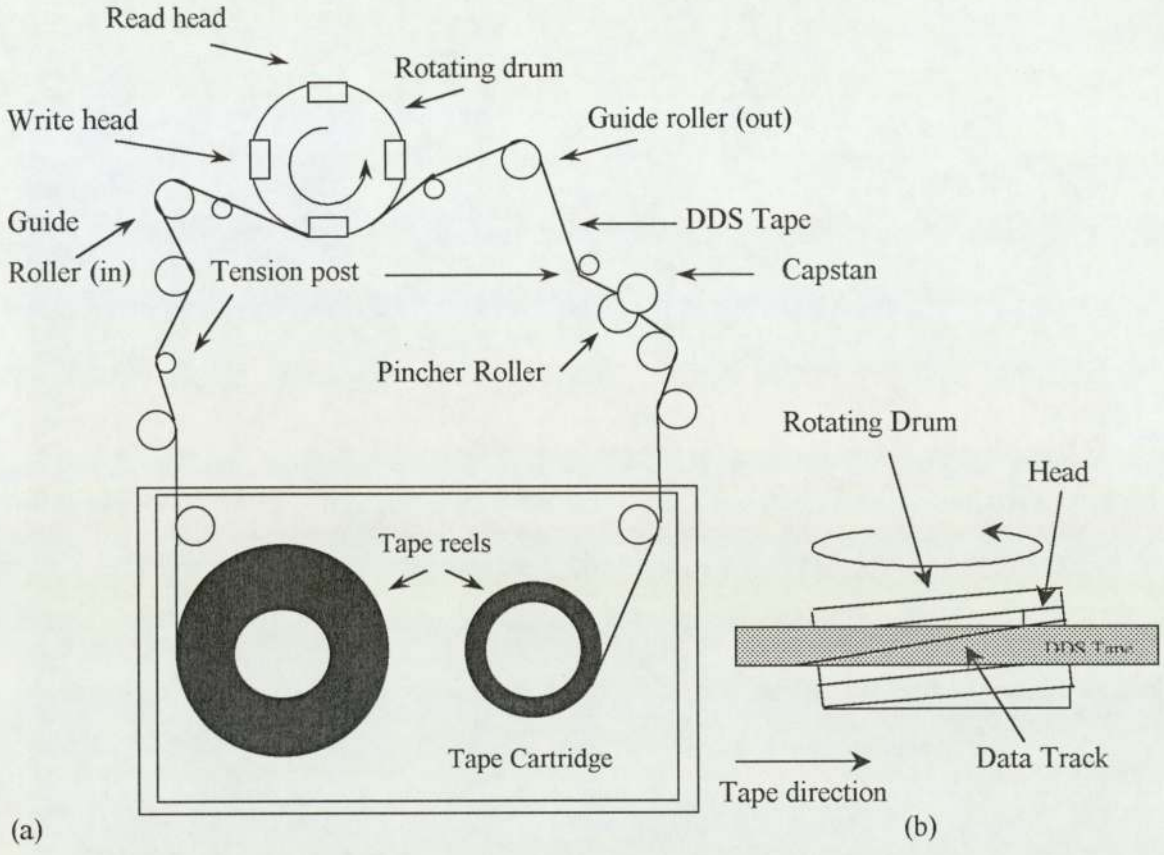

Figure 1 showing (a) a typical Helical Scan DDS set-up where the capstan drives the tape at constant speed, and (b) side view of a drum rotating with the head and tape in contact

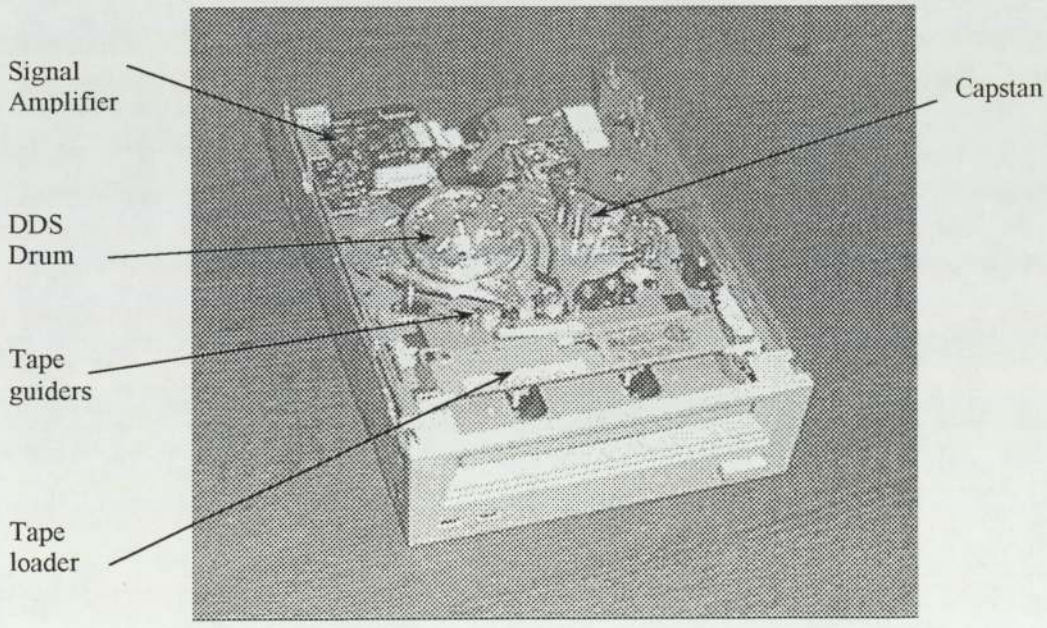

Figure 2 showing a picture of a commercial Digital Data Storage DDS tape drive

Advantages of the DDS format are that it maximizes the storage capacity by storing the data diagonally side by side. This format also offers compatibility with the existing storage command sets (QIC commands) and backwards compatibility with earlier DDS tape. Further enhancements to the DDS format are that it inherits the error correction capability (C1 and C2) from the previous data-DAT technology together with an extra level of error correction known as C3 (read-after-write). The next generation of DDS drives (referred to as the third generation, DDS-3) used in the proceeding experiments has a maximum data capacity of around 24 Gigabytes compressed. Whereas earlier drive generations such as DDS-1 and 2 have a maximum data capacity at around 4 and 8 Gigabytes respectively.

1.2 The principles of magnetism

To understand the principles of magnetic recording, basic ideas of magnetism (electromagnetism) need to be understood.

Magnetism is a property, which arises from the motion of electrons within an atom. Consider the model of an atom (that is the Bohr's model), where a negative charge electron orbits around a positive charged nucleus. The orbiting electrons result in a localized current, which contributes to the atoms magnetic dipole moment. That is, when the electron is stationary, then the electron has an electric field. However, when the electron is moving in a circular orbit the electric field translates to a magnetic field that is a moving electric field is equivalent to a magnetic field. A result based on the connection between the orbital contribution to the magnetic moment **m** and orbital angular momentum **L** of an electron can be calculated as

$$\mathbf{m} = \frac{-e\,\mathbf{L}}{2\,m_e} \qquad (1)$$

Where, e = Electronic charge (C)

m_e = Mass of the electron (Kg)

In addition to the orbital contribution to the magnetic moment, there is a contribution to the magnetic moment from each electron due to its intrinsic, or *spin* angular momentum **S.** This spin contribution to **m** is proportional to **S.** The proportionality constant is normally twice that of the orbital case.

The magnetic moment for an atom is then obtained by adding the contribution of all electrons. This results in many atoms having zero magnetic moment except for a few

examples like Fe and O. Therefore, in the case of spin angular momentum **S**, most electrons in a molecule pair up with opposite spins, so that the net pair gives a zero net spin contribution to the magnetic moment. Thus for molecules in which the pairing is incomplete, then the magnetic moment is due to the few unpaired electrons. These molecules are known as permanent magnetic moments for example Fe, etc. When there is a number of unpaired magnetic dipole moments **m** available within the material, the material possesses magnetisation **M.** The term *magnetisation* (Amps/m) is defined as the sum of the magnetic dipole moments per unit volume within the medium:

$$\mathbf{M} = \frac{\text{mean of the sum of magnetic dipole moments.}}{\text{Volume}} = \frac{< \Sigma \mathbf{m}_i. >}{V} \qquad (2)$$

For each magnetic atom (e.g. Fe), the resultant magnetic moment has two most common spin orientations, called spin-up or spin-down. When an external magnetic field is applied to the atoms, the spin orientations of the magnet moments of each atom point in a partial alignment giving the material magnetization as shown in figure 3. Figure 3 shows when you increase the magnitude of the applied external magnetic field, the field alignment of most of the magnetic particles points in the same direction and parallel to each other, resulting in the magnetisation of the material becoming fully saturated. This is called a ferrormagnet. However, when the external field is removed, the spin orientation of the magnetic moments of each magnetic particle becomes disordered resulting in the material loosing its magnetism. This is called a *paramagnet* or a soft magnetic. The soft magnet is referred to having low *coercivity* and magnet remanence. The definition of *coercivity* is the field strength required to reduce the magnetic remanence to zero. So higher the *coercivity* of the material greater the applied external magnet field required to reduce the magnetic remnance to zero. Whereas *remnance* magnetisation simply means the retained magnetism, when an applied external field is removed. Often the retained magnetism is less than the original external magnetic field due to the material having an internal field (called a demagnetising field), which opposes the surface magnetic flux, thus reducing the magnetisation **M** to a new equilibrium value. A soft magnet is normally used in a magnetic recording head, because there is no need to retain its magnetism when a magnetic field is removed.

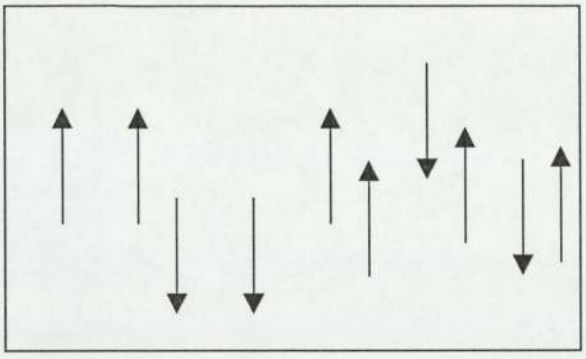

Figure 3 A typical paramagnetic where the arrows represent the resultant magnetic moments of each domain or magnetic atoms

When a material retains its magnetism after an applied external magnetic field, this is referred to as a *ferromagnet* or a hard magnet shown in figures 4(b). This type of material has high coercivity and magnet remanence characteristics, which can be used in magnetic tape to record data. In this form, most of the magnetic dipole moments of the magnetic particles are aligned in the same direction.

Another important property of a magnet is when you increase the current through a coil of wire wound around an iron torrid core you can obtain values of the components of **H** and **B**. Where **H**, is the magnetic intensity and is related to **B** by this definition: $\mathbf{B} = \mu_o (\mathbf{H} + \mathbf{M})$, μ_o is permeability, and **M** is the magnetisation of the sample. By plotting the values of **H** and **B**, you can get two types of curves as shown in figure 4(a) and 4(b). These curves show the process of irreversibility of the magnetic domain structure. This irreversibility process is referred to as a *hystersis loop*, where total area enclosed by the curve represents the total loss of energy through the process of core heating. When the external magnetic field is increased until the magnet core becomes fully saturated at point A i.e. **B** = a constant, this is referred to as saturated magnetism, and is labelled as $\mathbf{B}_s$. At this point, the magnetic particles are aligned in one direction, and any further increases in the external magnetic field **H** will not increase the magnetic flux **B** of the core. In figure 4(a), when the field **H** is reduced (from point A to B on curve of figure 4), that is when **H** tends to zero. This results in the iron core retaining its magnetism (remnance magnetism $\mathbf{B}_r$), after the external magnetic field is reduced to zero. If you continue from point B to C by reversing the field **H** ($\mathbf{H} < 0$), the resultant **B** field tends to zero. At this point, the B field is zero, which is referred to having negative coercivity $-\mathbf{H}_c$ of the material. By further increasing the reversed H field (C to D), again the magnetic core becomes saturated in the negative or opposite direction, which is referred to as $-\mathbf{B}_s$. When the **H** field is reversed again (D to F), so that it is becomes positive again, the **B** field reduces to zero at point F. When $\mathbf{H}_c$ is large, the magnet possesses high remnance magnetisation $\mathbf{B}_r$.

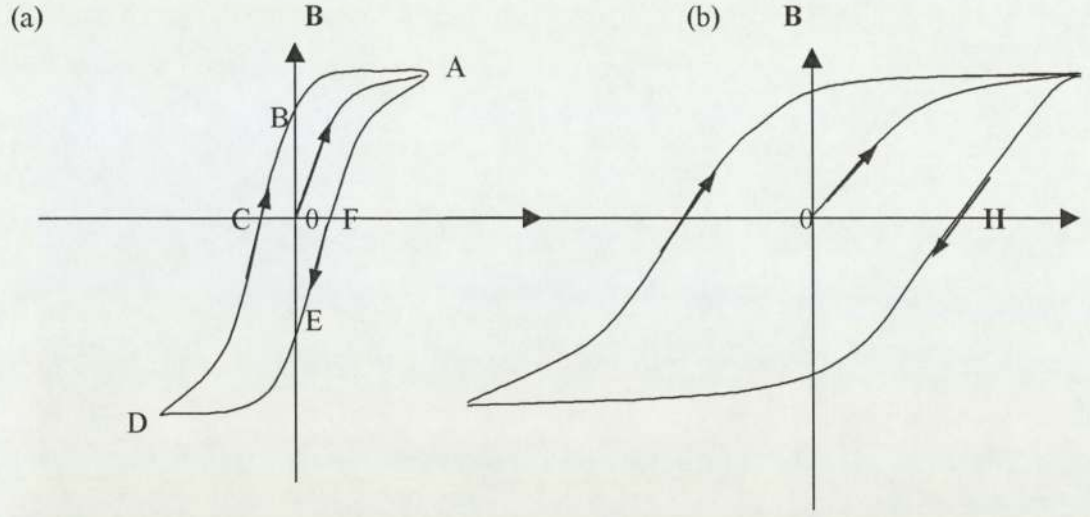

Figure 4 showing a typical (a) paramagnet or a soft magnet,(b) a Ferro magnet or a hard magnet

The *hystersis loop* shown above has two distinct shapes, which is dependent on the material used as a core. Firstly, the curve shown in figure 4(a) is long and thin with a small cross-sectional area, remnance magnetism $\mathbf{B_r}$ and coercivity $\mathbf{H_c}$. This is associated with a *soft magnetic*, which is used in magnetic reading/recording heads. Whereas, when the cross-sectional area of the loop is large the coercivity and magnetic remnance are high as shown in figure 4(b) the material is referred to as a *hard magnetic* and is used as magnetic particles within tape to record data, audio and video.

1.3 The principle of magnetic recording and playback

There are two modes used in magnetic recording and playback. Firstly there is analogue, which uses an analogue waveform or cosine/sine wave. The second mode is digital, which is made up of discrete units of 1's and 0's or high and low voltages respectively. A typical digital waveform is shown in figure 5(a).

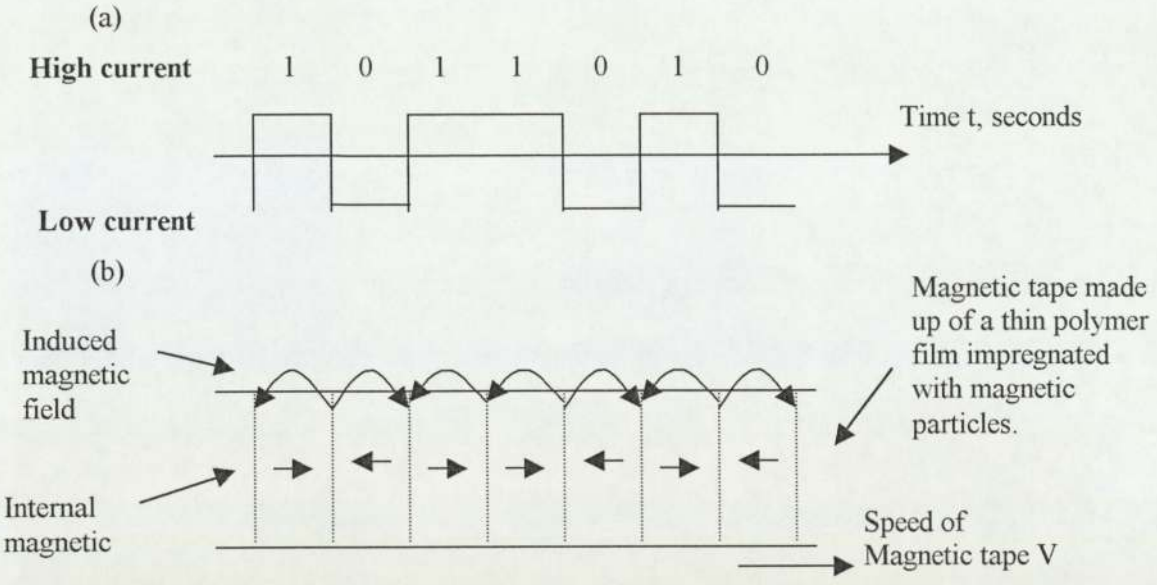

Figure 5 (a) the above diagram shows a typical digital waveform and (b) shows the corresponding magnetic fields deposited on a flexible magnetic tape

The digital waveform shown in figure 5(a) shows 2 discrete magnetic states within the magnetic media, these are the high = 1 and a low = 0. In the magnetic recording industry, each of these states represents a bit of data. The size of a bit can be described as a bit length, which is the size of magnetic particles or a single domain. Therefore, as the bit length decreases, the overall storage density of the magnetic tape or disc increases. You can also relate the size of the bit to the recording wavelength λ, so the bit size b is equal to $\lambda / 2$. By using the recording wavelength λ, the frequency f can be calculated from this relationship $\mathbf{v} = \mathbf{f}\lambda$, where v is the relative velocity of tape and head. So as the recording frequency increases, then the bit size decreases i.e. size of a magnetic domain decreases at constant relative speed.

There are two types of magnetic recording, which you can use in magnetic tape recording. Firstly is the popular *longitude* magnetic recording like the one shown in figure 5(b), where the magnetic field of the magnetic particles lie parallel to the plane of the tape. Secondly, *perpendicular* recording is when the magnetic fields of the magnetic particles are orientated perpendicular to the plane of the magnetic tape. This type of recording can store more data per square inch than *longitudinal* recording, resulting in higher recording densities.

1.3.1 Magnetic recording principles

Magnetic recording works by sending a signal i.e. a short pulse of current **I**, which energises two coils of a *gapped toroid* head and generates a fringe magnetic flux **B** between the head gap. The fringe flux then penetrates the passing magnetic tape, and magnetises the magnetic particles by changing the orientation of the magnetic moments in a direction parallel to the plane of the tape. When the current **I** is reversed, the direction of the magnetic moment of the magnetic particles changes in the opposite direction. This gives a flux pattern shown in figure 6, where the directions of the magnetic domains lie opposite to each other and are parallel to the plane of the tape.

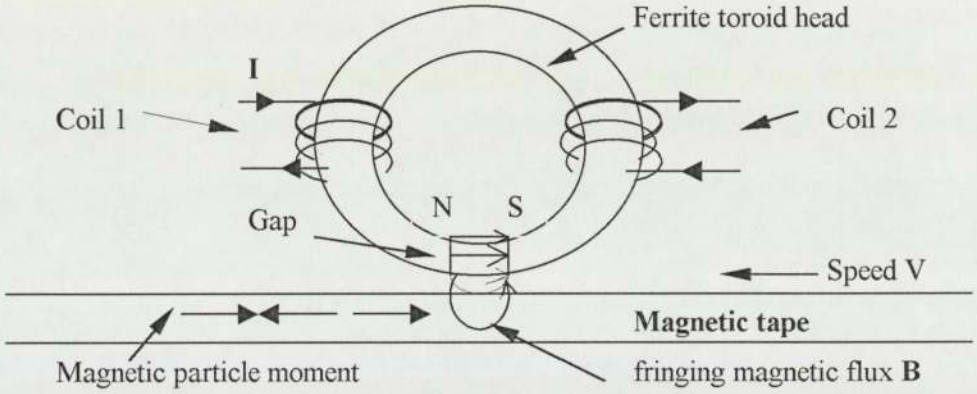

*Figure 6 showing a gapped toroid fringed magnetic field **B** penetrating passing magnetic tape*

When two magnetic moments oppose each other in longitudinal recording, that is when the opposing magnetic dipole moments start to demagnetise each other, then the resultant magnetic flux density becomes less than the original magnetic.

1.3.2 Magnetic playback principles

The physics of playback is based on the experiments performed by Michael Faraday in 1831. In his experiments, he passed a permanent magnet in one direction through an inductive coil made of copper wire, which was connected to a voltmeter or galvanometer. He observed a negative voltage (potential difference) from the coil. However, when he moved the magnetic in the opposite direction through the coil, he observed a positive voltage. As you increase the speed U of the magnet through the coil in either direction or simply increase

the number of coils respectively, the voltage or emf E increases. A simple relationship describing these observations is:

$$\text{Voltage, } V = -N\left[\frac{d\Phi}{dt}\right] = -N\left[\frac{d\Phi}{dx}\right]U \qquad (3)$$

Where Φ = Magnetic flux density (Weber);

N = Number of coils or turns;

x = Distance travelled by tape from the head (m);

U = dx/dt = Speed of passing tape relative to the head (m/s)

The voltage or emf (Electro-motive force) shown in equation 3 above is directly proportional to the rate of change of magnetic flux lines linking N loops or turns of a coil. As the rate of change of magnetic flux increases that is the number of flux a line linking one loop increases then the induced voltage or current measured increases proportionally. Alternatively, as the speed U of the magnetic increases so does the potential difference V. The potential difference V is created when negative charges of the coil are attracted to the North Pole of the coil and positive charges are repelled to the other side of the inductive coil, resulting in a charge imbalance. This charge imbalance and potential difference induces an electric current I. The negative sign, which appears in equation 3, is referred to as the sense of the induced current. Classically equation 3 is now known as *Faradays Law* who discovered this phenomenon.

The playback mechanism uses the above principle by using two copper coils wrapped around a horseshoe shaped ferrite core to represent an inductive head as shown in figure 5. Let's assume that the recording head shown in figure 5 is used as a reading head instead. When the magnetic tape passes very close to the inductive head, the magnetic flux linking the coils of the head induces a potential difference V or an emf E. When the magnetic flux from the magnetic particles increases, the number of field lines linking the coils of the head increases, so the reading signal (voltage) increases proportionally. Alternatively, as the speed U of the tape is increased, the potential difference V increases proportionally.

The reading voltage V should be equal to the original signal (recording signal), but in real terms, this is not exactly true. This is due to the magnetic particles having its own internal magnetic field resulting in demagnetising the external field at the surface of the magnetic tape. Thus the writing voltage $V_{writing}$ is not equal to the reading voltage $V_{reading}$.

During playback, where the magnetic tape is at a distance d from the gap due to debris or deposits located around the gap region of the head, the magnetic flux density from the magnetic particles decays exponentially. That is the magnetic flux density m is directly proportional to the exponential of the distance d-

$$\text{Flux density} = A\exp\left\{\frac{-2\mu d}{\lambda}\right\} \qquad (4)$$

Where, d = Distance between head and tape (in metres);

λ = Recording wavelength (in metres);

μ and A = Constant.

This deposit introduces a *spacing loss* or '*Wallace loss*' between the tape and head, resulting in a loss of read signal. This spacing loss can also be expressed logarithmic in decibels (dB):

$$\text{Spacing loss} = -\left[\frac{54.6\,d}{\lambda}\right] \text{dB} \qquad (5)$$

Where d = Distance between ferrite reading head and passing magnetic tape (m);

λ = Recording wavelength (m);

1.4 Flexible magnetic tape

There are at present two forms of magnetic flexible tape used in today's data/audio/video recording industry. These are metal particulate and metal evaporated (ME) tapes.

1.4.1 Particulate flexible tape

This type of tape is used by many platforms such as audio, video, and data storage as in the DDS format. The basic structure of a particulate tape such as the Digital Data Storage DDS-3 shown in figure 7 is a modern dual layer system. This system consists of a thin magnetic layer of the order of 0.2 μm and a thicker titanium layer of 1.8 μm bonded together

to form a single system. An earlier DDS generation such as DDS-2 has a single magnetic layer of around 2 μm bonded to a substrate, instead of a titanium and magnetic layer system as in DDS-3. Two major companies such Fuji and Maxell manufacture the DDS format thus differ slightly in the dimensions and formulations of the binder, substrate, and magnetic particles used in the tape.

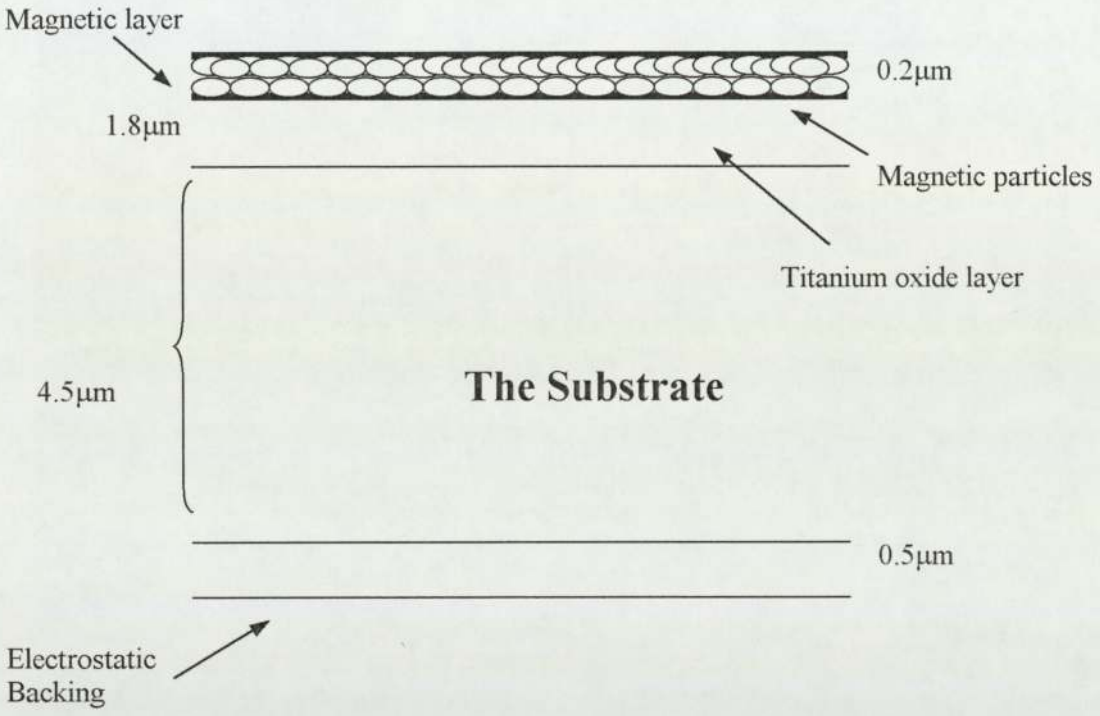

Figure 7 showing the basic structure of a dual layered DDS particulate flexible tape (in this case a DDS-3tape was used in this work.

The magnetic layer of a DDS-2 tape is made up of gamma iron oxide, which is bound together within a polymeric binder. Whereas for the DDS-3 system passivated iron oxide particles (metal particles) are used. The same substrate is used by both DDS formats of the order of 4.5 μm in thickness. Each of these components is described in more detail in the following sections.

1.4.1.1 The Binder

To form a cohesive and durable magnetic coating of defined thickness and surface structure, the magnetic particles are disposed into a polymeric binder together with head cleaning agents, lubricants, and antistatic agents as in the case of the DDS-2 system. In the DDS-3 system, the lubricant is deposited in the titanium layer underneath the magnetic layer/binder.

The binder is made of flexible co-polymer such as polyester-polyurethane or poly-vinyl chloride-polyurethane, which exhibits two phases or states; these are the 'rubbery' and 'glassy' states. The 'rubbery' state - polyester or poly-vinyl chloride gives the tape the property of flexibility so that the tape conforms to the contours of the head and the 'glassy' state- polyurethane gives the tape surface hardness (durability), so that the binder has lower wear rates. The latest binder formulation used in today's DDS tape system is polyester or poly (vinyl chloride) with polyurethane.

1.4.1.2 The Magnetic Particles

In particulate tape, there exist many types of magnetic particles including γ - Fe_2O_3 (gamma ferrite oxide), cobalt modified gamma-ferrite oxide, chromium oxide, passive metallic iron and barium ferrite. The particles gamma ferrite oxide, cobalt modified gamma ferrite oxide are not used anymore except in DDS-2, but at present passive metallic iron is used in DDS-3 particulate tape. For future magnetic recording, barium ferrite could be used in perpendicular media due the unique properties mentioned later. Each of these particles is described in more detail below.

(I) Gamma ferrite oxide

Gamma ferrite oxide γ - Fe_2O_3 has been used for some time and remains one of the principle recording materials used in today's audio tape. The main properties of this particle are that it is needle-like (acicular) with dimensions of around 250-750 nm in length and 50-150 nm in width. These particles have high coercivity and remnance magnetisation of 300 Oe, but are not high enough for high-density recording, therefore were used in earlier low-density data recording and audio. Such example is DDS-2 tapes that are used in these experiments

(II) Cobalt modified gamma iron oxide

With cobalt added to gamma iron oxide (Co-γFe_2O_3), an increase in coercivity of around 1000 Oe is achieved. The drawback with this particle is that the magnetic properties are thermally unstable at high temperatures, such that the cobalt diffuses into the particle. These particles are mostly used in videotapes.

(III) Chromium oxide

Chromium oxide CrO_2 has superior magnetic properties in comparison to the particles mentioned earlier, but they have a tendency to oxidise when exposed to the environment. Normally a thin layer protective layer is added to the surface to reduce oxidisation and protect the surface.

Chromium oxide is grown by hydrothermal process at high temperatures and pressures. These particles have very high remnant magnetisation and coercivity, but are not used nowadays due to having very high abrasivity, which wears away recording heads very quickly.

(IV) Passive metal particle

These are iron particles referred as metal particles (MP) are acicular in shape but are much smaller than standard iron oxide particles used in DDS-2 tape. The shape of these particles has a ratio of 7:1 or a length of 60 nm, and width of 8 nm. The coercivity is very high at around 1500 Oe and is commonly used in high-density magnetic recording such as DDS-3 tapes. The highest at present is around 2200 Oe, but are not on the market yet. The passivating layer around the metal particle is a thin oxidising layer of a defined thickness, which is used to protect the particle from further corrosion due to the atmosphere. If the passivating layer is too thick, the magnetic properties of the particle are reduced. With further refining, the thickness of the passivating layer can be reduced to a minimum, so that the magnetic properties can be increased to a maximum value.

(v) Barium ferrite

The shapes of barium ferrite particles BaFe are very different to any other particles mentioned above. They have a platelet shape. This particle has stirred up a lot of interest due to the possibility of using the particle for perpendicular magnetic recording. With further modifications, these particles can offer very high linear recording densities at relative high coercivity.

It has been reported that the coercivity is too high of around 3500 Oe to be of any practical use. This is due to the internal demagnetising field of the magnetic particle. To reduce this value, BaFe was modified with the substitution of Fe^{3+} for Co^{2+} - Ti^{4+} to lower the coercivity to a suitable value.

1.4.1.3 The Substrate

The substrate is a biaxially orientated polymer, examples of which include polyethylene terephthdate (PET), polyethylene naphthalene (PEN), aromatic polyamide (ARAMID) and polyamide (PI). Work done by [1] to measure the dynamic mechanical behaviour of PET, PEN, and PI substrates used in magnetic tape, has found that advanced PEN and ARAMID tapes tend to have higher modulii than PET tapes. Other work [2] has shown that PEN and ARAMID have superior characteristics when compared to PET. Such characteristics are that PEN and ARAMID have higher elastic modulii of 4-54 GPa and 10 GPa respectively and thermal and hygroscopic expansion measurements show that PEN and ARAMID are typically superior to PET.

1.4.1.4 Lubrication

The lubrication in the form of fatty acids esters and natural or synthetic hydrocarbons are normally used in particulate tape. The function of a lubricant is to reduce wear and friction between two surfaces in contact by separating the head and tape at a small distance apart during contact. In the early days of low-density magnetic tape recording, an air bearing to separate the head and flexible tape was used instead of a lubricant. This reduces the wear and friction between head and tape, thus prolonging the life of the head and tape.

With the advent of high-density magnetic and head-to-tape contact recording, there is a need for incorporating the lubrication within the binder system of the tape. With modern dual layer tapes (DDS-3 tapes), the lubricant is held within the TiO_2 layer. This type of lubrication system works when you exert pressure on the surface of the tape; the lubricant within the TiO_2 layer diffuses to the surface of the tape and replenishes the depleting lubricant during head-tape contact. The lubricant fills in the pores or defects on the surface of the tape, making the surface smoother (minimize surface roughness), thus reducing the friction coefficients. When there is too much lubrication on the surface of the tape, this leads to running and durability problems such as stiction and meniscus forces. Hishida et al [3] investigated the amount of lubricant on the surface of a particulate magnetic recording media using X-ray photoelectron spectroscopy (XPS) and contact measurements. They found that in topical lubrication, it is possible to obtain lower friction coefficient than internal lubrication. In addition to obtain low friction coefficient of the tape, it is necessary to have large coverage ratio and sufficient amount of sub-surface lubricant.

1.4.1.5 The head cleaning agent (HCA)

Originally the head-cleaning agent composing of an abrasive particle was added to the binder to remove deposits or tape debris on the magnetic head, so that the head is kept clean keeping the head and tape in direct contact. The particles used to keep the head clean are very hard and are added at around 2 to 6% by relative weight to the magnetic particles. The head-cleaning agent is normally made of aluminium oxide (Al_2O_3). These particles have dimensions of around 0.2-0.4 μm in diameter. These days the function of HCA is also to improve the mechanical properties of the tape by acting as a bearing surface instead of removing staining and tape debris.

It was reported [4], that an increase in HCA or roughness reduces propensity of head stain, resulting in better signal reproduction at the expense of higher head wear. However, there seems to be a limit to improving the reproducing signal with an increase in HCA.

1.4.2 Metal Evaporated tape

The structure of this type of magnetic recording tape is shown in figure 8 overleaf. This figure shows it is constructed with a thin single film of $(Co_{80}Ni_{20})_{80}O_{20}$ magnetic particles, which is evaporated onto the polyester (PET) base. The evaporated film is made of columnar particles of an intermixture of Co and Co-Ni crystallites. These particles are grown in a <002> direction.

During evaporation, O_2 is added in order to improve the corrosion resistance and to reduce the noise from head-tape contact. It was found that the greater the oxygen O_2 flow rate during evaporation, the finer the magnetic particles become. By Auger analysis, it was found that the relative concentration of O_2 in an evaporated film increases with flow rate, which in turn improves the durability and hardness of the tape.

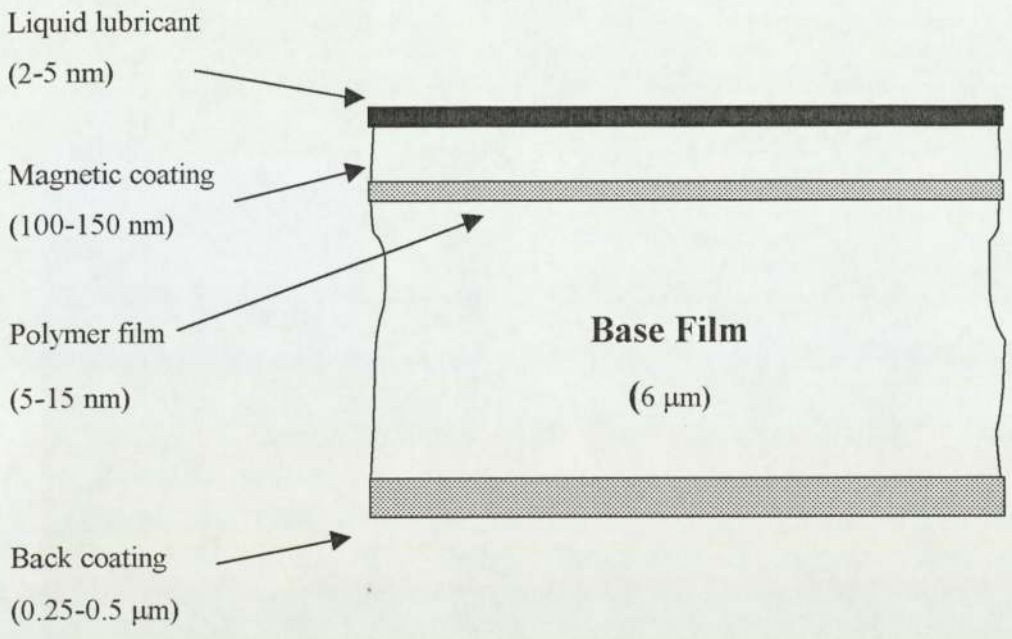

Figure 8 showing the structure of a metal evaporated (ME) tape

With ME, it offers higher coercivity and remnance magnetisation in comparison to particulate tape, but the disadvantages associated with ME tape are that it is more prone to corrosion, higher wear rates, and friction. To prevent corrosion of the metal film, an overcoat is added to the surface, but inherits an undesirable spacing loss. A typical overcoat is rhodium, silicon dioxide, or graphite.

A topical liquid *lubricant* (typically perfuoropolyether with reactive polar ends) is applied to the surface of the magnetic coating to reduce the friction and wear of the tape. The secondary function of the lubricant is to enhance the durability of the magnetic coating and inhibit the highly reactive nature of the metal coating.

A *backing coating* primarily made of carbon is added to the back of the magnetic layer so that it balances the stresses of the tape and reduces the static build-up. Backing coating used by particulate tape is inadequate due to the problems of the transfer of polymeric binder and pigment (magnetic particles) resulting in excessive dropouts and head clogging.

The base film is made of PET, which has been processed, by a polymer pre-coat film on both sides of the substrate. The function of the pre-coat is to reduce the roughness and provide a good adhesion with a ME film. Inorganic particles are added to the pre-coat to control the real area of contact and consequently the friction between the finishing tape and the head surfaces. The particles used are generally made up of SiO_2 and the size is typically of

the order of 100-200 nm in diameter. The areal density of these particles (10,000-particles per mm^2) is varied to obtain an optimum compromise between head output level and friction.

1.4.2.1 The durability of Metal Evaporated tape

The durability of this type of tape is improved by using small protrusions on the surface of the tape. This prevents the increase in the real contact area between the head and tape causing wear. After some time, these protrusions wear away, drastically increasing the friction to the point of breakdown. However, if the protrusions are too high, spacing losses occur, therefore a loss of signal. Thus, optimisation between the height of the protrusions and spacing loss is required.

Hempstock et al [5] studied the durability performance of two tape types ME and metal particle (MP). A correlation was made with mechanical and physical changes to the surface of the tape to the recording error measurements. It was found that MP tapes exhibit far greater durability than ME tapes.

1.5 Head types

To date there is two main types of heads used in the magnetic recording industry these are the *inductive* head used in *helical scan* and *linear* tape technologies and the magnetoresistive heads (MR head for short) used in hard drives and linear tape drives. The inductive head is shown below.

1.5.1 The inductive head

The basic structure of an inductive head (or more precisely a ferrite inductive head) is very similar to a DDS-3 system as shown in figure 9. This figure shows a *reading* head with two ferrite cores and two copper coils wrapped around each core. The gap is filled with bonding glass to give the head stiffness since the head is subjected to high differential forces when the tape passes the head with high tension.

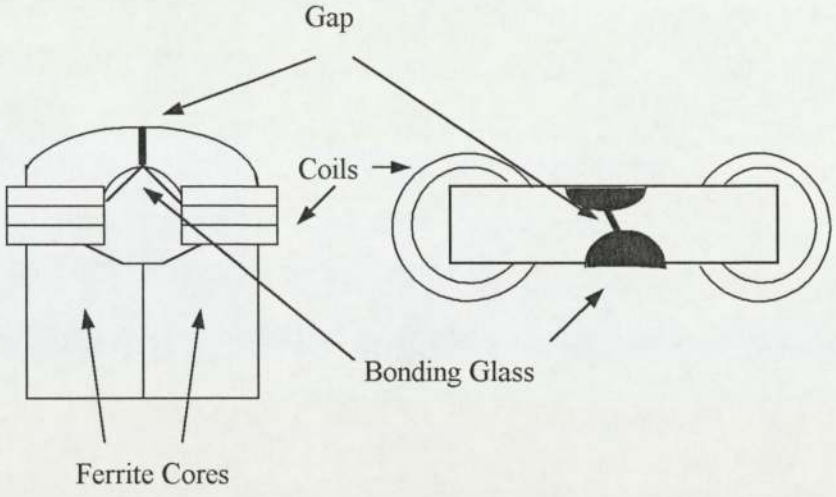

Figure 9 showing the basic construction of a DDS-2 and DDS-3 ferrite inductive reading head

In the past few years, there has been a rapid increase in recording densities, with an improvement in ferrite head technology, resulting in the reading head and gap dimensions becoming smaller. A typical dimension for the gap width is around 250 nm for a DDS-3 system and the head has an overall size varying from 20 –70 μm by 1.2-50 mm, with a contact area of tape-head at around 70 μm. The core is made of manganese-zinc ferrite in a polycrystalline form delivering a high level of saturated magnetism and low coercivity to read very short wavelengths (high bit density) from high coercivity tape. Low coercivity and remnance magnetisation is needed so that the head is sensitive to rapid changes in magnetic flux at the gap.

In the case of a ferrite read head shown in figure 9 the gap is modified with sputtered films deposited on the gap faces. This type of head is referred to as a *metal-in-gap* (M.I.G) head, and is used as a writing head. This is shown in figure 10. The idea behind the MIG is to improve the magnetic flux density at the gap, which leads to an increase in the recording wavelength amplitude. Again, the bonding glass is used to give the head rigidity. Again for the DDS-3 systems the gap size is around 250 nm, and the length of the head is around 1.2 mm, with a head-tape contact length of around 700 μm.

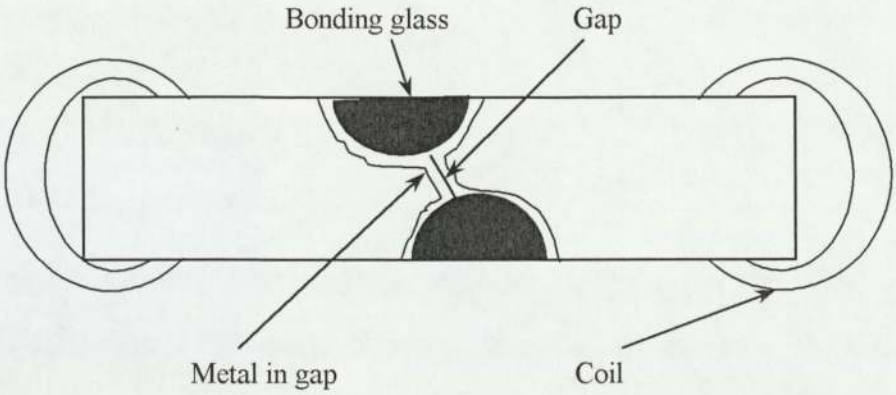

Figure 10 showing a DDS-2 and DDS-3 ferrite metal in gap inductive writing head

Other materials' used to construct a reading/recording head is *Permalloy.* The composition of Permalloy is 80% Ni and 20% Fe, which gives the material high saturation magnetisation of around 12,500 Gauss

1.6 The tribology of the head-tape interaction

Tribology of head-tape interactions is a special branch of classical tribology that is concerned with the friction and wears between magnetic tape and recording/reading heads. This new branch of tribology has come about, due to the increase in bit densities resulting in intimate contact between the head and tape. In this section, the reader will be introduced to basic principles of friction and wear, the 2-body and 3-body interactions, corrosion, transfer layers and the latest research work done by other researchers in tribology.

1.6.1 Wear

The wear ω defined as volume of material removed per unit sliding distance of the magnetic tape and a read/write head during contact can be described by this simple relationship: the *Archard Wear Law* [6].

$$\omega = K W / P_m \qquad (6)$$

Where, W = load (in Newton's, N); P_m = flow pressure or hardness of the mating material;
K = coefficient of wear.

This law, equation 3 shows that as the flow pressure increase i.e. the hardness increases, and then the wear rate ω decreases. Whereas, when you increase the load W during contact between the two mating surfaces the wear rate ω increases proportionally. To reduce wear the two mating surfaces (that is, the head and tape) a thin lubricant needs to be applied to separate the two surfaces. A compromise is made with the thickness of the lubricant so that the wear is reduced and spacing loss is kept to a minimum.

At contact area between the head and tape, the 'real area of contact' is always less than the apparent area of contact (i.e., when you observe at the macroscopic level). At a microscopic level, the 'real area of contact' is when the surface of the head and tape are in contact at asperity points along the surface. Asperities are peaks of various sizes and spacing along the surface, so for real area of contact, the tips of these peaks are in contact with the mating surface. By referring back to the Archard Wear Law [6], as the load W increases, the real area of contact increases and more asperity tips are in contact resulting in the increase in the wear rate.

The asperities can be deformed in two modes: elastic or plastic. In the elastic mode, the asperity deforms to its original shape after a load W is removed. The second mode is plastic, this occurs when the asperity deforms to a new shape after a load is removed. These modes can be described by a Bhushan plasticity index ψ and the metal plasticity index based on the relationship developed by Greenwood and Williamson [8]. The Bhushan plasticity index shown in equation 7 describes the plastic behaviour of polymers so can be used to calculate the asperity deformation modes of any polymer such as tape binder when in contact with another surface. Equation 7 can also be modified to take into account metal surfaces such as recording head.

$$\psi = E^* / \gamma \, (\sigma / \, r_a)^{1/2} \qquad (7)$$

Where, E^* = complex modulus of elasticity; r_a = mean radius of the asperities peaks; σ = Standard deviation of asperities height; γ = Yield strength or hardness of contact surface;

From equation 7, it can be calculated that when $\psi < 1.8$, the contact between the head and tape is elastic, whilst for $\psi > 2.6$, the contact is plastic. In practice, contact between the head and tape is always elastic. For $1.8 < \psi < 2.6$, the contact between the head and tape is semi-elastic and semi-plastic surface deformation.

A great deal of research has been done in the field of wear over the years especially the interactions of magnetic tape and Mn-Zn ferrite heads. Bhushan [9] has found that wear of Mn-Zn ferrite heads is dependent on water vapour. At mid-relative humidity (around 50% RH), water acts as a lubricant, which mitigates the wear and friction of the ferrite head. Whereas, at high humidities, the wear and friction increase dramatically, due to the formation of menisci bridges at asperity contacts resulting in high friction due to adhesion and the increase in abrasive wear from the agglomeration of debris. The wear and friction increases steadily up to 65% RH. Beyond this point wear and friction catastrophically destroys the surface of the ferrite head and magnetic tape with stress fractures.

Further work [10] on the wear and friction mechanisms of particulate (metal particle and barium ferrite) and metal evaporated (M.E) magnetic tape in rotary head systems, have found that particulate tapes has a longer wear lifetime in comparison to M.E. tapes. This was followed by a catastrophic failure of the surface of the tape and tape breakage was observed by [9]. The tape failure may be due to the fatigue of the tape, which was set to the pause mode in the video recorder.

Based on these modes and the model on the area of contact, there are five mechanisms of wear during head and tape contact. Firstly:

1.6.1.1 Abrasive Wear

Abrasive wear is observed as scratches on the surface of a soft material. These scratches can be referred to as the 'ploughing' effect, where the harder material removes the softer material during contact, creating small grooves and tape debris. Figure 11(a) demonstrates this effect of a 2-body interaction. The 'ploughing' effect can also be thought of as a three body, where the harder debris between two surfaces in contact causing scratches to appear on the surface of a softer material. This is shown in figure 11(b). A simple model describing the 'ploughing' effect is shown below in equation (8).

$$V = \frac{K\,L\,D\,\tan\theta}{H_D} \qquad (8)$$

Where L = load applied to asperity (N); K = constant; D = distance of sliding (m); H_D = hardness of material; θ = Angle between a hard asperity and surface of a softer mating material;

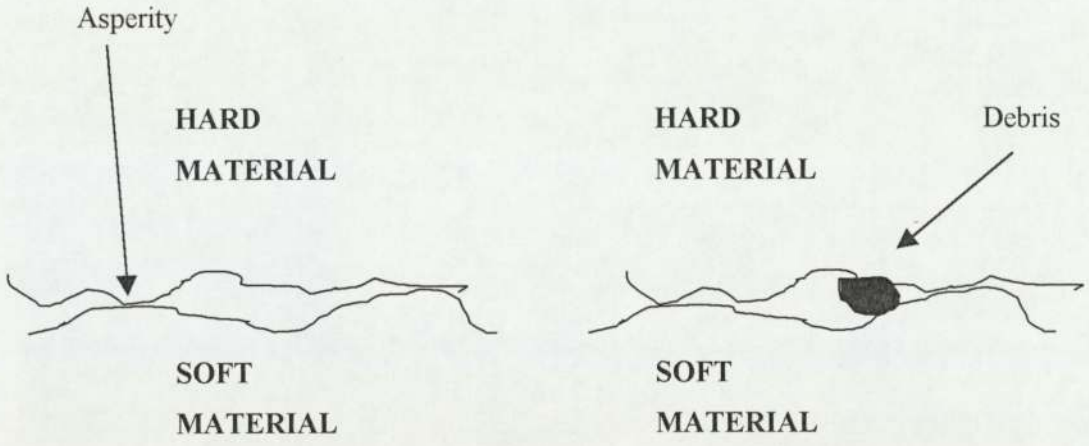

(a) A two body interaction

(b) A three body interaction

Figure 11 showing (a) a two-body interaction and (b) a three-body interaction

From equation 8, you can see that when the material is hard, then the volume of debris removed V is smaller, but when the sliding distance is increased, then the volume of the debris V is increased. Note that the hard asperity must have an angle θ greater than 0 degrees and less than 90 degrees to result in the 'ploughing' effect.

When considering the mechanical properties of wear there is a considerable amount of work done during sliding, this is measured using the area under a stress/strain curve. A simple calculation deduces that the work done W is approximately equal to the breaking strength S times the elongation at break point e: W = S e. A further calculation gives the wear rate of 1/S e.

1.6.1.2 Erosive Wear

Erosive wear occurs when solid abrasive particles behaving as a fluid, slowly erode a small crevice at the surface of the ferrite head. The wear rate is dependent on the angle of incidence of the eroding particles and the solid surface. This wear mechanism is different for a surface, which is either brittle or ductile. For a brittle surface, material is removed by the interaction of cracks that radiate out from the point of impact of the eroded particle. Whereas for ductile surfaces, the material will undergo wear by process of plastic deformation in which the material is removed by the displacement or cutting action of the eroded particle.

1.6.1.3 Fatigue Wear

Fatigue wear is a single microcutting effect from repeatingly stressing a given area. This can develop into abrasive wear when the two surfaces are in continuous contact at the same area e.g. when videotape is left in pause mode.

1.6.1.4 Corrosive Wear

Corrosive wear is a chemical reaction, which occurs at the interface of the surface of the material with the environment. In the case of the head-tape interface the two surfaces are protected with a topical lubricant excreted to the surface of a tape. Chemical corrosion occurs in a highly corrosive environment and in high temperatures and humidities

1.6.1.5 Adhesive Wear

Adhesive wear occurs when strong intermolecular forces at the asperity points transfers material from the surface of a soft material such as magnetic tape onto the surface of the harder ferrite head. This transfer of material starts with an irregular spotty deposit, which in time develops into a thin film with a distinct thickness. This transfer layer becomes smooth with a lower friction coefficient, which inherently decreases the wear rate of the surface of the much harder ferrite head. Often the transfer film starts with scratches on the surface of the head due to abrasive wear.

The forces involved in adhesion wear may be physical (Van der Waals bonding) or chemical (covalent, electrostatic, or ionic). Sullivan [11] suggested that for metal and polymer interactions such as the magnetic head and tape, chemical forces like covalent and Van der Waals forces might be involved. Since the polymer atom is arranged chain-to-chain, ion-dipole attractions can occur between the head and tape, resulting in shearing within the bulk of the magnetic layer. This process can be referred to as a transfer layer or staining on the surface of the ferrite head.

1.6.2 Transfer films

A transfer film, which is commonly known as head 'stain' is an adherent layer of substance transferred from magnetic tape onto a magnetic reading/recording head. The substance transferred to the ferrite head can be either organic or inorganic in nature, where organic is polymeric and inorganic is metallic. Early work done by Bhushan [12], analysed

the transfer layer from particulate tape to find that its primarily made up of inorganic magnetic iron oxide particles together with a small amount of organic tape binder and lubricant. Chandler [13], Stahle [14], Prabhakaran [15] and Gupta [17] have also confirmed this. A transfer film has been observed as either a loose powder-like or an adherent deposit. Diffraction has revealed that stain has four distinct colours: brown (most common), blue, transparent, or white. When the film is observed as a brown 'stain', Raman spectra showed it is mainly iron oxide and inorganic compounds as confirmed by Y.F.Liow et al [16].

Chandler et al [13] measured an increase in transfer layer thickness of around 20 nm at low humidity, resulting in a 1 dB spacing loss between the magnetic head and tape. This spacing loss inherently causes data errors in helical scan DDS systems or a reduction in signal at high recording frequencies. Gupta et al [17] analysed the thickness variation of the stain on a metal-in-gap core formed by Co-γFe_2O_3 and metal particle (MP) tapes using an Atomic Force Microscope. Found that for Co-γFe_2O_3 and MP tapes produced stain with a thickness of 30-120 nm and 20 nm respectively. Gupta et al [17] also observed stain as patchy or streaky.

Further experiments done by other researchers [18] and [19] have found that stain is encountered at low humidity (less than 30% relative humidity RH and high temperatures of around 40°C). The most common appearance of a stain is small patches of around 20 nm in height. Figure 12 shows a typical example of a transfer film. In this figure, the stain has started at the trailing edge, which then forms stripes from the gap and glass region of the head.

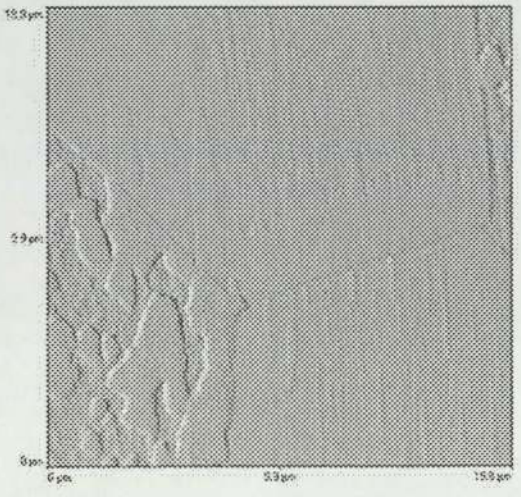

Figure 12 showing an AFM scan of a transfer film 'stain' on a ferrite inductive reading head. This scans shows large patches of staining on the glass region and stripes lying parallel to the direction of the tape. DDS-2 (M120) tape was cycled at 25°C/10%RH

In the past there has been an intention to encourage stain formation, so that it reduces the wear of the head by acting as a smooth protective layer. At present greater data storage densities have been achieved so direct contact between the surfaces of the ferrite head and tape is required, resulting in head staining becoming a significant problem at smaller recording wavelengths (or higher frequencies).

Stain has also proven to be harder to remove from the surface of the head than loose tape debris probably due to the high adhesion from the organic components of the stain. Normally HCA is used within the tape to remove the stain at the expense of the increase in head wear.

Work done by T.Kamei et al [20] found that a chleting agent on the magnetic tape could drastically suppress the loss of signal amplitude caused by stain. In addition, found that chleting agent reacts with iron oxide of brown stain to make metal complexes, and the complexes are easily removed by chemical lapping, reducing the need for a head-cleaning agent incorporated within the tape system.

W.W.Scott et al [21] studied the generation of tape debris in linear tape drives when running MP tapes against AL_2O_3-TiC and Ni-Zn ferrite heads. Found three types of debris: magnetic particle rich, polymer rich, and adherent (stain). Each type of debris was found at distinct locations along the thin film AL_2O_3-TiC and Ni-Zn ferrite heads, but AL_2O_3-TiC generated more than Ni-Zn. Adherent debris (stain) collected near the poles of the heads and was difficult to remove. This potentially poses a head-tape spacing problem. A relationship of debris generation versus tape speed, tape tension and head wrap was deduced. Found that loose debris generation increased as tape speed decreased and as tape tension and head wrap increased.

Head staining has also been associated with head clogging where loose tape debris has been deposited on either side of the head-tape contact region of the recording head as studied by H.Osaki et al [22]. It was found that tape debris forms agglomerate contacts at the surface of the tape and is deposited. The following head picks it up on the rubbing surface and a spacing loss occurs with a consequential decrease in the reproducing signal.

H.Ota [23] studied brown stain on VCR heads. It was found that stain occurs at low humidity and low tape tensions as confirmed by other researchers. Further into this study, the researcher had found that the wear volume of the head decreases when brown stain occurred-

this suggests that stain can reduce head wear. A temperature rise was measured and occurred at the head-tape interface when stain appeared. This temperature rise was found to be limited to the temperature recrystallation of the metal, friction and flash temperatures.

1.6.3 Friction

Friction is a force between two interacting surfaces sliding against each other. Bhushan et al [24] studied the behaviour of friction and wear of high-density magnetic tape and found that the effect of tape roughness on friction is dependent on the hardness of the material and friction increases with an increase in surface roughness. However, friction decreases with an increase in roughness of a hard ferrite surface, which is consistent with the asperity contacts being elastic in nature. There are two forms of friction involved to describe these interactions: dynamic and static friction, each obeying the laws of friction.

1.6.3.1 Laws of Friction

Friction is the resistance to motion of two sliding bodies in contact or a shearing of adhesion bonds formed over the real area of contact.

Law 1: Friction F_a is directly proportional to the applied load L.

$$F_a \alpha L$$

$$\Rightarrow \quad F_a = \mu_a L \qquad (9)$$

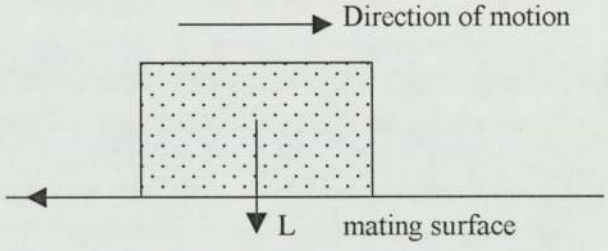

Law 2: Frictional forces between two bodies are independent of the apparent area of contact, but are dependent on the real area of contact.

The second law of friction means that on a microscopic scale, the surfaces are in contact at the points of the asperities. Thus, the real area A_r of contact is always less than the apparent area A_p of contact or observed area of contact. As the load is increased, the number of contact asperities increases, so the friction between the two sliding surfaces increases. The deformation of the asperities can be classified as plastic or non-recoverable interaction.

Since friction is associated with the shearing S of the adhesion bonds at the tips of the asperities (called cold weld), then friction F_{ad} can be calculated as:

$$F_{ad} = A_r S \quad (11)$$

The total friction F between the two surfaces is the sum of the adhesion and deformation forces:

$$F = F_{ad} + F_{def} \quad (12)$$

The deformation force can have the effect of ploughing, plastic, and elastic or a combination of all these forces. The definition of each of these effects is explained in earlier sections of this chapter.

1.6.3.2 Dynamic friction

The definition of dynamic friction is the force resisting motion between two surfaces in contact at relative speed to each other. This force is the summation of the adhesion and deformation as shown in equation 12. In the case of the magnetic layer on the flexible tape is visoelastic in nature, so the total deformation component is negligible. Therefore, the friction comes from the adhesion part. The dynamic friction force is related to the relationship: $F = \tau A_r$, **(13)** where τ is the shear/stress force per unit area, and A_r is the real contact area.

With particulate tape, fatty acid or fatty acid ester is used as a lubricant to reduce the dynamic friction. These types of lubricant acts like a reservoir to preserve and replenish the magnetic layer. Equation 13, can be modified to take into the account of the lubricant, to give this new relationship of dynamic friction:

$$F = A_r (\tau (1- \alpha) + \tau_l \alpha) \quad (14)$$

Where, α is the fractional areal lubricant coverage and τ_l is the shear stress of lubricant.

Early experiments have shown that an increase in the coefficient of friction was observed with an increase in running time of tape [24]. This is due to the surface of the head and tape becoming smoother.

1.6.3.3 Static friction

The definition of static friction is the force required to initiate motion between two interacting surfaces. It has been found that this static frictional force is always greater than the dynamic friction, due to the magnetic layer being in a visoelastic state when operated at normal temperatures (where the strain rates is dependant). Thus, the real area of contact increases with time, therefore an increase in the initial frictional- static friction.

Research work has observed that static friction is very high at high levels of humidity. The possible reason for this is that the water condenses between the head and tapes creating a meniscus effect (where surface tension attracts itself) or water plasticity of the polymer. More likely, the increase in humidity creates pasteurisation.

1.7 Signal and Noise

Noise in the form of electronic, thermal fluctuations, and from the recording medium can be very troublesome when operating a data-recording device at low signal output. So higher the ratio of signal-to-noise (SNR) then lower the noise needs to be thus increasing the reproducing signal. The signal to noise ratio is characterised by the decibel (dB), which is the logarithmic ratio of the power output of a given signal to the noise power in a given bandwidth:

$$SNR = 20 \log (V_{signal} / V_{noise}) \quad (15)$$

The signal to noise ratio can be as big as 30 dB at a bandwidth of 25 MHz and at transition densities of 1000 flux reversals/mm, when using today's technology.

As mentioned above, noise can be in three basic forms during head/tape interactions of a data tape recording system. Each of these forms is explained in more detail below:

1.7.1 Electronic noise

Electronic noise is caused by the random fluctuations in time of electric charge carriers through the magnetic recording head. It is normally neglected at medium to high frequencies, but at low frequencies, electronic noise becomes very significant.

1.7.2 Head noise

The magnetic fluxes in both read and write heads are subjected to thermally induced fluctuations. When the write head is subjected to high flux densities, a low resultant noise is neglected. However for read heads, the flux densities can be low, resulting in the noise becoming significant as in the electronic noise. To understand this phenomenon, the Nyquist noise theorem can be applied.

This theorem state's that any device, which dissipates energy when connected to a power source, will generate noise power as a passive device such as resistor. The magnitude of this noise is:

$$E^2_N = 4\,k\,T\,Re\,(z)\,\Delta f \qquad (16)$$

Where k = Boltzmann's constant; T = absolute temperature (K); Re (z) is the real part of impedance of load W; and Δ f is the frequency (Hz).

In general, the dissipative impedance of the head has two parts: the hysteria loss and the resistance of the coil. In manganese-zinc ferrite heads, coil resistance is very small, so noise is generated by hystersis losses. When areal densities increases, noise in whatever form will become a major problem. To reduce noise, the tracks on the magnetic tape are narrowed as the areal density is increased. Narrowing the head dimensions can further reduce the noise.

There are two forms of head noise, which occur. Firstly, noise is generated when the magnetic material has non-zero magnetostriction. Secondly, the acoustic waves generated by head rubbing during contact causes fluctuations in the magnetic flux threading in the head coils. This noise is called 'white noise', where the acoustic noise is randomised. To reduce this noise, a polycrystalline material is used so that the random orientation of the crystals permits cancellation of the magnetostriction. Note that the properties of the head, such as geometry often cause the rubbing noise, which peaks at a certain mechanical frequency. In the final case of a thin film head, the Barkhausen noise is observed. This is caused by the changes in the domain wall structure of the thin film.

1.7.3 Recording medium noise

Recording medium noise comes from the uncertainty or randomness of the property of the magnetic tape. The basic random process in magnetic recording tape is the uncertainty

of the positions of the magnetic particles or grains. If the particles are packed according to Poisson statistics (of equal probability in equal volumes), the noise is additive. Additive noise is present whether the signal is recorded or not. Multiplicative noise (modulation noise) varies with the level of the recording signal.

1.8 Surface Analysis Techniques

There are three methods used in surface analysis; firstly the Atomic Force or Scanning Probe Microscope used to study the changes to the topography of a surface (that is mapping a surface using the forces between the contact tip and the surface). X-ray Photoelectron Spectroscopy and Auger Electron Spectroscopy are used to study any chemical changes that occur at the surface of the tape and head during head-tape contact. To describe how these devices work are as follows:

1.8.1 The Scanning Probe or Atomic Force Microscope (AFM)

The Atomic Force Microscope (AFM) relies on a mechanical probe for magnifying images. An AFM comprises of a sensor probe, piezo-electric ceramics, a feedback electronic circuit, and a computer for generating and presenting images. An essential component of an AFM is the sensor probe that offers a very high spatial resolution. A common type of probe used in AFM is a Force Sensor.

A force sensor measures the deflection of a cantilever shown in figure 13. A tip is mounted on a cantilever such that when the cantilever moves the light beam from the small laser moves across the face of four-section photodetector (sensor). The degree of motion of this cantilever can be calculated from the difference in the light intensity on the sectors. The light intensity on the photodetector is converted to a sensor current, which is used to adjust the z-piezoelectric ceramic and generate z-data on the computer. A piezoelectric ceramic is device, which changes its physical size when an electric field (or voltage) is applied. Therefore, for a small potential the size of the piezo ceramic is small, and when the voltage is increased the size of the ceramic increases accordingly. In basic terms, the piezoelectric ceramic moves the tip in accordance to the sensor current measured from the laser light deflected from the tip.

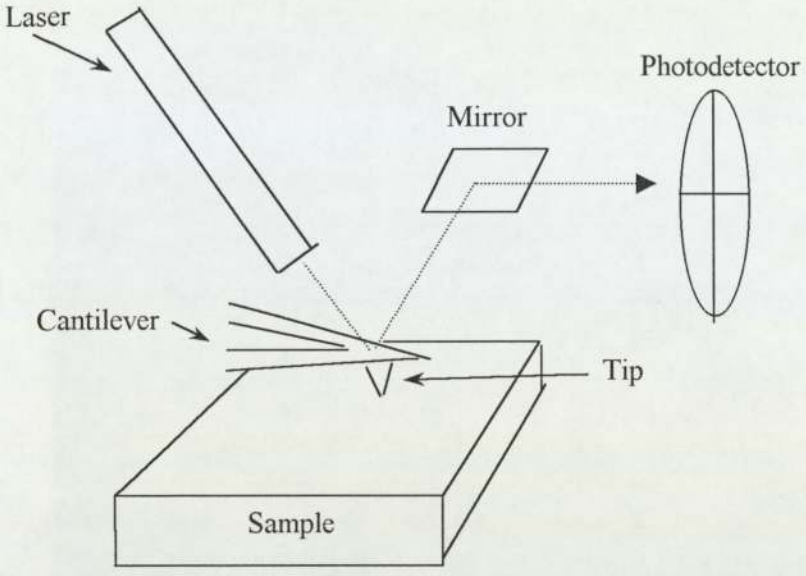

Figure 13 showing a Force Sensor device used by the Atomic Force Microscope AFM

As the probe is brought close to a sample it is attracted to the surface of the sample due to Van der Waals forces. When the probe gets too close to the surface, the electron orbital of the atoms on the surface of the probe and the sample start to repel each other. As the gap decrease between the tip and sample surface the repulsive force neutralises the attractive force due to Van der Waals and the tip is in contact with the surface. This is referred to as atomic force contact scanning.

At this point, the tip is as close to the surface as possible, and the feedback electronics combined with the piezo-ceramics creates a feedback loop, which keeps the tip position at a fixed distance from the surface. When the tip moves towards the surface the output of the sensor electronics increase. The difference between the increased voltage and the reference voltage is corrected using a differential amplifier. The corrected voltage or error signal excites the piezoelectric ceramics such that the sensor is pulled away from the surface at a required distance.

When adding two piezo-ceramics to the X-Y plane to scan the sensor voltage, the computer captures the error signal from the integrator circuit to the positioning device. An image of the surface is generated by rastering the sensor over the surface and storing the piezo driver signal on the computer.

1.8.2 X-ray Photoelectron Spectroscopy (XPS)

In XPS, the surface of a sample is irradiated with X-rays, which produce photoelectrons from the core levels (labelled K, L, M, with sub shells 1, 2, and so on for each level) of an atom near to the surface. This is referred to as the photoelectric effect and is described by this simple expression: $E_k = h\nu - E_B$ **(17)** or Kinetic energy of the emitted electron = energy of the X-ray photon - binding energy of the atom. From this expression the energy of the X-ray photon needs to be equal to or higher than the binding energy of the atom, so that a photoelectron with energy E_k is emitted from the core levels of the atom. When a photoelectron is emitted, an outer electron falls into the inner vacant level, and a secondary electron is emitted carrying off the excess energy from the fluorescent X-ray photon. This secondary electron is referred as an Auger electron.

The energies of the photoelectrons are characteristic of the elements, small variations of the chemical state and the environment of the element. The emitted photoelectrons are collected and analysed according to the energies of the photoelectron to allow classification of the elements at the surface of the sample. In addition, the binding energies of the inner electrons are sensitive to chemical states, therefore chemical information can be gained from this technique. To determine the relative concentration of the elements at the surface of the sample, the peak intensities and elemental sensitivity are taken into account.

1.8.3 Auger Electron Spectroscopy (AES)

This technique uses a beam of energetic electrons (1 – 10 KeV) to irradiate a surface of a sample. This results in ionisation of the atoms at the surface. The Auger electrons emitted have energies E_x associated with the core states of the irradiated atoms, so that the emitted Auger electrons have the characteristics of the parent atoms and the associated chemical states. Thus, energy analysis of the Auger electrons is done by means of an electrostatic analyser enabling the elements present in the surface of the sample to be identified.

The primary electron beam can be focused and used to give spot analysis on selected points on a surface. In addition an electron beam can be used to raster across a given area and Auger line of the elements of interest is then collected. This is called mapping mode. Another useful feature of AES is that focussed electron beams can be used as a Scanning Electron Microscopy (SEM) giving a secondary electron image of the surface of the sample can be produced.

Chapter 2 The Experimental Work

In this chapter, the experimental work done during this research project will be described. Firstly, background work includes writing the necessary software or code to operate the tape drives used in the following experiments together with the setting up of the necessary experimental equipment.

2.0 The Background Work

The background work consists of understanding the basic concepts in controlling the H.P DDS-3 data tape recorder and devising useful techniques of microindenting so that wear rate at the surface of the ferrite heads can be determined. Additionally techniques such as Atomic Force Microscopy AFM to study the physical changes to the surface of the tape and heads, and Auger Electron Spectroscopy AES and X-ray Photoelectron Spectroscopy to study the chemical changes to the surface of the head and tape.

2.0.1 Basic apparatus used in project

The basic apparatus used in the main experiments is shown in figures 14 and 15. The Hewlett Packard DDS tape drive in figure 15 is controlled and programmed using the Hewlett Packard Unix workstation (HP9000-700 or 300 series) like the one shown in figure 14. The DDS tape drives was connected to the workstation via a SCSI interface cable and a 12-volt power supply was used to supply electrical power to operate the drive.

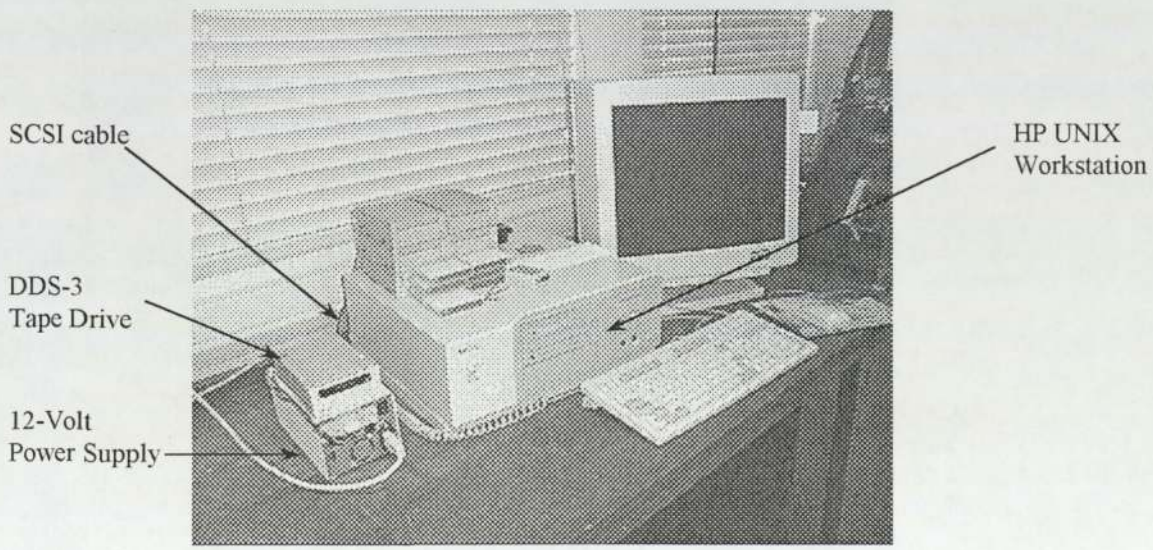

Figure 14 showing the basic apparatus used in the following experiments

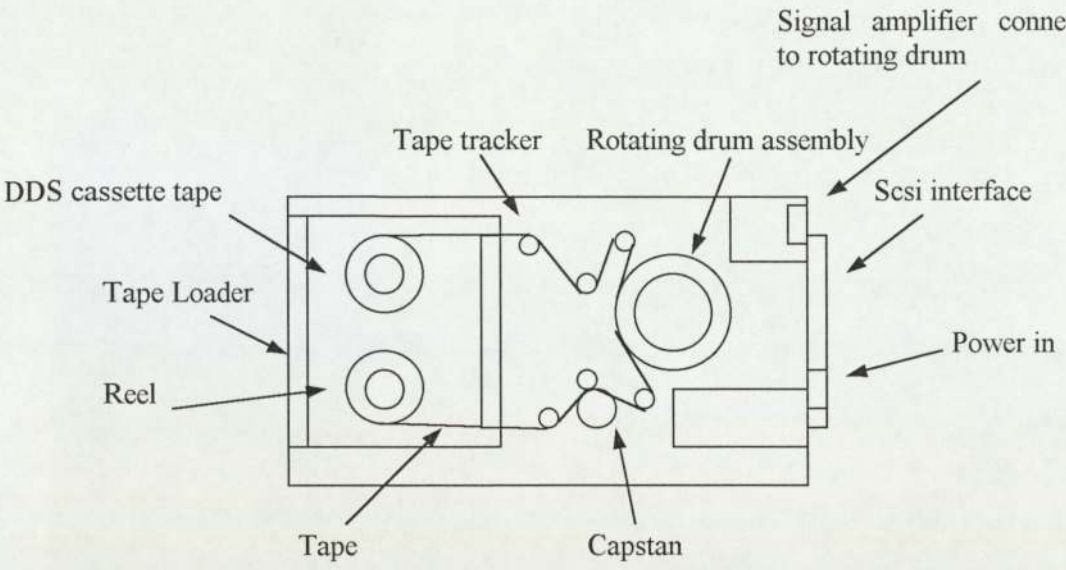

Figure 15 showing a schematic diagram of a DDS-2/DDS-3 tape drive

The DDS tape drive shown in figure 15 used in the following experiments was controlled via the SCSI interface cable and the HP Workstation as shown in figure 14. The main components of the DDS drive are as follows:

1) The signal amplifier circuitry amplifies the signal from the read heads of the rotating drum. An oscilloscope can be connected to the circuit so that you can measure the raw reading signal from the heads.

2) The rotating drum referred to as a helical scanner has four protruding heads-two read and two write each at 90 degrees to each other. A read head is a simple ferrite head shown in figure 8 and an write head is a metal-in-gap head as shown in figure 9. The drum rotates at around 5000 rpm.

3) The tape loader simply loads and unloads any DDS tape.

4) The capstan function is to forward the tape past the rotating drum at a constant speed. When the tape is set rewind or fast forward the capstan and tape pincher is released from the tape.

5) Tape trackers functions are to guide the tape and wrap the tape around the rotating drum when loading, and to remove the tape from the drum when the cassette was ejected.

Other essential equipment used in the project were X-ray Photoelectron Spectroscopy (XPS), Auger Electron Spectroscopy (AES) for the purpose of analysing the changes to the surface of the tape and inductive read heads respectively during head-tape contact. The ESCALAB VG ESCALAB 200D was used for XPS and AES analysis.

A Heraeus Votsch Environmental chamber was used to regulate the desired humidity and temperature. To obtain a range of temperatures and humidities the environmental chamber was operated was from 0 to 100°C and from 35 to 100% relative humidity (RH). For humidities less than 35%RH at 25°C, the humidity was regulated with a dry external air source, which was pumped from an air compressor through an air drier out into the chamber.

The Atomic Force Microscope (AFM), TopoMetrix Explorer was used to analyse the surface of the magnetic recording heads and various tape types as the tape was cycled at different environmental conditions. The surface measurements made with the AFM were scanned at resolutions of 400*400 with an area of $40*40\mu m^2$ to $100*100\mu m^2$ depending on the surface of the sample.

2.0.2 Unix software to operate the HP DDS tape drive

To control the tape drive via the Unix workstation i.e. in real-time, the software called 'smtc0' was run at the command box of the Unix system. This software allows the user to load/eject, forward and rewind a tape at various speeds depending on the tape format being used. The tape formats used are DDS-1, DDS-2 and DDS-3, which are first, second, and third generation tapes. The uncompressed data densities of these tape formats are 4 Gbytes, 8 Gbytes and 12 Gbytes respectively. At these formats, the tape drive changes the settings of the capstan, drum speed and tape tension using the calibration command 'h'. In DDS-3 format the tape speed was set at 10 mm/s and for DDS-2 the tape speed was 15 mm/s. At these tape speeds the drum speed remains the same. Normally these settings are set by manufacture by pre-storing the calibration information of the tape format in the EEPROM (Erasable Electronic Programmable Read Only Memory) of the tape drive.

To operate the Hewlett Packard HP tape drive remotely i.e. independently of the Unix workstation, a computer language called Manufacturing Test Control Language, MTCL was used by downloading a set of batch commands into the EEPROM of the drive. This language is a special set of instructions called firmware, which was used as a development tool for the engineer to test the drives mechanism and circuit board. Another function of

MTCL is to provide accurate fault information, so that with a minimum of effort the faulty components can be isolated and replaced.

These sets of instructions were used in the proceeding experiments to operate the drive with DDS tape at various settings, such as head/tape speed, and tape tensions mentioned earlier. Another useful feature of MTCL is that the error rate or the performance of the tape drive may be measured using the read-after-write (RAW) technology incorporated within the drive's electronics. This measurement consisted of counting the number of blocks of data, which were in error, when data is written to and read from the tape. A typical example of a set of MTCL instructions or batch commands referred to as a 'batch file' or a script is shown below.

```
SERVO_CMD (RESET)
SERVO_CMD (IGNORE_LURK)
SERVO_CMD (EJECT)
LDT    ONE25_METRE_TAPE
LED    RECOVERING
SERVO_CMD (CAPS_FWD_MID)  /* forwarding at *4 speed for 30 secs */
WAI    LONG_TIME_DELAY, 1
SERVO_CMD (EJECT)
SERVO_CMD (STOP)
 CAL
```

In this simple example, the script starts by resetting the electronics and ejecting any tape if loaded in the drive (line 1 to 3). Next, the script prompts the user for a tape by flashing a light at the front of the tape drive (line 4). The drive loads in the preferred tape, then forwards at times four speeds for 10 seconds (line 5 to 7). After 10 seconds, the tape stops and ejects. This is followed with the tape reloading which resets the tapes counter to zero. The final line calibrates the tape by altering the tape tension and drum-to-tape speeds, provided by the calibration information stored in the drive electronics. The commands shown in the mtcl script will be explained in more detail in a later section of this chapter.

When the script has been written the file needs to be compiled as a binary file, so that it can be downloaded into the tape drive. To compile and download the script into the tape drive, a program called 'XMDB' was executed at the command line under Unix. Before downloading, the dipswitches under the drive are set to a configuration of: switch 4 is set to off, and the rest of the other switches are set to on. This is shown in figure 16. In addition, the address of the tape drive is set to 42, so that the XMDB can communicate with the tape drive.

Its good practice to flush out the previous mtcl script stored in the EEPROM of the drive, before the new mtcl script is downloaded.

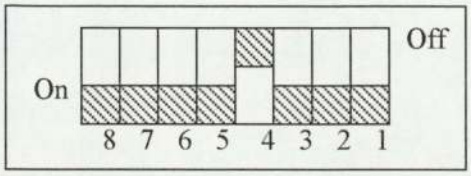

Figure 16 showing the dipswitch configuration for downloading an mtcl script into the DDS tape drive

When the mtcl script was loaded into the drive, a message was reported in the window of XMDB saying that the script has been loaded into the drive, ready to reboot. To reboot, the dipswitches are now set to this configuration: switch 8 is off and the rest (switch 7 to 1) is set to on. This was followed with the powering up of the drive. In this configuration, the drive with the downloaded mtcl script was then run independently of the workstation, so that the drive could be transferred to the environmental chamber together with its own power supply. To extract the RAW error rates stored in the drive after an experiment, the dip-switches was set as follows: switch 8 was set to on and 4 was off. The data can now be extracted from the tape drive via the program 'XMDB'. The error rate ER data was then copied over to the workstation as a 'filename.res'. Where the syntax 'filename' is the name given to the file used to store the data. The extracted data was viewed as two columns, the first column is Positive Channel and the second column is the Negative Channel.

2.0.3 Manufacturing Test Code Language (MTCL) programming

In this section, the reader will be introduced to the basic structure of an mtcl script and the most commonly used commands. The basic structure of an mtcl script shown in figure 17 consists of three main sections. Firstly, the script declares all the variables, constants and header files, then resets the tape drive electronics, and if there was a tape already loaded the drive ejects the tape.

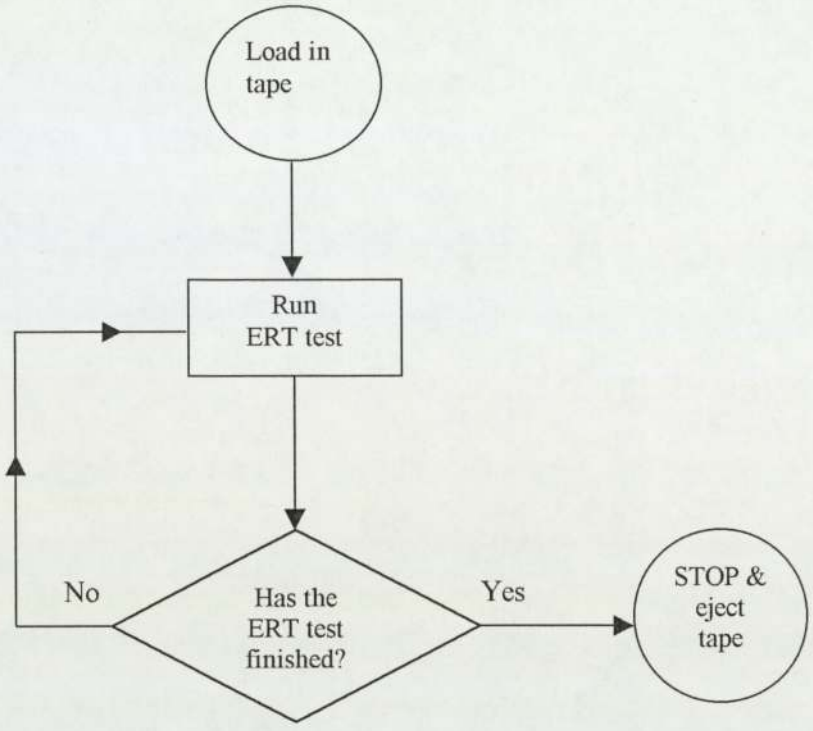

Figure 17 showing the basic structure of an mtcl script

This is normally written at the start of the script. The second section of the diagram is the main body of the script composing of the batch commands such as forwarding/rewinding the tape at various speeds, pausing, stopping, and error rate testing ERT. Finally, when all the batch commands have been completed in the main body of the script, the script stops and ejects the tape. However, if there are any operating errors within the drive, the tape is ejected and an orange light is indicated at the front of the drive.

The header files labelled 'filename.h' declared at the start of the script are programs (subroutines) written in mtcl. The main mtcl script then calls up these header files so the program could be executed. Without these header files the program 'XMDB, will not be able to compile the mtcl script. There are four main header files used by the script, which is described briefly below. All these files are shown in the appendix at the end of this thesis.

Servo.h is a set of macros to control the drive servo-mechanism such as load/eject tape, capstan control: forwarding/rewinding, pause, stop, rewinding etc;

Leds.h to define the led patterns on the front of the drive to give the programmer feedback on what the tape drive is doing at the present time;

Mtcl.h and Genmtcl.h are a set of standard mtcl parameters used by the main script. Such parameters are tape type, register names, error rate types like random, etc;

Turn_ffe_off.h is a set of commands, which turns off the error correction electronics that protects the end user from the uncorrected data errors. The reason for this is to give the programmer the true errors rate performance of the drive during the operation of reading and writing of data on the magnetic tape.

An example using the above header files are shown in the next page, starts by loading in a tape, then forwards at times 4 speed for 30 seconds, and an error rate test was performed. This example ends by the tape forwarding at times 4 speeds for 30 seconds.

```
LDT ONE25_METRE_TAPE
CAL
TURN_FFE_OFF

LED   WRITING
LOG   EVERYTHING
SRS
WER   DATA_RANDOM, START_HERE,FAIL_IF_EXCEED,WRITE_ERT_LENGTH,WRITE_ERT_LIMIT
SRS
LOG   ERRORS_ONLY

LED   RECOVERING
SERVO_CMD (CAPS_FWD_MID)
WAI   LONG_TIME_DELAY, 28

LOG   EVERYTHING
LED   WRITING
SRS
WER   DATA_RANDOM, START_HERE, FAIL_IF_EXCEED, WRITE_ERT_LENGTH, WRITE_ERT_LIMIT
SRS
LOG   ERRORS_ONLY
SERVO_CMD (EJECT)
```

To explain in more detail how this example works, the first command LDT asks the operator to load in a 125m (DDS-3) tape, where the parameter ONE25_METRE_TAPE is equal to 13 in hexadecimal and is written in the mtcl.h header file. When the tape was loaded, the tape was calibrated with the command CAL according to the tape format DDS-1, 2 and 3 used. Line 3, TURN_FFE_OFF disables the error correction electronics. Next in line, the LED's on the

front of the tape drive are set with the green light on saying that the drive is about to do a ERT. This line calls up the header file leds.h. The status of the servo is reported and stored in the drive.

The next line starts the error rate test ERT, using the command WER (write error rate test), which writes blocks/frames of data to the tape. There are five parameters associated with this command. The first parameter tells the drive to write random data to the tape. The second and fourth parameter tells the drive to start writing x number of frames of random data to the tape at a point on the tape. Note that the x number of frames is written as a hexadecimal, not a decimal number. The last parameter gives the limit of the frames to be written to the tape, which is written as FFFFh in hexadecimal. The number of frames and its limit are normally written at the start of the mtcl script, and are referred as constants. As the ER test are finished, the command SRS report and stores the status of the servo in the drive. The errors were logged and stored in the random access memory (RAM) of the drive, using the command LOG EVERYTHING. The LED's on the front of the drive changes from a green to yellow indicating the drive is recovering i.e. moving forward. Next, the servo command starts moving the tape at mid speed. A wait statement WAI is used to govern the period of which the tape moves forward. In this example, the period is for 20 minutes, where the last parameter of the WAI statement is given has 28 in hexadecimal. This last parameter is equivalent to 40 in decimal, so this equates to 40*30/60 = 20 minutes, when using 1 decimal unit = 30 seconds.

The next few lines repeat's the command WER for a further 3 minutes as mentioned early on in the mtcl script. Again, the errors are logged after a WER is completed. The final line simply ejects the tape, and then stops the tape drive.

All mtcl scripts written for the proceeding experiments will use these batch commands similar to ones shown in the example above, but there may be some variation depending on the type of experiment. A typical variation could be with repeating several times the WER batch command and rewind to the start of random data, so that the same section of the media was reused. At the very start of the proceeding staining experiments a selected number of DDS drives was subjected to a 'long reconditioning process'. An MTCL script was devised to perform this task.

2.0.4 The long reconditioning process

Initially, the heads of the H.P DDS-3 tape drives supplied by Hewlett Packard was re-profiled using virgin Fuji 125m (DDS-3)- F125 tape at environmental conditions of 25°C/80% relative humidity (RH) for 2 days. Virgin tape was used due to its high initial abrasivity, so the wear rates are at their highest. The whole of the tape was cycled for two days, so that the heads within the drum assembly were re-profiled according to the new tape settings such as virgin Fuji 125m (DDS-3)- F125. The reason for this was the requirement for the heads to be in a stable condition so that the error rate output of the drive was stable before each experiment. This type of head reprofiling was named as the 'long reconditioning process'.

The mtcl script, Long_recondDDS3.mtcl was developed for this process. The operation of the long reconditioning process is shown as a flow diagram in figure 18. The process started by loading in the F125 tape and calibrating. The tape was forwarded well away from the clear tape of the tape at a mid-speed for 10 seconds and the tape was reloaded, so that the tape counter was reset to zero.

Next, the first error rate lasting for 2 minutes (1.2m) or the equivalent of 2000 hex frames was written as random data. A green light was observed at the front the drive and the ER data was stored in the EEPROM of the drive. When this was completed, the drive continues to move the tape forward at normal speed for 65 minutes (39 m), and a green and yellow light was observed at the front the drive indicating the drive was recovering. The last two steps were then repeated another two times.

When the last two steps were completed, the tape was rewind to the start of the first error rate ER at high-speed lasting 15 minutes. When the tape had completed a forward cycle (lasting 3 hours) and rewound to the start of the first error rate, this was referred to as a 'pass' or a 'cycle'. All these steps except for loading in the tape were repeated for 16 cycles. After this, the tape was ejected after 2 days of experimentation. At this point, the ER data stored in the drive was downloaded into the UNIX workstation as described in section 2.0.2 of this chapter.

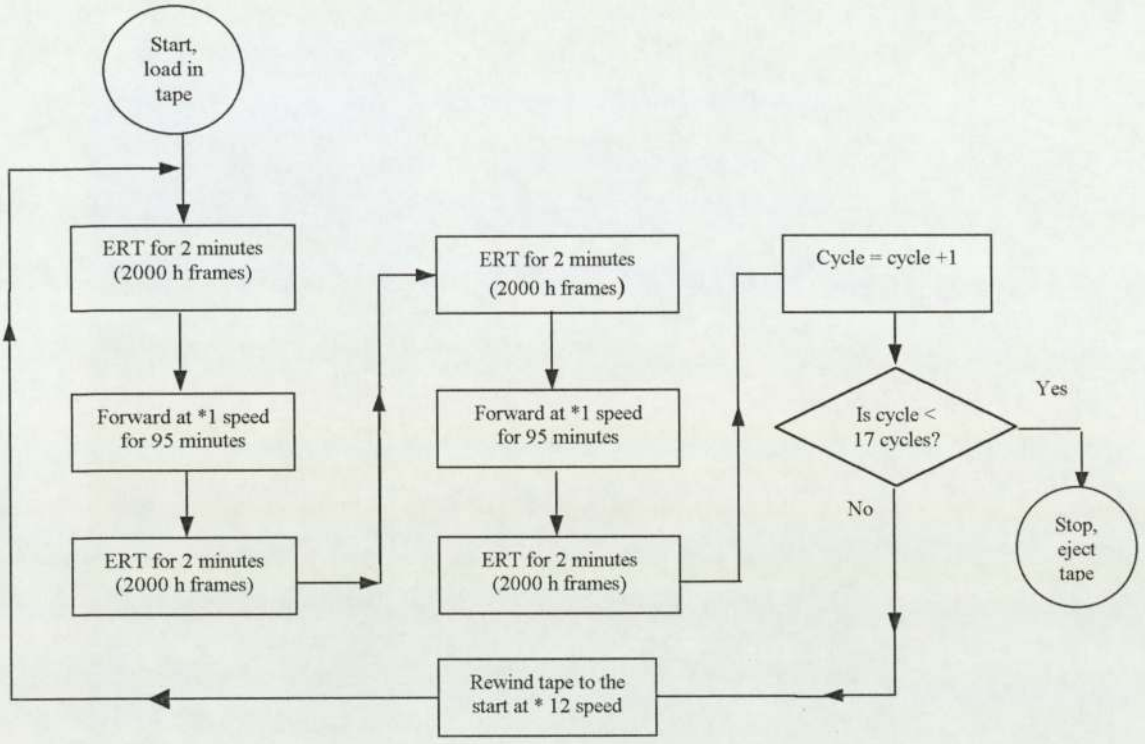

Figure 18 showing a flow diagram of the long reconditioning mtcl script. The increment counter: cycle was set to 0 at the start of the mtcl script

As mentioned early, the tape was forwarded for 10 seconds, so that first error rate testing is well away from the clear section of the tape. By doing this, experiments were conducted on the magnetic section of the tape not on the clear section. During forwarding, the media was in contact with the tape, resulting in a very slight change in the profile of the head and tape. To avoid this, the drum was removed from a discarded DDS-3 tape drive allowing the tape to forward at any speed without any head-tape contact. This was done before each experiment. To do this specific task, an mtcl forwarding script was written.

2.0.5 Tape forwarding script

The tape forwarding mtcl script is simple program, which loads in any tape, then calibrates the tape. Now the tape was forwarded at high speed for 10 seconds, and ejected. The script then goes back to the start in a continuous loop waiting for another tape to be loaded into the drive. Using the two scripts long reconditioning and forwarding the next stage of the project was the repeatability testing.

2.1 The Experimental Work

The aims of these experiments were to study how staining and its formation was effected by humidity and temperature, the length of tape used, tape type, tape cycling and head wear rate on the error rate of ten helical scan DDS-3 tape drives. Relationships of stain thickness and stain-to-ferrite separation with error rate and head wear rate was determined. AFM analysis of the heads was conducted at intervals of 1, 10, 100, 1000 and 5000 tape cycles and stain thickness/stain-to-ferrite measurements was made. AFM was also conducted on virgin and cycled to study the changes to the surface roughness of the tape. After each experiment Auger Electron Spectroscopy AES was conducted on cycled inductive read heads at 25°C/35%RH and 40°C/10%RH to determine what is stain and to confirm the presence of this stain on the surface of the inductive head. Before experimentation error rate repeatability testing was conducted on a number of tape drives to identify the drives showing consistent error rate.

2.1.1 Repeatability Error Rate Testing

Repeatability testing involved measuring three times, the error rate of the ten DDS-3 tapes drives (labelled 1 to 10) and virgin DDS-3 (F125) tapes at 25°C/35%RH. Between each repeatability test lasting 36 hours, each drive was subjected to the long reconditioning process (explained in section 2.0.4) for 2 days at 25°C/80%RH. The reconditioning process was required so that the drives heads could be returned to it original state before each experiment. The error rate data extracted from the reconditioned drives was plotted. Before and after each experiment and reconditioning process, Atomic Force Microscopy AFM was performed on these inductive read heads to study the changes in the surface topography.

A comparison of the three error rate data extracted from each drive was required to determine whether the error rate data from the following drives error rate could be repeated. When the drives show stable and consistent error rates, these were selected for the next phase of the experiments.

The mtcl script developed for repeatability testing was similar to the long reconditioning script, except each cycle lasts for 15 minutes (9 m of tape). The basic layout of this script is shown in figure 19. The script starts by loading a virgin DDS-3 (F125). This was indicated as a flashing orange light at the front of the drive. Next, the tape was forwarded until it reaches a point on the tape where there is no data. At this point, the tape was ejected and reloaded so that the tape counter was reset to zero. When the tape was reloaded, the tape

was calibrated according to the tape format used, and a logged error rate test lasting 2 minutes was executed. This was followed with a further two unlogged error rate lasting 13 minutes. The tape was rewound at normal speed to the start of the first error rate. When the total number of cycles equals 58 (or equivalent of 58 error rate), then the tape was ejected. When logging, the error rate is stored in the drives EEPROM.

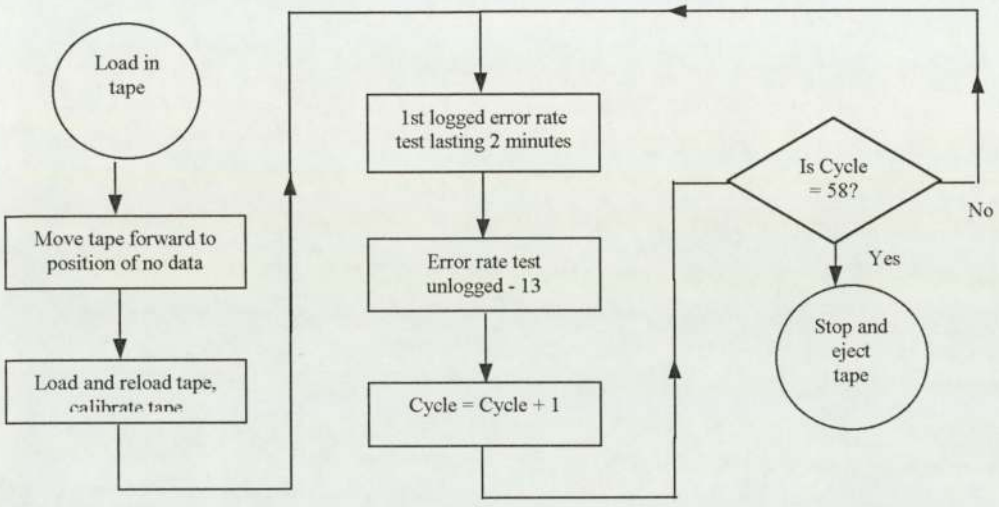

Figure 19 showing a flow diagram demonstrating the repeatability testing mtcl script. The increment counter: cycle was set to 0 at the start of the mtcl script.

Data from each drive was extracted with two error rate columns representing the positive channel and negative channel. Again, the DDS tape drives were subjected to the long reconditioning process as described earlier.

2.1.2 The Staining Experiments

The aims of the staining experiments presented were to study how staining and its formation was effected by humidity and temperature, the length of tape used, tape type, tape cycling and wear rates on the error rate of ten helical scan DDS-3 tape drives. Three environmental conditions were employed: 25°C/35%RH, 25°C/10%RH and 40°C/10%RH, and tape type used were DDS-2 (M120) and DDS-3 (M125) are manufactured by Maxell, and DDS-3 (F125) is manufactured by Fuji. Denotes: M120 and M125 are Maxell 120m and 125m tapes respectively and F125 is Fuji 125m tape. DDS-2 and DDS-3 are second and third generation tapes with a data capacity of 4 and 12 Gbytes uncompressed respectively. AFM was used to measure the stain thickness and stain-to-ferrite separation at tape intervals 1, 10, 100, 1000 and 5000 tape cycles and the error rate measurements were conducted.

Initially a short experiment was conducted at 25°C/35%RH to study whether staining occurs after a few short tape cycles. Virgin DDS-2 (M120) tape was cycled four times and AFM scans were performed at intervals of 2 and 4 cycles and any stain found the thickness was measured. AES was conducted on the inductive read heads after the forth cycle to establish whether there were any stain deposited on the head.

2.1.2.1 The Initial Staining Experiments at 25°C/35%RH

These experiments involved cycling virgin DDS-2 (M120) tape for 4 cycles at 25°C/35%RH, where 1 cycle = 20 seconds (0.3 m of tape). Contact Atomic Force Microscopy AFM was used to analyse the surface topography of the inductive read head after reconditioning, 2 and 4 tape cycles.

2.1.2.1.1 AFM scans and surface analysis

The AFM scans of a reconditioned positive inductive read head was used as a comparison to the AFM scans at 2 and 4 cycles of DDS-2 (M120) tape. The head was scanned at locations around the gap and glass region as shown in figure 20. The size of AFM scan was performed at 41 μm^2 with a resolution of 400.

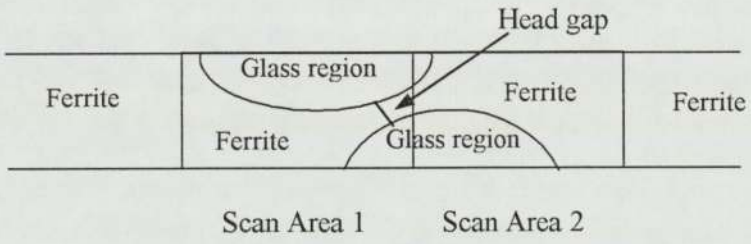

Figure 20 showing locations of the AFM area scans along an inductive read head.

Using these AFM scans the stain thickness and stain-to-ferrite measurements were conducted as follows using this technique.

2.1.2.1.1.1 Stain thickness and stain-to-ferrite separation measurements

To measure the stain thickness an average value was calculated from the difference between the maximum height and the base of all of the possible stain. To do this, the AFM image of the head was "second ordered levelled" to remove any curvature. The processed AFM image was then smoothed and analysed using lines transposed on top of the 2-D AFM

image (x-y plane) as shown in figure 21(a). Along the line scan heights P were selected at the base and maximum height of the stain as shown in the example of figure 21(b) and the difference h between the two results (P3, P8) is the thickness of the stain. Using similar results the average stain thickness can be calculated for X number of tape cycles.

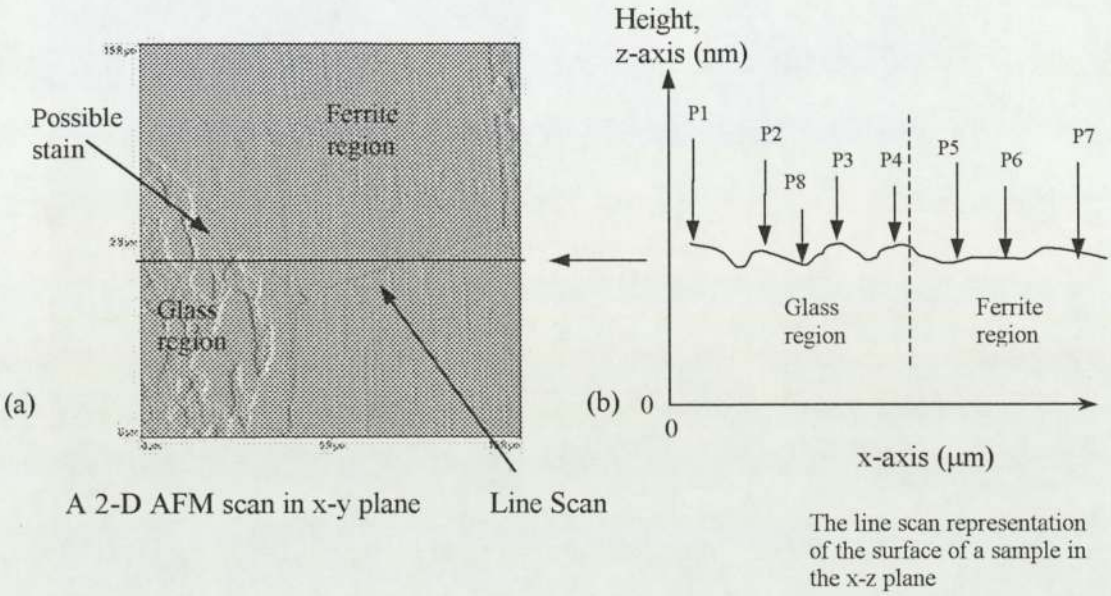

Figure 21(a) and (b) showing an AFM example and the corresponding line scan used in AFM analysis. Figure 21(a) shows possible stain on both the ferrite and glass region after several tape cycles of DDS-2 (M120) tape at 40°C/110%RH. Figure 21(b) shows a series of points P1 to P8 along the line, which represents various heights measured in nanometers (nm). Several points such as P5 to P7 at the ferrite region were used to measure an average height of the ferrite, which was referred to as a reference point for measuring the stain-to-ferrite separation. The stain-ferrite separation is the difference between the height of the stain on the ferrite and/or glass region and the height of the reference point at the ferrite region. This overall stain-to-ferrite separation was correlated with the changes in the error rate per tape cycle.

To measure the stain-to-ferrite separation after X tape cycles, the average reference point on the ferrite region was calculated by measuring a series of heights along the z-axis at points P5 to P7 in the example shown in figure 21. The line was then moved up and down the AFM image and further height measurements on the ferrite were recorded. An average reference point was calculated and used to determine whether stain was protruding above the ferrite or below. Furthermore the calculated stain-to-ferrite separation was correlated with the changes in the error rate after X number of tape cycles.

The height of the stain at the glass region and/or the ferrite of the head are measured at points P1, P2, P3 and P4, shown in the example in figure 21 and the average height of the stain was calculated. In this example figure 21, the average stain-to-ferrite separation H of the stain relative to an average reference point along the ferrite can be calculated as H = average

stain height at the glass and/or ferrite regions – average height of the ferrite region = ((P1+P2+P3)/4) – ((P4+P5+P6)/3). Thus the average stain-to-ferrite separation at the glass region is the average height of the stain at the glass region minus the average height of the ferrite region. This is similar to the stain-to-ferrite separation at the ferrite region, except the average height of the stain lies at the ferrite. This is also approximately equivalent to the stain thickness at the ferrite region. H<0 the stain is below the ferrite, whereas for H>0 the stain is protruding above the ferrite. Using this technique, the average stain-to-ferrite separation was calculated for 2 and 4 cycles of DDS-2 (M120) tape at 25°C/35%RH.

To confirm that stain was on the glass region of the inductive read head, the head was analysed using AES survey after a 4 tape cycles (1 cycle = 20 seconds) of DDS-2 (M120) tape at 25°C/35%RH. Again the AES survey of the elements detected and the corresponding relative percentage atomic concentrations [AT]% at these locations were measured and recorded.

Next, wide scans of all elements at the glass region of read head were performed and the elements were identified. As a comparison a reconditioned read head was compared with a cycled read head. The AES analysis was performed with a Fisons Instruments VG ESCALAB 200-D multi-techniques spectrometer which includes x-ray photoelectron spectroscopy XPS.

2.1.2.1.2 Auger Electron Spectroscopy (AES) survey of the surface of an inductive read head after reconditioning and cycling of DDS-2 (M120) tape at 25°C/35%RH

The two positive read heads cycled with the DDS-2 tape were carefully removed from the drum. Each head was then subjected to multi-point AES at locations along the surface of glass, gap, and ferrite regions as shown in figure 22, where ARHP and ARP1 experiments are the positive and negative read heads respectively, and P1 to P4 are the locations of the AES analysis. From AES survey scans the relative percentage atomic concentrations [AT]% of all the detected elements are recorded and averaged for each element. The locations of the points on the head are also included. Using this data, the etched positive reconditioned read head was used as a reference for future experiments.

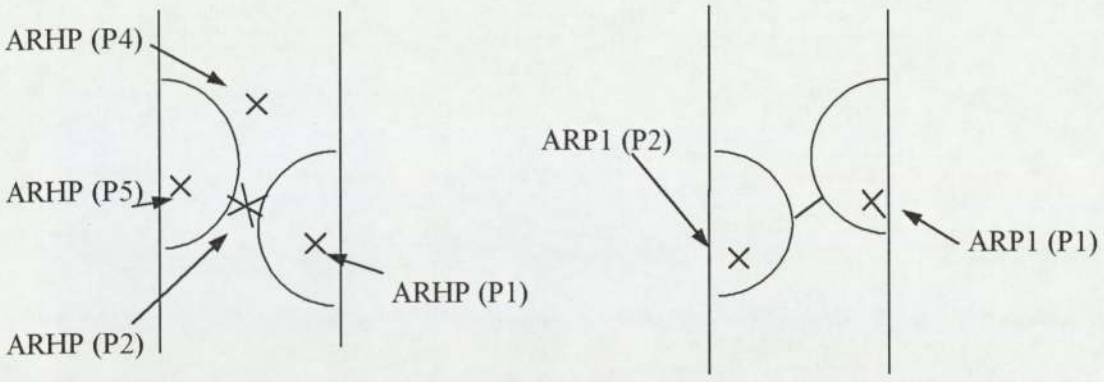

Figure 22 showing the locations of the AES survey along the inductive read head after 4 cycles of DDS-2 (M120) tape at 25°C/35%RH

The same process was repeated again for a reconditioned read head, which was used as a comparison to a cycled head. The drive was 'long reconditioned' and prepared for the next stage.

2.1.2.2 Main staining experiments at 25°C/35%RH, 40°C/10%RH and 25°C/10%RH

The purpose of these experiments was to study the effects of tape cycling; humidity and temperature (25°C/35%RH, 40°C/10%RH and 25°C/10%RH) and tape type interchange at 25°C/10%RH, head wear rate and tape surface roughness on head staining with error rate. A population of ten HP DDS-3 drives were used with tape type M120 at 25°C/35%RH and 40°C/10%RH, where the same length of M120 tape was cycled for 2 minutes (1.8m) in these experiments. And at 25°C/10%RH, 15 seconds (0.225m) of tape was cycled and there was a tape type interchanging of M120, F125, M125 and M120.

Before these experiments, ten DDS-3 drives were long reconditioned at 25°C/80%RH for 2 days cycling using virgin DDS-2 (M120) tape. Reconditioning was indicated by a stable read-after-write (RAW) error rate. The error rate is the measure of the number of frames of random data written and read back which are in error.

A drive was selected and a positive read head was scanned at two locations along the surface using contact Atomic Force Microscope (AFM). These locations shown in figure 23 show the gap, glass and ferrite regions of the inductive read head.

The positive inductive read heads of the reconditioned drives designated as 1, 6 and 7 were analysed with the AFM. Whereas, drive 8 was used for chemical analysis (XPS for the tape and AES for the head) and drive 3 was used for wear rate measurements. All these drives

were run simultaneously under the same environmental conditions using DDS-2 (M120) media. The drives were subjected to environmental conditions 25°C/35%RH, and 40°C/10%RH and the tape was run for 1, 10, 100, 1000 and 5000 tape cycles, where 1 cycle = 2 minutes (1.8m). The mtcl script sss.mtcl was modified according to the size of the cycle and number of cycles required.

2.1.2.2.1 Atomic Force Microscopy AFM analysis of stain thickness/stain-to-ferrite measurements at 25°C/35%RH and 40°C/10%RH

Initial these experiments started by running drives 1, 6, 7, and 8 at pseudo-ambient conditions 25°C/35%RH and DDS-2 (M120) tape was cycled 5000 times. After the first cycle of tape the first error rates results were collected from the four drives, and the positive inductive read heads were examined with AFM as described earlier. The average stain thickness was measured and calculated after 1 cycle of tape. This is described in section 2.1.2.1.1.1. Next, additional 9 cycles (10 cycles in total) were cycled against the inductive read heads of the four drives using the same length of tape. This was repeated for a further 100, 1000 and 5000 cycles of drives 1 and 7 were added together to give a total of 5000 cycles each. The average stain thickness on the positive read heads of drives 1, 6, and 7 at intervals of 1, 10, 100, 1000 and 5000 cycles were measured. After 5000 cycles the positive read from drive 8 was removed from the drum assembly and prepared for AES analysis.

After the previous environmental condition at 25°C/35%RH, the drives were reconditioned again at 80%RH/25°C for 2 days using the method outlined in the previous experiments. Seven drives were chosen for the proceeding experiments, three for AFM analysis, three for wear rate measurements, and the final one for AES/XPS analysis. The drives used for AFM analysis was labelled as 1, 6 and 7, whereas drives 2, 3 and 9 were used for wear rate measurements, and drive 5 for XPS/AES analysis (XPS of the tape and AES of the head). The positive read drive head of drive 5 was removed from the drum and prepared for AES analysis.

Initially drives 1, 6, 7 and 5 were run at intervals of 1, 10, 100, 1000 and 5000 cycles of tape at 40°C/10%RH using the modified sss.mtcl script and each cycle of tape was set to 2 minutes (1.8 m). The three drives labelled 2, 3 and 9 were used for measuring the wear rates at intervals of 100 and 1000 cycles using the equivalent mtcl script sss.mtcl. The drives positive inductive read heads were scanned by the AFM at intervals of 1, 10, 100, 1000 and 5000 cycles and the average stain-to-ferrite separation and stain thickness were measured at the glass and ferrite region as described in section 2.1.2.1.1.1. The positive read heads of

drives 1, 6 and 7 were scanned with the AFM at 7 locations along the inductive read head as shown in the figure 24 below. The numbers 1-7 represents the locations of the 55*55 μm^2 scan.

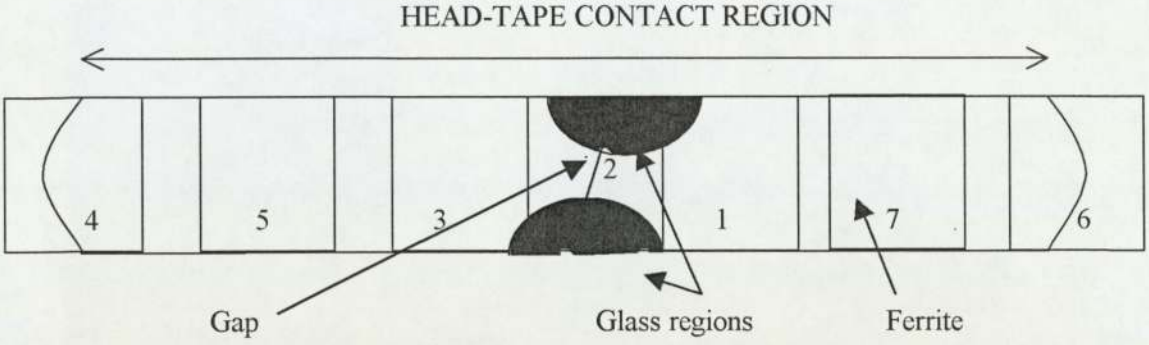

Figure 24 showing the locations of the AFM scans along the inductive read head.

2.1.2.2.2 Error rate measurements at 25°C/35%RH and 40°C/10%RH

The error rate measurements ware extracted from the drives at the same time as the drives read heads were analysed with the AFM as described in section 2.1.2.1.1.1. The error rates from 1 to 10, 10 to 100, 100 to 1000 and 1000 to 5000 cycles were added together and displayed for each of the designated drive. This was repeated for both conditions and virgin tape was used for each drive.

2.1.2.2.3 Head wear rate measurements using DDS-2 (M120) tape at 25°C/35%RH and 40°C/10%RH

At 25°C/35%RH and 40°C/10%RH the positive inductive read head of three drives were indented at the same locations along the head since most of the indents were removed during reconditioning. The head wear rate experiments were run simultaneously from 0 to 5000 cycles of M120 tape. The changes in length of the indents were measured and the wear rate (= change in depth of indent / length of tape cycled over the head) was calculated at intervals of 100, 1000 and 5000 tape cycles. When the three drives had completed 100 cycles, one tape was removed in order that the surface of the tape could be analysed by AFM. The remaining two drives were run for a further 900 cycles (1000 cycles in total) at which stage a second tape was removed for AFM/XPS analysis. Another tape was then removed from the two remaining drives in order to perform surface analysis. The remaining drive was allowed to continue cycling for a further 4000 cycles (5000 cycles in total).

A Knoop Micro-Hardness Indenter with a load of 25 grams force was used in these experiments. The shape of a Knoop indent is shown in figure 27. Before and after a tape run, the length of the indents were measured and the wear rates was calculated as the change in the depth of the indent per total amount of tape pulled over the head. The wear rate was calculated as $\Delta l/(30.1*L)$ as shown in section 2.1.2.2.3.1, where Δl is the change in the length of the indent, and L is the total length of tape cycles over the head. The experiment was repeated three times using virgin tape to obtain good repeatability. To calculate the error in these measurements an indent was re-measured several times and the averaged value together with a standard deviation of the measurements was calculated. The position along the surface of the head is indicated as either positive or negative relative to the gap, where the positive positions is referred to as the trailing edge and the negative positions is the leading edge. The leading edge of the head is a position where virgin tape has first contact with the surface of the head and the trailing edge is where the head is in contact with non-virgin tape. At the gap region of the head, the position is defined as zero.

Head A (inductive write head)

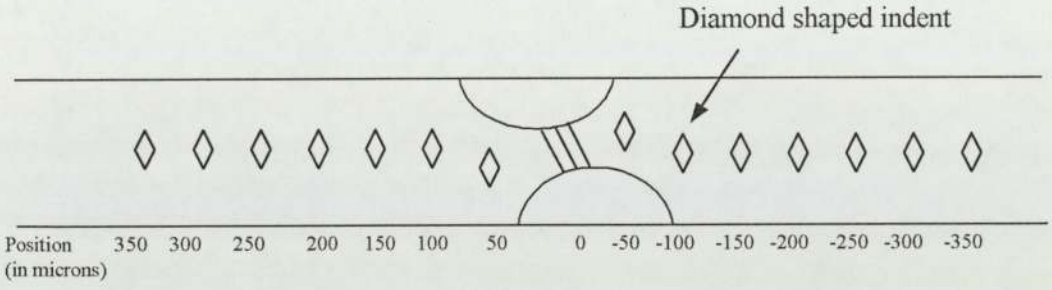

Figure 25 showing position of the indents along the inductive write read

Head B (inductive read head)

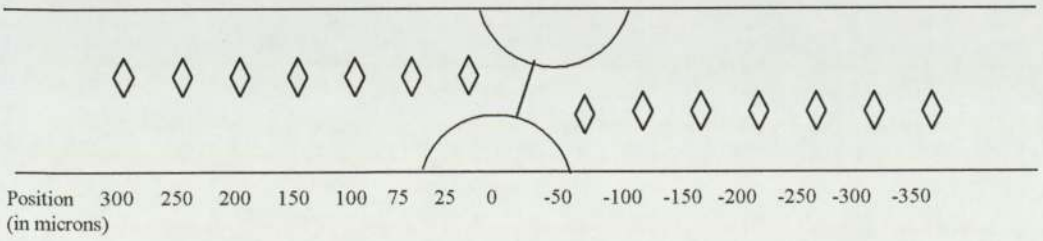

Figure 26 showing position of the indents along the inductive read head

2.1.2.2.3.1 Measuring and calculating head wear rate

When the triangular indent was made, the size of the indent (length l of the indent horizontally) was measured using the micrometers on the indenter as shown in figure 27. A record of the length of these indents was made. Before and after indenting, the drums were removed and placed carefully back into the tape drive using gloves, so that the drums/heads are not damaged and the chances of fingerprints on the drum/heads are reduced to a minimum.

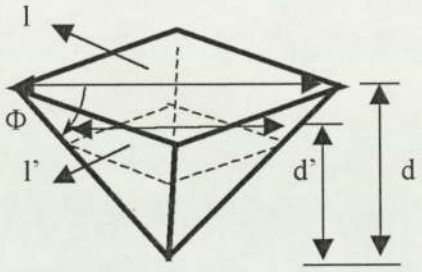

Figure 27 showing a Knoop diamond indent used in micro-indenting

After indenting and tape was passed over the heads for a set time, the drums are dismantled from the drive, and the new sizes l' of the indent are measured again. Another record can be made. The wear rate may be calculated from the knowledge of the calculated depth d of the indent before and after the tape has been run over the heads. The wear rate calculation is shown below:

Since, $\tan \Phi = d / l = 1/30.1$, and $\tan \Phi = d'/l'$, where d is the old depth and d' is the new depth of the indent.

Therefore, depth of indent $d = l / 30.1$ and $d' = l' / 30.1$
And change in depth of the indent is $\Delta d = d - d' = (l - l')/30.1 = \Delta l / 30.1$,

So, wear rate WR = change in depth of indent / total length of tape used

$$= \Delta l / (30.1 * L) \qquad (17)$$

The experimental errors are calculated from the average change in length of the indent Δl at the corresponding position X and the standard deviation of the average change in length of the indent Δl at position X / square root of the total number of drives used.

2.1.2.2.4 Surface roughness measurements and characteristics of virgin and cycled DDS-2 (M120) tape at 25°C/35%RH and 40°C/10%RH

In order to study the changes in the surface topography and roughness R_a (rms.) of DDS-2 (M120) tape before and after 5000 cycles at 25°C/35%RH and 40°C/10%RH and to determine whether there is a link between surface roughness and head wear rate. Three tapes from drives 1, 6 and 7 were analysed with Contact Atomic Force Microscope AFM. The scan was performed at angles of 0 and 270 degrees, where 0 degrees lies parallel to the plane of the tape and 270 degrees lies perpendicular to the plane of the tape. In addition, two area scans were conducted at 10*10 μm^2 and 100*100 μm^2.

At 40°C/10%RH, the M120 tape were again analysed with the AFM after 5000 cycles of tape using the tape from the previous wear rate experiments. The AFM scans of the tape were performed in two directions as in the previous surface roughness study.

An AFM scan of virgin DDS-2 (M120) tape was recorded at 10*10 μm^2 to identify any magnetic particles present at the surface of the tape including any other features or characteristics.

2.1.2.2.5 Auger Electron Spectroscopy AES survey analysis at the surface of an inductive read head after 5000 cycles of DDS-2 (M120) tape at 25°C/35%RH and 40°C/10%RH

Auger Electron Spectroscopy (AES) survey scan was conducted to determine the surface elements present and its relative atomic concentrations [AT]% at the glass and ferrite regions along an inductive read head after 5000 cycles of DDS-2 (M120) tape at 25°C/35%RH and 40°C/10%RH, where 1 cycle = 2 minutes (1.8m) and to the identify the presence of stain on the heads.

Before AES analysis the surface of the head was etched with Argon gas to reduce surface contamination such as carbon. Six random AES area analysis along the ferrite and glass regions (3 scans for each region) were performed so that an average atomic concentration present on the head can be calculated. AES survey of a reconditioned head are include as comparison to the heads after tape cycling at 25°C/35%RH and 40°C/10%RH. For tape reconditioning refer to section 2.0.4.

2.1.2.2.6 X-ray Photoelectron Spectroscopy XPS survey of virgin DDS tape

The purpose of performing XPS survey of virgin DDS tape was to analyse the composition, measured in relative percentage atomic concentrations [AT%] of the surface of virgin tape. The analysis also includes the identification and composition of the elements present in the binder, which also includes identifying the lubricant, the magnetic particles and the head-cleaning agent (HCA). The surface of the DDS tape was bombarded with an Mg K_α X-ray source.

Three tape types was used, these were DDS-2 (M120), and DDS-3 (M125 and F125) tapes, where M120 is 120 m Maxell tape, M125 is 125 m Maxell tape and F125 is 125m Fuji tape. DDS-3 (M125 and F125) tapes were used as a comparison to the main tape DDS-2 (M120). X-rays was targeted at the surface of the sample then the emitted photoelectrons were collected at 0° take-off angle (TOA) and 70° TOA to the normal to the surface of the sample. The normal is imaginary line, which is perpendicular to the surface of the sample and where all take off angles were measured. Several locations along the tapes surface were used to calculate the average relative percentage atomic concentrations [AT]%.

2.1.2.2.7 The stain thickness versus error rate with DDS tape type interchange at 25°C/10%RH

The aim of these experiments was to determine the relationship between stain thickness and error rate with the effects of tape type interchanging at low humidity/temperature: 25°C/10%RH using 10 seconds (0.18 m) of DDS tape.

An mtcl script called sss.*mtcl* was written and a block flow diagram of the script used is shown in figure 28. The script starts by loading DDS-2 (M120) or DDS-3 (F125) tape, then calibrated (where tape calibration adjusts the head-tape speed, tape tension and drum speeds) according to the tape type used. The tape was forwarded for 10 seconds (0.6 m) at mid-speed so that the first error rate starts well away from the beginning of the tape. The tape was ejected and reloaded so that the tapes counter is set to zero. Next, a 10-second (0.015 m) error rate was recorded or logged. The tape was rewound at high speed for 3 seconds to the start point, where the tape was loaded. The last two steps were repeated 40 times and the tape was ejected. The whole cycling process was repeated again for other tape types. In this script the error correction electronics was turned off, and an error rate measurement was logged every two cycles.

Before each batch of tape type interchanging experiments, the selected drives was subjected to a *short reconditioning* process, which simply removes any tape debris on the inductive read heads. The *short reconditioning* process is split into three parts: (1) load in tape and perform an error rate for 3 minutes at normal speed; (2) forward the tape at mid-speed (*4) for 20 minutes; and (3) another error rate for a further 3 minutes at normal speed then eject tape.

The first experiment includes operating eight tape drives at the similar environmental conditions of 25°C/10%RH as before with 10 seconds of tape cycled, but four tape types were used during interchanging DDS-2 (M120), DDS-3 (F125), DDS-3 (M125) and DDS-2 (M120) to study the effects error rate and stain build-up with tape interchanging. This test was repeated three times for the purpose of experimental repeatability. AFM scan and analysis was used to determine any stain present on the head and its thickness.

The second stage of experimentation included tape type interchanging at 25°C/10%RH, the mtcl script shown in figure 28 in the form of a flow diagram was further modified to use two tape types only: DDS-2 (M120) and DDS-3 (M125), instead of four-tape as in the previous experiment. This test was repeated three times for the purpose of repeatability. AFM scans and analysis of a read head was conducted after tape type interchanging to determine the stain thickness and any other surface features after two-tape type interchanging.

The final stage of experimentation includes one tape type interchange of DDS-3 (M125) tape and a total number of cycles was increased to 400, so that an error rate was logged every 10^{th} tape cycle instead every 2^{nd} tape cycle. Again, the chosen drives were subjected to the same environmental conditions of 25°C/10%RH. Between each stage, the drives were subjected to the short reconditioning process as explained earlier in this chapter and the AFM was used to measure the transfer layer thickness on the glass and ferrite regions of the inductive read head.

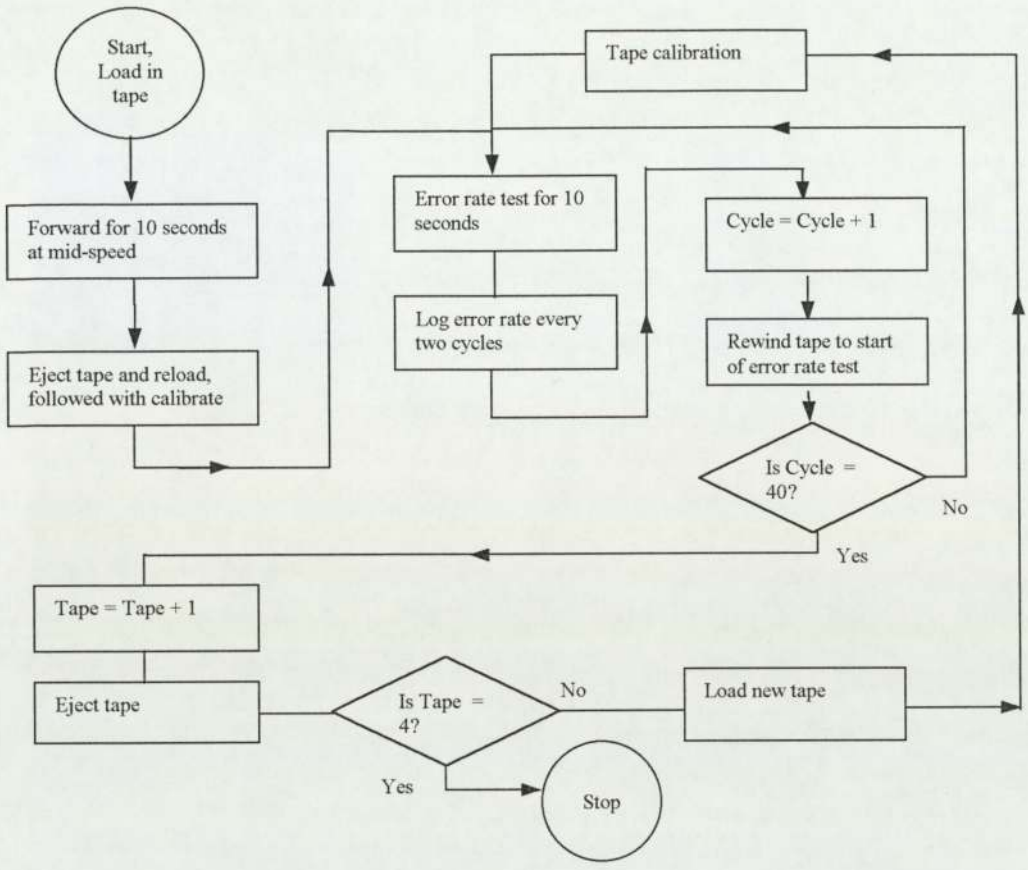

Figure 28 showing a flow diagram of a typical mtcl script (sss.mtcl) used in type tape interchanging at 25°C/10%RH. Cycle and tape are increment counters where for every tape cycle and tape type the counter is increased by one. At the start of the script the increment counters: cycle and tape was set 0.

Chapter 3 The Results

In this chapter, the results obtained from the experiments outlined in chapter 2 will be shown. The first set of experiments involved repeatability testing where a number of DDS-3 drives was tested for consistent error rate performance at a fixed temperature and humidity.

3.0 Repeatability Error Rate Testing

Presented below in figures 29 to 31 shows the three error rate curves versus number of tape cycles for one drive using DDS-3 (F125) tape under the same environmental condition of 25°C/35%RH, where each tape cycle lasts 15 minutes (9 m). The three error rate curves were compared with each other and a set of drives was chosen for the proceeding experiments. An average error rate was calculated between the positive and negative channel.

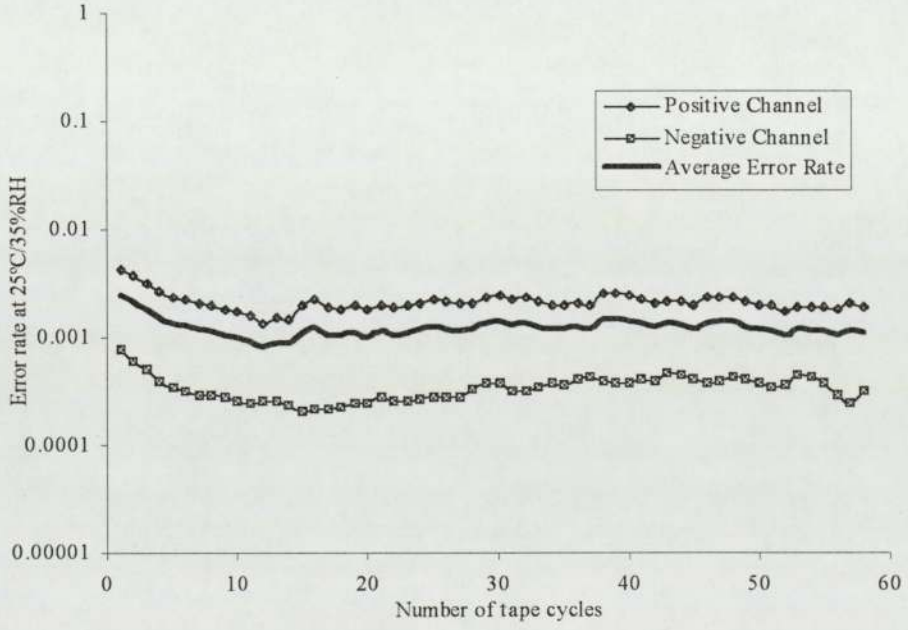

Figure 29 showing the error rate of the repeatability testing 1 of DDS-3 (F125) tape at 25°C/35%RH, (1 tape cycle = 15 minutes = 9 m).

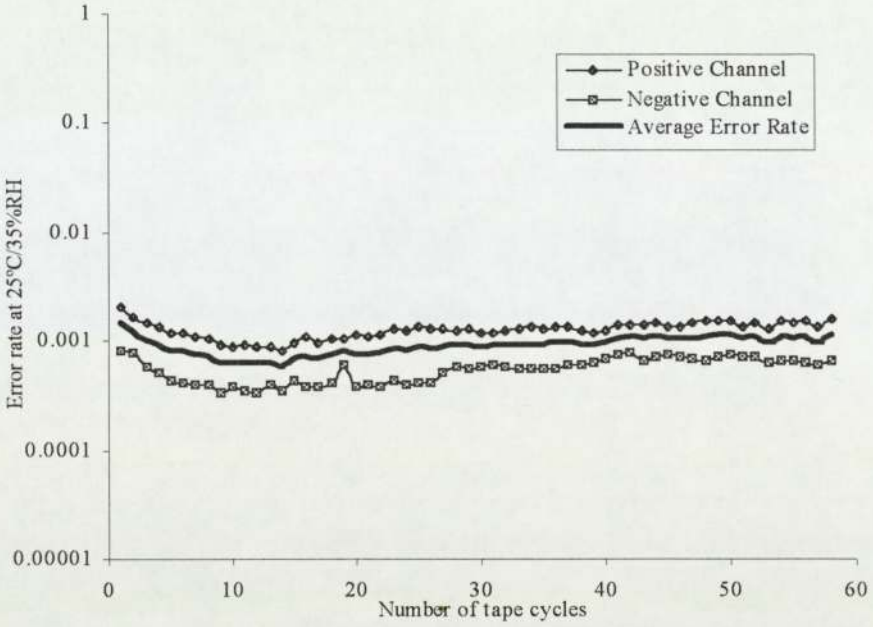

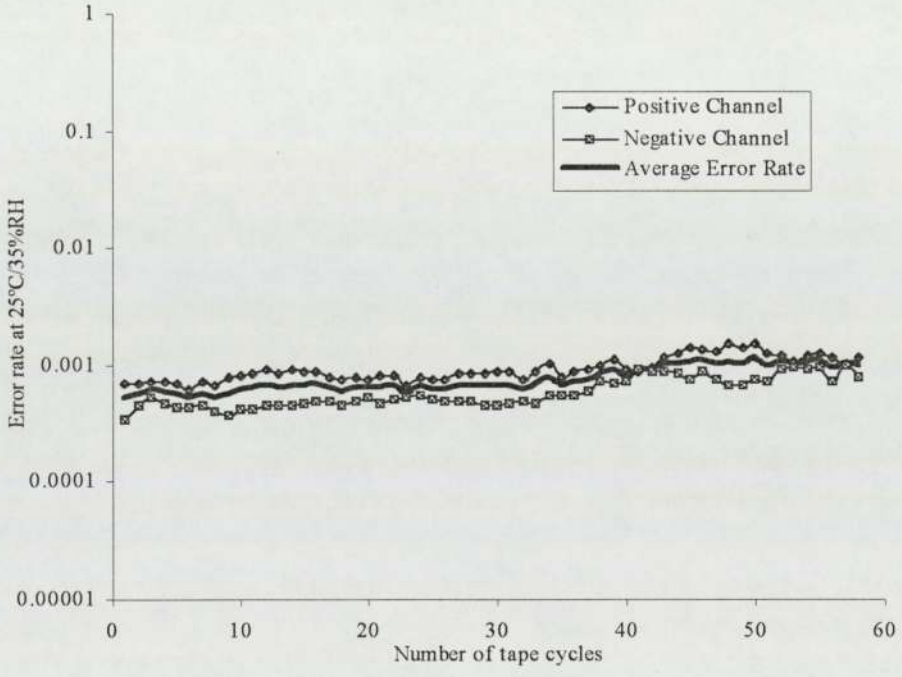

Figures 30 top and 31 bottom showing the repeatability testing 2 and 3 at 25°C/35%RH respectively using DDS-3 (F125) tape (1 tape cycle = 15 minutes = 9 m).

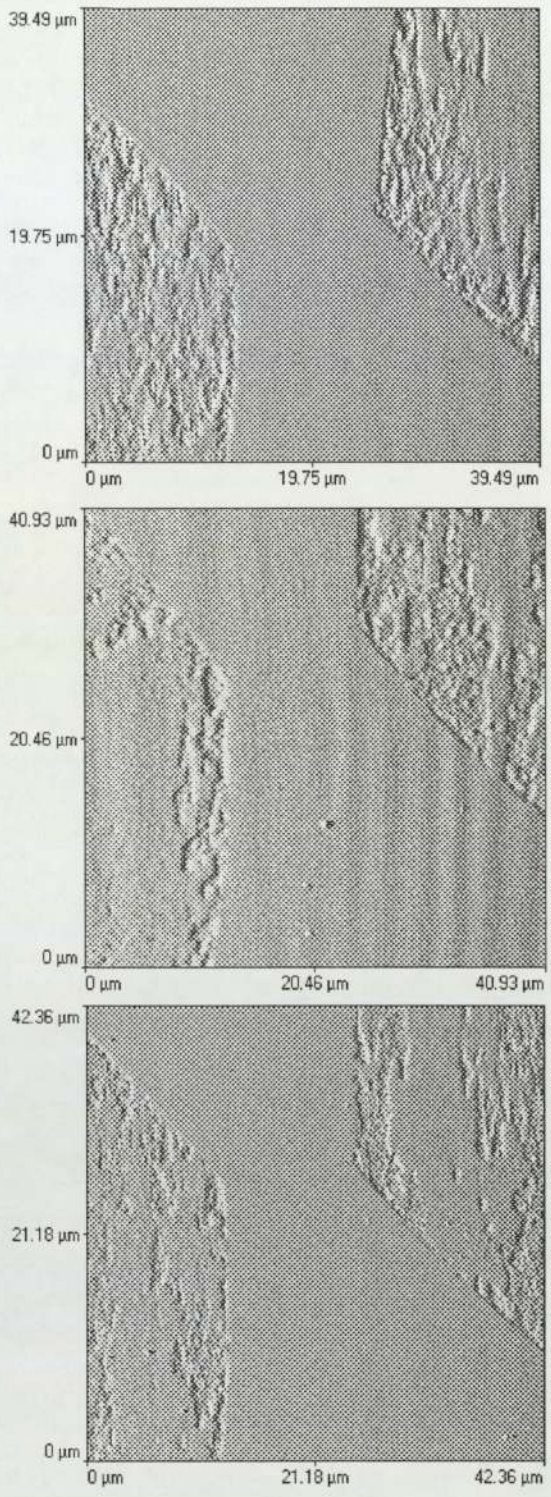

Figure 32 showing AFM scans after repeatability testing of three inductive read heads from a population of ten DDS-3 drives after cycling DDS-2 (M120) tape at 25°C/35%RH, (1 tape cycle = 15 minutes = 9 m). Any evidence of head curvature was removed by second order levelling before analysis.

Figures 29-31 show some degree of repeatability, especially tests 2 and 3, this was due to the successful reconditioning process that recovered the previous error rate start point.

AFM scans of the inductive read head taken after repeatability testing (1 to 3), figure 32, show large areas of possible stain on the glass region and fine abrasion marks on the ferrite region of the read head. The middle AFM scan also shows a vertical 'rippling effect' which is due to the stray AFM laser light reflected from the curved surface of the sample read head.

In the appendix a summary of error rate results of all the drives used during the repeatability testing are shown. The start and end error rate of each drive are used as a comparison, so that the drives, which exhibit good repeatability were chosen for the proceeding experiments.

3.1 The Initial Staining Experiments at 25°C/35%RH

These experiments involved cycling virgin DDS-2 (M120) tape for 4 cycles at 25°C/35%RH, where 1 cycle = 20 seconds (0.3 m of tape). After four cycles the error rate readings were extracted and plotted. Contact Atomic Force Microscopy AFM was used to analyse the surface topography of an inductive read head after 2 and 4 cycles.

3.1.1 AFM scans and surface analysis

The resulting AFM scans of an inductive read head are shown in figures 33, 34 and 35 together with the associated line scans. The AFM scans have shown no change in the surface characteristics as the tape was cycled from 0 to 4. Abrasion marks are evident on the glass region of the positive read head and on the ferrite region after reconditioning. At the gap region tape debris was observed after head reconditioning. The rippling effects evident in figure 35 were artefacts due to the stray laser light reflecting from the surface of the read head. This can alter the results and affect the surface detail. AFM analysis revealed abrasion marks on the glass region probably due to the Head Cleaning Agent (HCA) within the tape

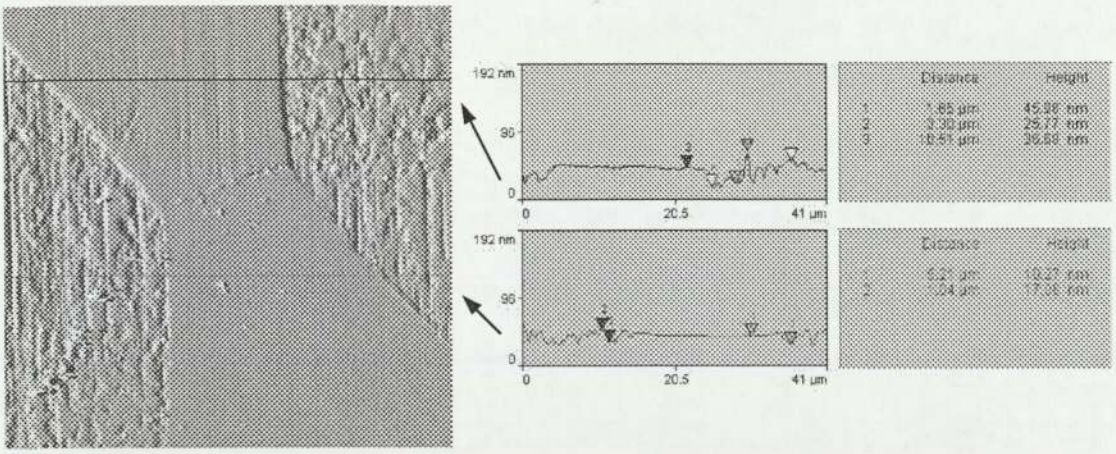

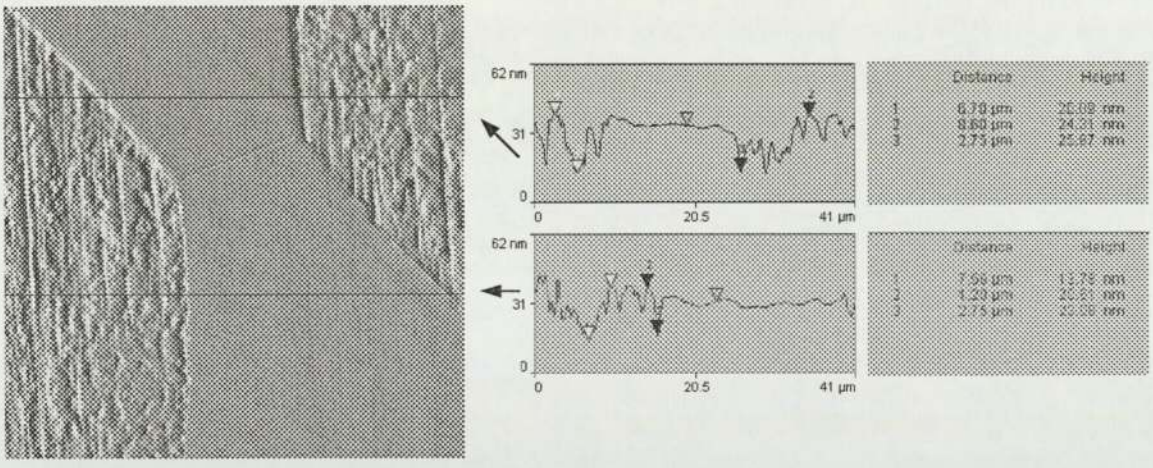

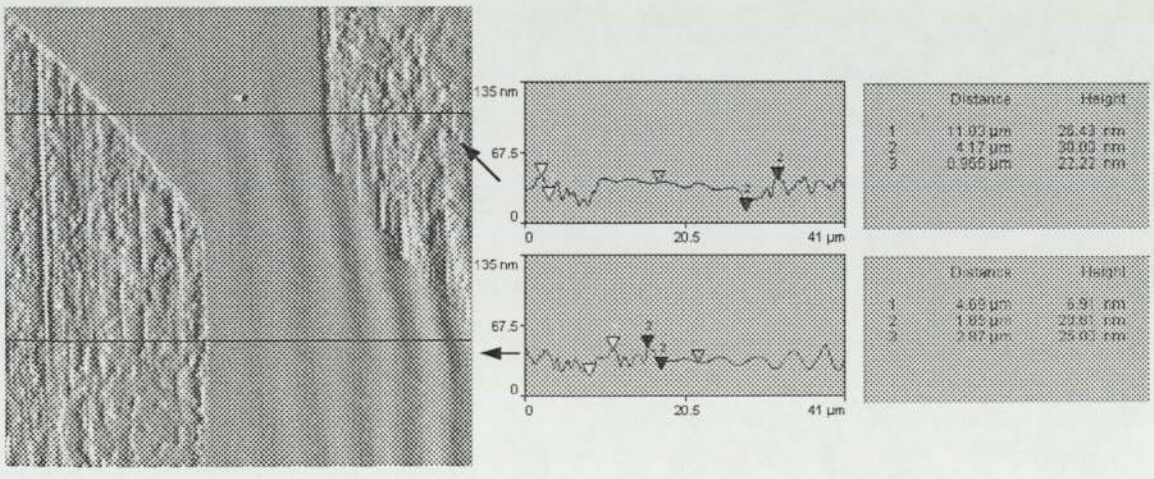

Figures 33, 34 and 35 showing from the top to the bottom AFM scans of an inductive read head after reconditioning, 2 cycles and 4 tape cycles respectively of DDS-2 (M120) tape at 25°C/35%RH, (1tape cycle = 20 seconds = 0.3 m). Any evidence of head curvature was removed by second order levelling before AFM analysis.

3.1.1.1 Stain-to-ferrite separation and average stain thickness at 25°C/35%RH

Referring to figures 33, 34 and 35, the line scans of an inductive read head have showed that after reconditioning the glass-to-ferrite separation at the glass region relative to the ferrite was measured to be 7.51 +/-10% nm above the ferrite. After 2 and 4 cycles of DDS-2 (M120) tape, the stain-to-ferrite separation at the glass region decreased slightly from 7.86 +/- 10% nm to 7.15 +/- 10% nm. Tables 1 and 2 shows a summary of the stain-to-ferrite separation and average stain thickness versus number of tape cycles.

	Stain-to-ferrite separation (nm)	
Number of tape cycles	2	4
Average	7.87	7.15
Error	0.78	0.71

Table 1 showing stain-to-ferrite separation of an inductive read head versus number of tape cycles of DDS-2 (M120) tape at 25°C/35%RH, (1tape cycle = 20 seconds = 0.3 m).

	verage thickness of tain on the glass region f an inductive read head (nm)	
umber of tape cycles	2	4
verage thickness.	27.19	24.44
rror	1.14	2.01

Table 2 showing average stain thickness at the glass region of an inductive read head after cycling DDS-2 (M120) tape at 25°C/35%RH, (1tape cycle = 20 seconds = 0.3 m).

There was some correlation between the error rate, and stain-to-ferrite separation for 2 and 4 cycles of DDS-2 (M120) tape at 25°C/35%RH, but further investigations are required to determine the relationship between error rates, stain-to-ferrite separation and stain thickness beyond 4 tape cycles.

3.1.2 Auger Electron Spectroscopy (AES) survey at the surface of an inductive read head after reconditioning and cycling DDS-2 (M120) tape at 25°C/35%RH

Tables 3 and 4 show AES survey of point analysis results of the elements detected and the percentage atomic concentration at the surface of a reconditioned inductive read head and after cycling of DDS-2 (M120) tape. The AES percentage atomic concentration data together with the positions along the reconditioned read head are shown in table 3 and figure 36 respectively. Whereas, table 4 and figure 37 shows the average percentage atomic concentrations and locations of the AES points along the inductive read head respectively after 4 cycles of DDS-2 (M120) tape at 25°C/35%RH.

		AES survey results of elements detected and the atomic percentage concentration [AT]% at the surface of a reconditioned inductive read head from point analysis			
Scan region	Position	C KL1	O KL1	Fe LM2	Si LM1
Glass	P1		76.47		23.53
	P2		73.78		26.22
	P3		73.94		26.06
	P5		74.74		25.26
	P9		71.53		28.47
	P10		73.74		26.26
Average Concentration.		**0.00**	**74.03**	**0.00**	**25.97**
Ferrite	P4		33.83	66.17	
	P6	13.75	48.74	37.52	
	P7	17.39	46.82	35.86	
	P8	10.69	51.07	38.24	
	P11	12.16	47.28	40.56	
Average Concentration.		**13.50**	**45.55**	**43.67**	**0.00**

Table 3 showing the AES survey results of the average percentage atomic concentration [AT%] and elements present on reconditioned an inductive read head after etching. Average percentage atomic concentrations from the AES points shown were calculated for the elements C, O, Fe and Si at the glass and ferrite regions of the read head.

Silicon Si and oxygen O was present at the glass region in the form of SiO_x was expected, where subscript x of oxygen in unknown. Carbon C contamination was not present probably due to surface etching- the removal of surface contamination, prior to AES. On the other hand, the ferrite region showed abundance in oxygen O and iron Fe in the form of iron oxide Fe_3O_4 as expected, whereas carbon C contamination was still evident after etching.

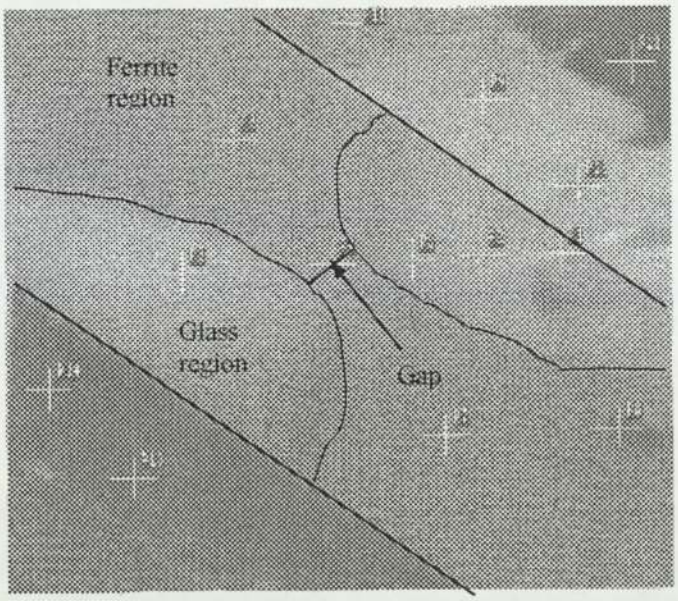

Figure 36 showing the AES points along the reconditioned inductive read head after etching with Argon.

		AES survey results of elements detected and the percentage atomic concentration [AT]% at the surface of an inductive read head after 4 cycles of DDS-2 (M120) tape			
Scan region	Position	C KL1	O KL1	Fe LM2	Si LM1
Glass	P1	58.40	24.50	9.50	7.20
	P3	No data			
	P5	24.50	48.50	14.80	12.30
Average Concentration.		**41.45**	**36.50**	**12.15**	**9.75**
Gap	P2		73.78		26.22
Average Concentration.		**0.00**	**73.78**	**0.00**	**26.22**
Ferrite	P4	53.50	19.70	26.50	
Average Concentration.		**53.50**	**19.70**	**26.50**	**0.00**
Glass	P1	31.10	53.20	5.70	9.70
	P2	36.00	43.00	5.90	14.30
Average Concentration.		**33.55**	**48.10**	**5.80**	**12.00**

Table 4 showing the AES survey results of the elements detected and the average percentage atomic concentrations [AT]% on an inductive read head after 4 cycles of DDS-2 (M120) tape at 25°C/35%RH, (1 tape cycle = 2 minutes = 1.8 m). Average atomic concentrations from the AES points shown were calculated for the elements detected at the glass and ferrite regions of the read head. No chlorine Cl was detected.

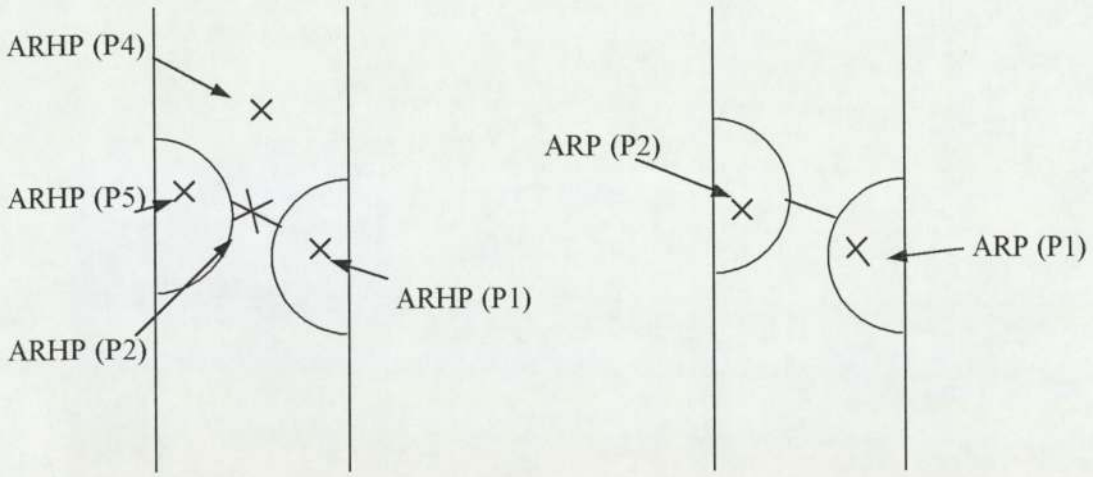

Figure 37 showing the location of the AES scans along an inductive read head after 4 cycles of DDS-2 (M120) tape at 25°C/35%RH, (1 tape cycle = 20 seconds = 0.30 m).

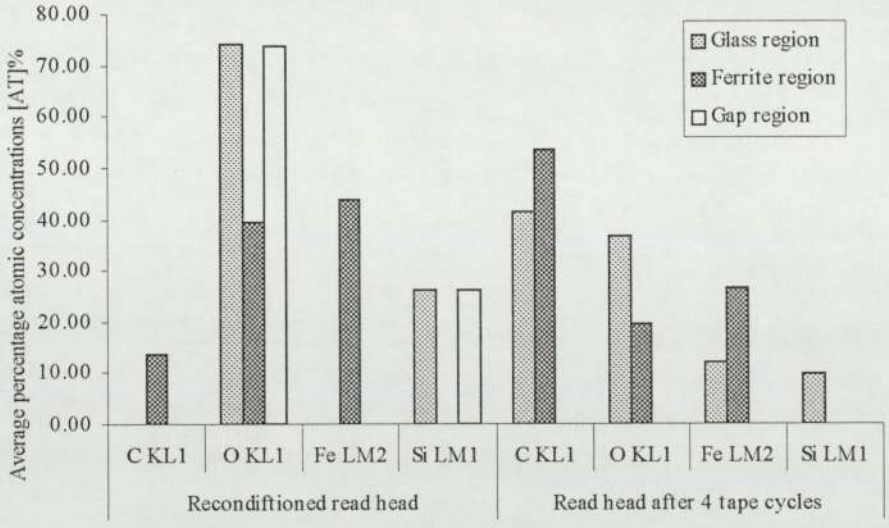

AES survey of elements detected at the ferrite, glass and gap regions of an inductive read head after reconditioning and tape cycling of DDS-2 (M120) tape at 25°C/35%RH

Figure 38 showing AES survey of elements detected at the ferrite, glass and gap regions of an inductive read head after reconditioning and tape cycling of DDS-2 (M120) tape at 25°C/35%RH.

These results show that staining (consisting mainly of iron Fe particles) was observed on the glass region of the read head after 4 tape cycles of DDS-2 (M120) tape even though 1.2m of tape was cycled, where 1 tape cycle = 20 seconds = 0.3 m of tape. Oxygen O and carbon C was detected everywhere along the head. Silicon Si was present on the glass region, since glass is in the form of silicon oxide SiO_2.

3.2 Main staining experiments at 25°C/35%RH, 40°C/10%RH and 25°C/10%RH

This section presents the results of the effects of the length of tape used, the number of tape cycles, humidity and temperature, wear rate and tape type interchanging on staining and error rate. Stain thickness and stain-to-ferrite separation are correlated with error rate as the tape was cycled, and AES was used to analyse the surface chemistry changes of the stain. Wear rate measurements are also shown to study the effects of head wear rate with staining as tape was cycled and to the changes to the humidity and temperature.

3.2.1 Atomic Force Microscopy AFM analysis with stain thickness/stain-to-ferrite measurements at 25°C/35%RH, 40°C/10%RH

Figures 39 through to 50 show AFM line scans of an inductive read head of one tape drive versus number of tape cycles at 25°C/35%RH, 40°C/10%RH.

3.2.1.1 Atomic Force Microscopy AFM scans of a read head at 25°C/35%RH

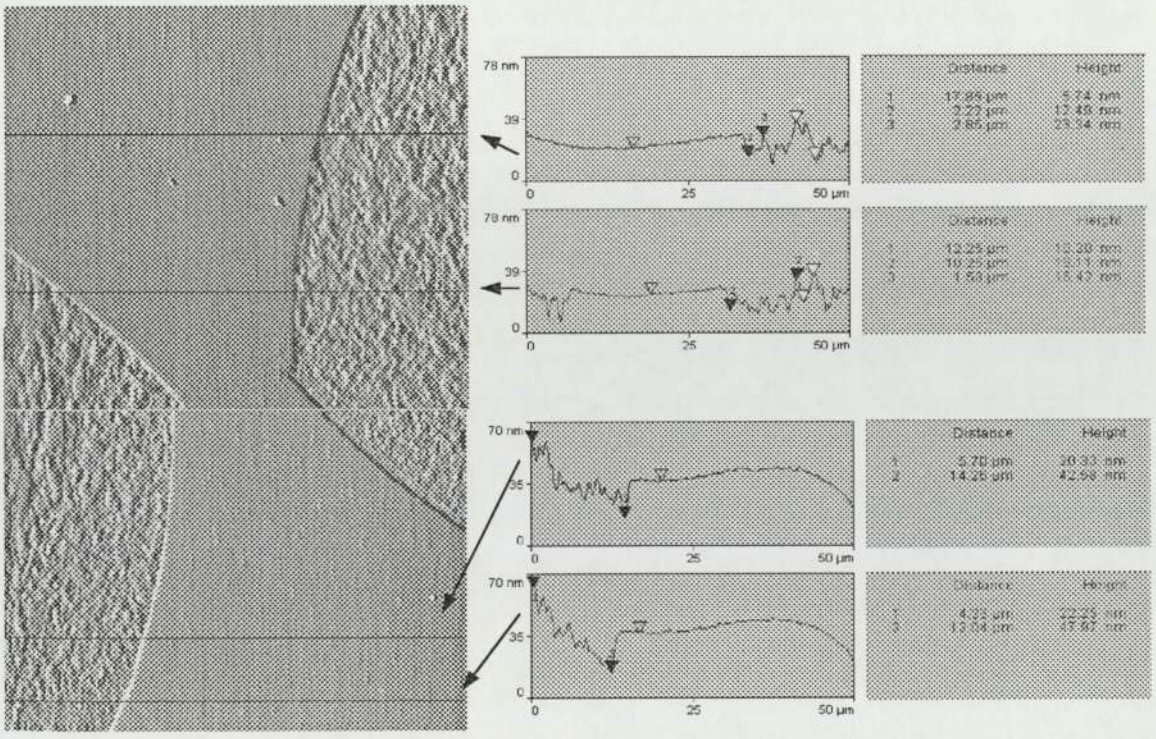

Figure 39 showing AFM scan and associated line scans of an inductive read head after reconditioning at 25°C/80%RH, (1 tape cycle = 2 minutes = 1.8 m). Any evidence of head curvature was removed by second order levelling before AFM analysis. As in this case second order levelling did not remove any curvature.

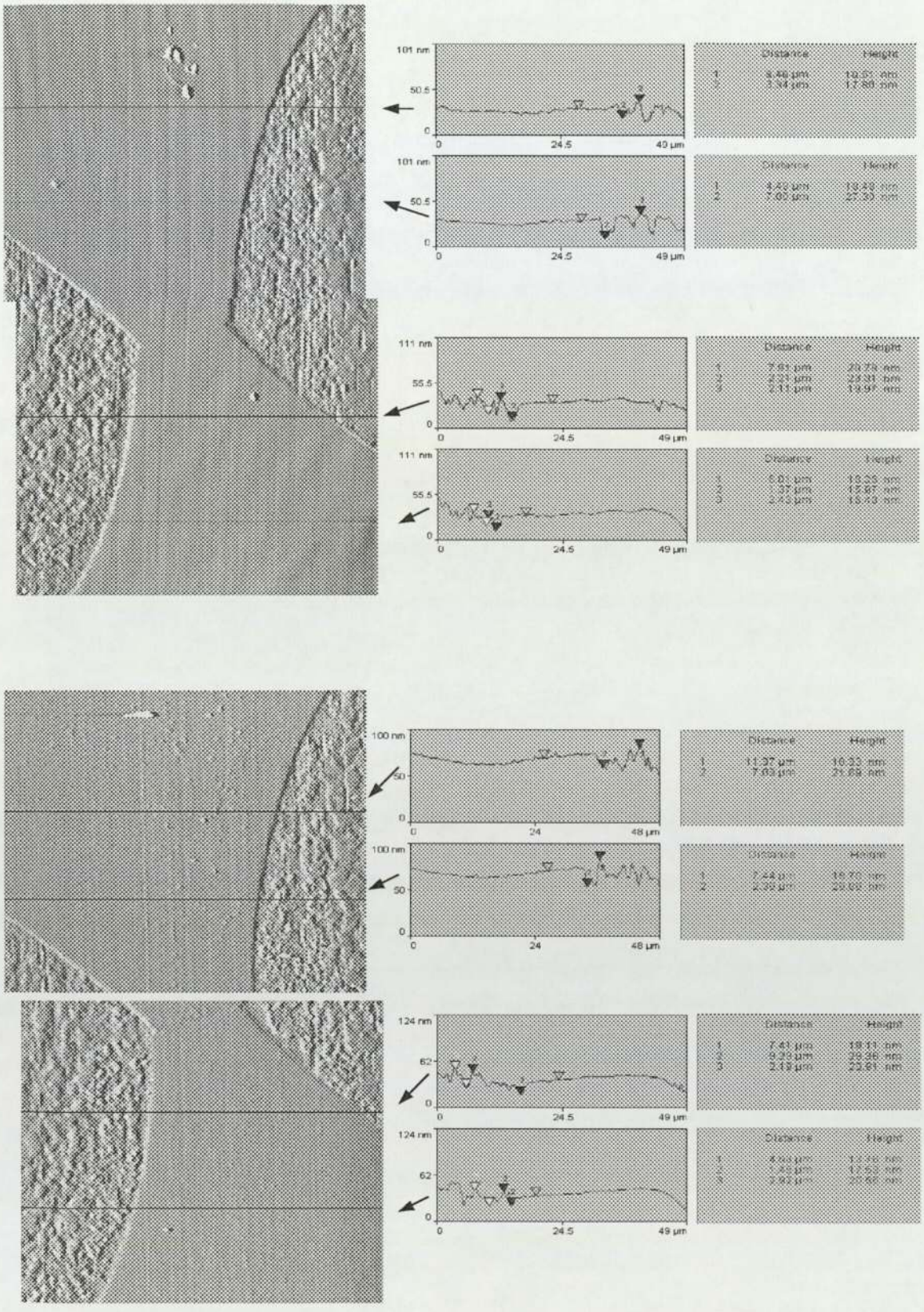

Figures 40 and 41 from top to bottom showing AFM scans and associated line scans an inductive read head after 1 and 10 tape cycles of DDS-2 (M120) tape respectively at 25°C/35%RH, (1 tape cycle = 2 minutes = 1.8 m). Any evidence of head curvature was removed by second order levelling before AFM analysis.

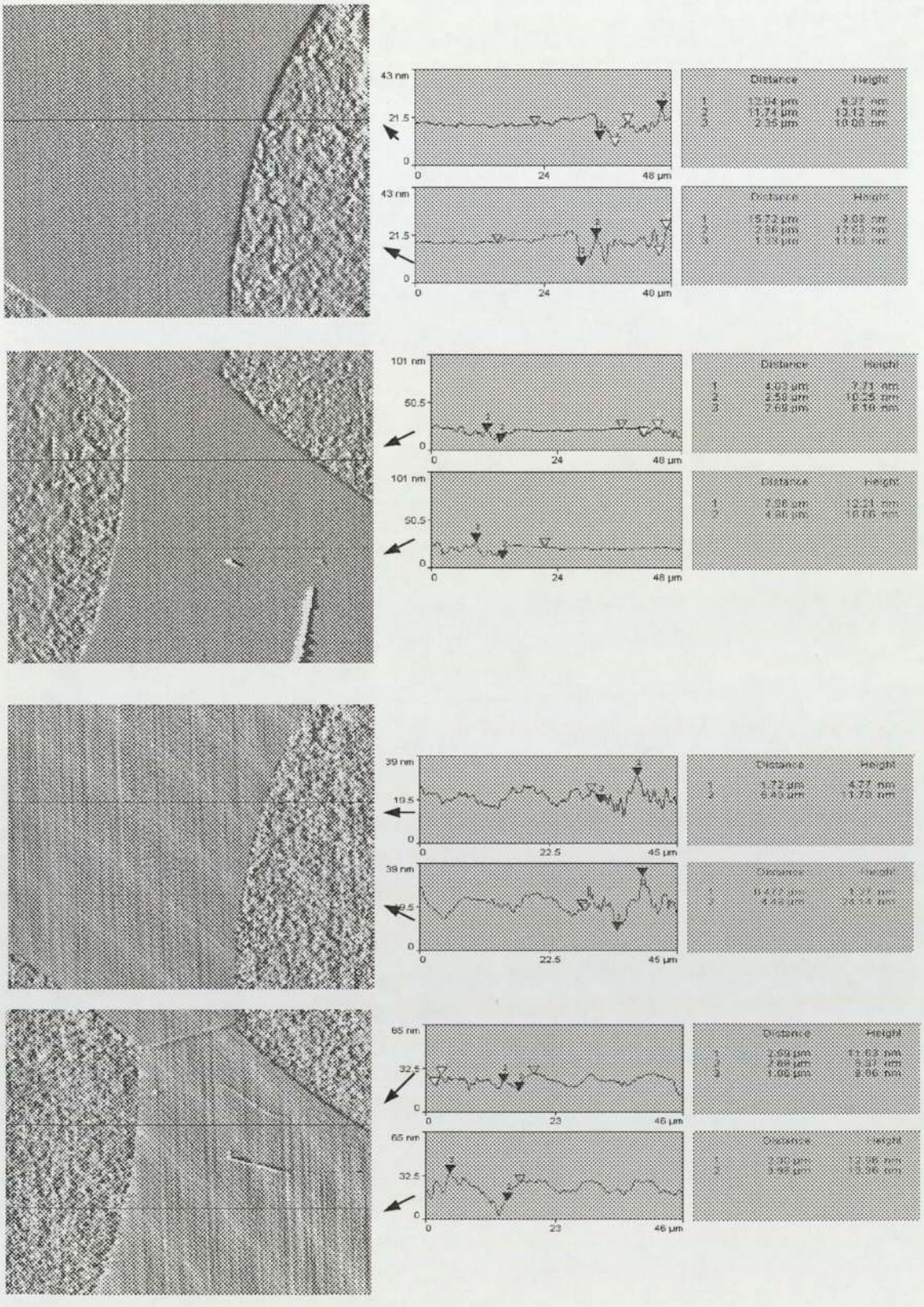

Figures 42 and 43 from the top to the bottom showing AFM scans and associated line scans an inductive read head after 100 and 1000 tape cycles of DDS-2 (M120) tape respectively at 25°C/35%RH, (1 tape cycle = 2 minutes = 1.8 m). Any evidence of head curvature was removed by second order levelling before AFM analysis.

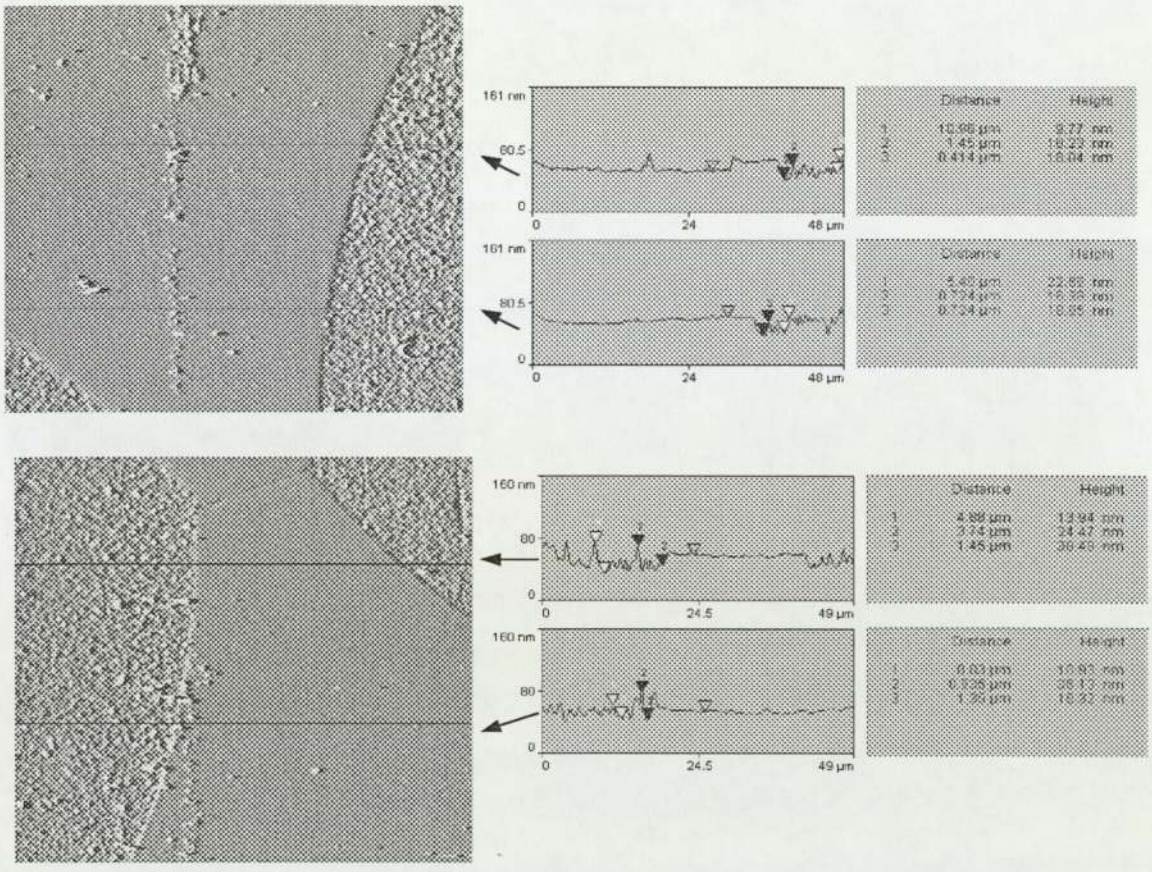

Figure 44 showing AFM scans and associated line scans of an inductive read head after 5000 tape cycles of DDS-2 (M120) tape respectively at 25°C/35%RH, (1 tape cycle = 2 minutes = 1.8 m). Any evidence of head curvature was removed by second order levelling before AFM analysis.

Initial examination of the AFM images figures 40 to 44 shows that at 25°C/35%RH, stain was identified on the glass regions of the head only as confirmed by the AES analysis shown later on in this section. Comparing figures 40 and 41, the glass region showed an increase in the stain coverage. After 10 cycles (figure 43), there was further evidence in the increase in the stain coverage at the glass region and patchy areas of stain were not observed at the ferrite region of the read head, although debris was present. After 1000 and 5000 cycles (figures 43 and 44) the structure of the stain on the glass region has changed from patchy deposits from 1 to 100 cycles (figures 40 to 42), to small particulate deposits and an increase in the areal coverage. At 25°C/35%RH, analysis of the heads revealed abrasion marks on the ferrite and initially there were only abrasion marks on the glass region. After a few cycles, the stain started to cover the glass region.

3.2.1.2 Atomic Force Microscopy AFM scans of a read head at 40°C/10%RH

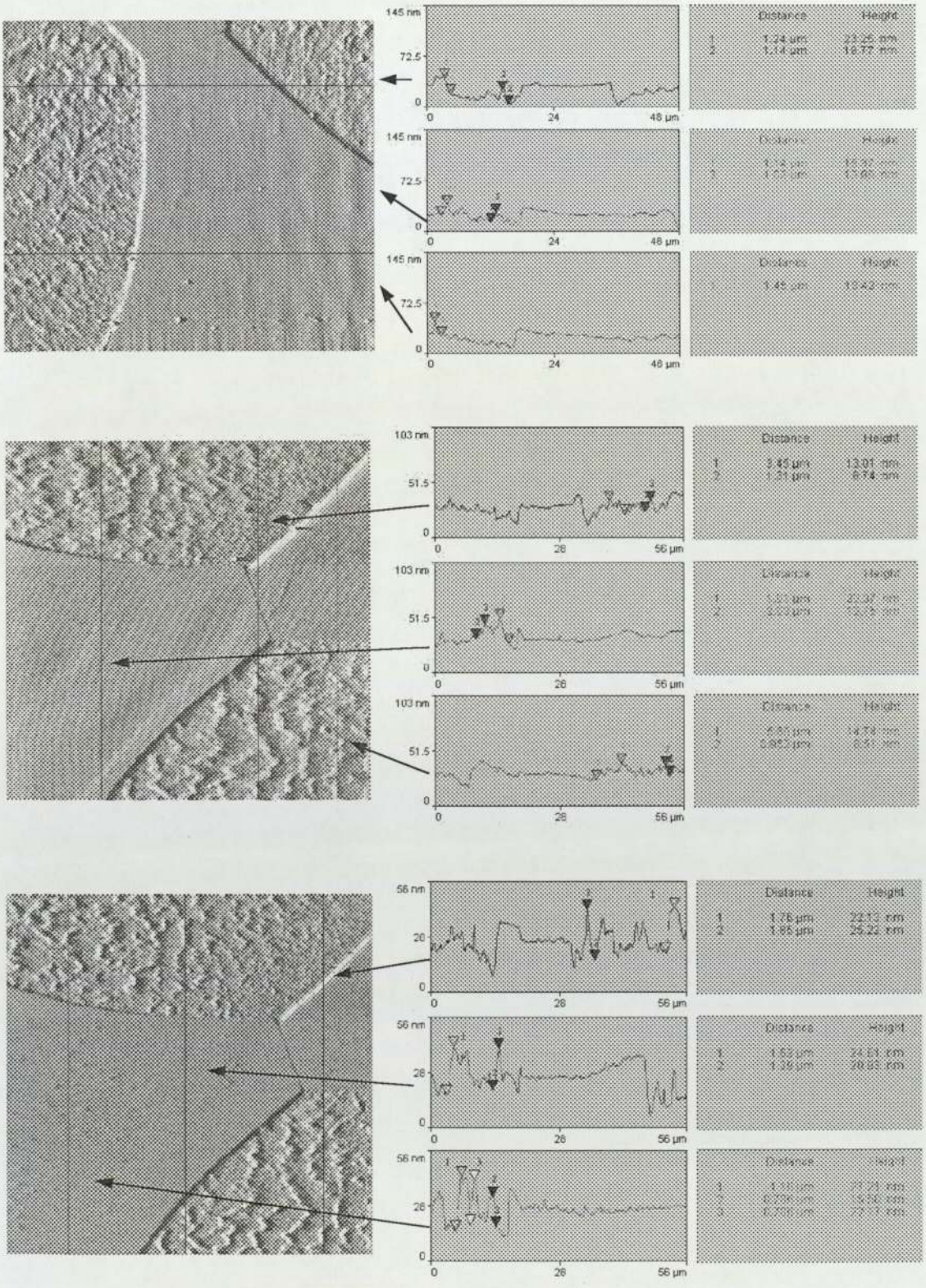

Figures 45, 46 and 47 from top to bottom showing AFM scans and associated line scans of an inductive read head after reconditioning at 25°C/80%RH, 1 cycles and 10 cycles of DDS-2 (M120) tape at 40°C/10%RH respectively, (1 tape cycle = 2 minutes = 1.8 m). Any evidence of head curvature was removed by second order levelling before AFM analysis.

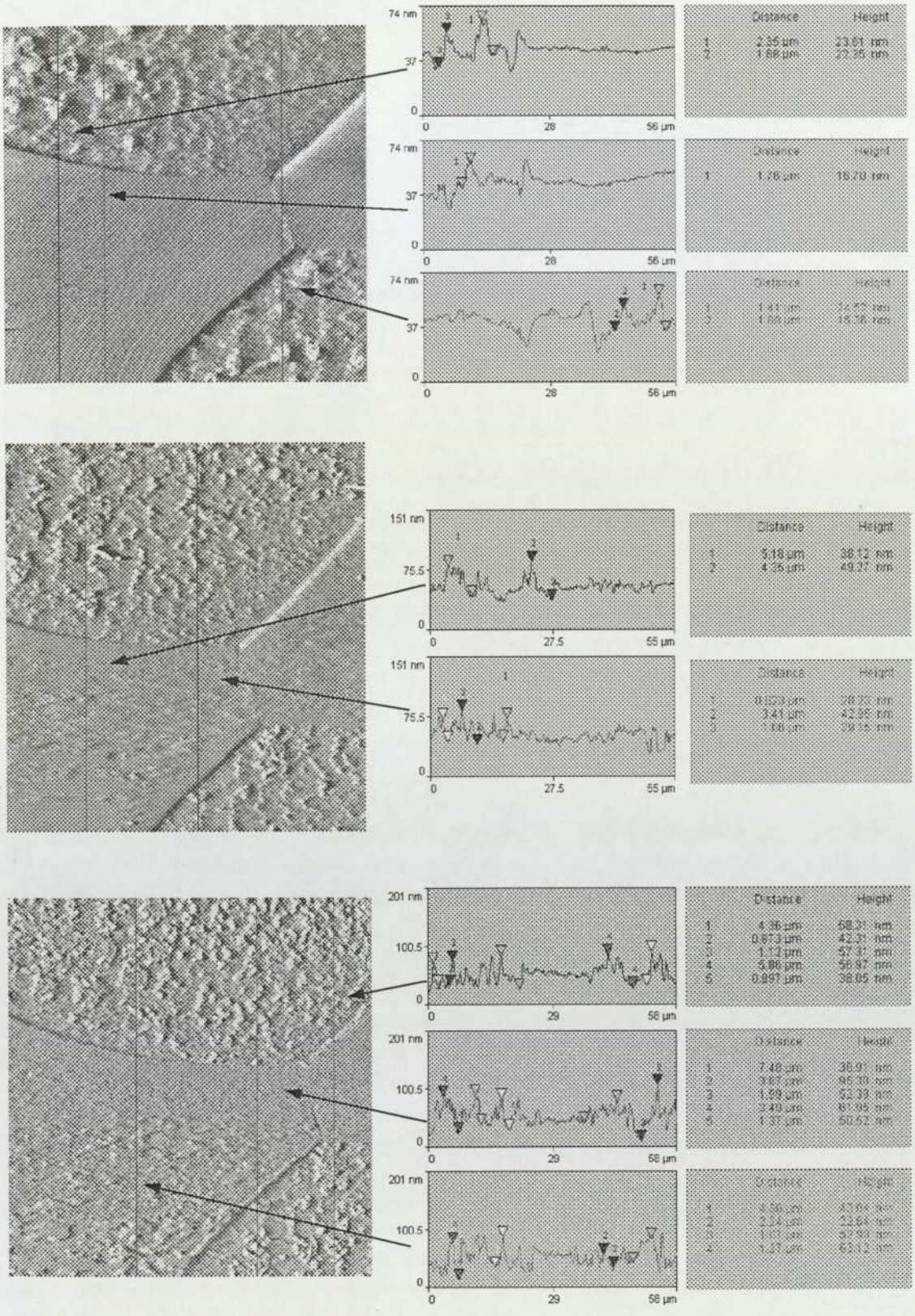

Figures 48, 49 and 50 from top to bottom showing AFM scans and associated line scans of an inductive read head after 100,1000 and 5000 tape cycles of DDS-2 (M120) tape at 40°C/10%RH respectively, (1 tape cycle = 2 minutes = 1.8 m). Any evidence of head curvature was removed by second order levelling before AFM analysis.

Figures 45 to 50 show staining present on the glass and ferrite regions. An increase in the areal stain coverage from the glass region to the whole of glass and ferrite regions of the read head as the tape was cycled was evident. Stain started to occur on the ferrite region at around 1000 tape cycles and large lumps of stain were observed at the glass region from 100 tape cycles, which progressively became smaller as the stain areal coverage increased.

3.2.1.3 Stain thickness/stain-to-ferrite measurements of Atomic Force Microscopy AFM scans at 25°C/35%RH and 40°C/10%RH

The results presented in tables 5 and 6 with figures 51 and 52, and tables 7 and 8 with figures 53 and 54 show the average stain thickness and stain-to-ferrite separation versus number of tape cycles of DDS-2 (M120) tape at 25°C/35%RH and 40°C/10%RH respectively. Tables 5 and 6, and figures 51 and 52 shows stain thickness and stain-to-ferrite separation at the glass region of an inductive read head only as there were no stain present on ferrite region. Table 6 and figure 52 show stain thickness and stain-to-ferrite separation at the glass and ferrite regions at 40°C/10%RH. An average stain thickness was calculated at the glass region after 1, 10, 100, 1000 and 5000 tape cycles for drives 1, 6, and 7 -right hand column of table 5 and from 1 to 5000 tape cycles of drives 1, 6 and 7 at the bottom of table of table 5.

3.1.1.3.1 Stain thickness and stain-to-ferrite separation measurements at 25°C/35%RH

	Stain thickness at the glass region (nm) of an inductive read head at 25°C/35%RH			
Number of tape cycles	Drive 1 Glass region	Drive 6 Glass region	Drive 7 Glass region	Average
1	21.30	15.63	12.50	16.48
10	26.24	23.24	25.75	25.08
100	19.14	20.03	19.50	19.56
1000	20.95	23.25	16.10	20.10
5000	28.26	12.31	15.35	18.64
Average stain Thickness (nm)	**23.18**	**18.89**	**17.84**	**19.97**

Table 5 showing a table of stain thickness at the glass region versus number of tape cycles of drives 1, 6 and 7 at 25°C/35%RH using DDS-2 (M120) tape, (1 tape cycle = 2 minutes = 1.8 m). An average stain thickness was calculated at the glass region after 1, 10, 100, 1000 and 5000 tape cycles for drives 1, 6, and 7 -right hand column of table 5 and from 1 to 5000 tape cycles of drives 1, 6 and 7 at the bottom of table of table 5.

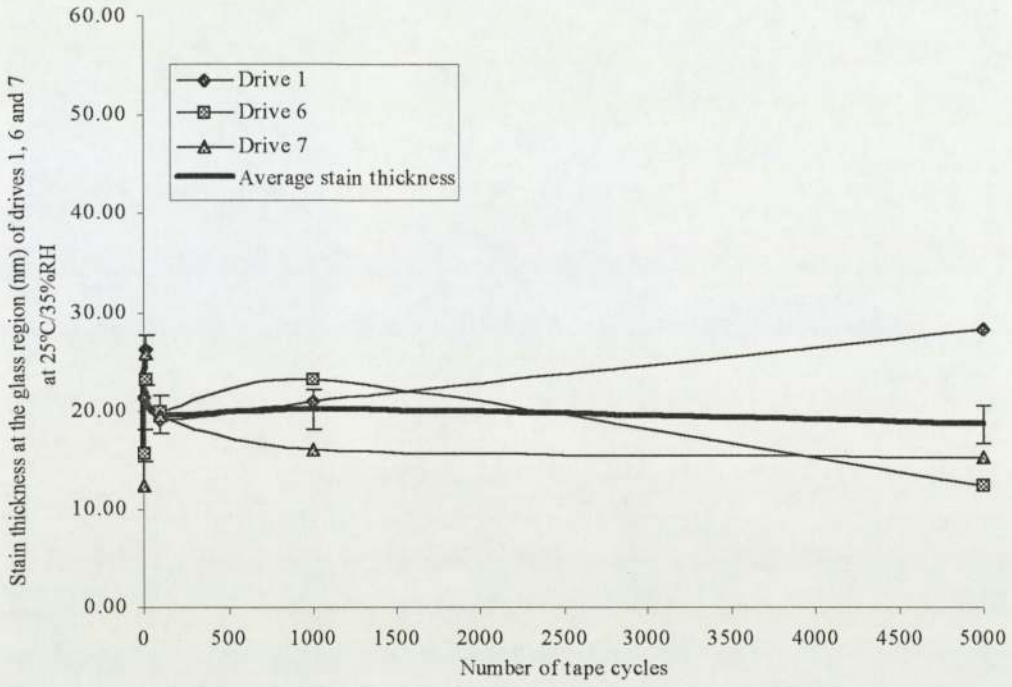

Figure 51 showing a plot of stain thickness at the glass region versus number of tape cycles of drives 1, 6 and 7 at 25°C/35%RH using DDS-2 (M120) tape, (1 tape cycle = 2 minutes = 1.8 m). An average stain thickness was calculated at the glass region after 1, 10, 100, 1000 and 5000 tape cycles for drives 1, 6, and 7. No staining was found on the ferrite region of the inductive read head.

	Stain-to-ferrite separation at the glass region (nm) of an inductive read head at 25°C/35%RH			
Number of Tape cycles	Drive 1 Glass region	Drive 6 Glass region	Drive 7 Glass region	Average
1	5.18	4.41	3.13	4.24
10	7.13	5.54	8.10	6.92
100	4.97	7.98	5.75	6.23
1000	5.94	5.75	5.56	5.75
5000	13.39	4.96	7.15	8.50
Average Stain-to-ferrite separation (nm)	**7.32**	**5.73**	**5.94**	**6.33**

Table 6 showing stain-to-ferrite separation at the glass region versus number of tape cycles of drives 1, 6 and 7 at 25°C/35%RH using DDS-2 (M120) tape, (1 tape cycle = 2 minutes = 1.8 m). An average stain thickness was calculated at the glass region after 1, 10, 100, 1000 and 5000 tape cycles for drives 1, 6, and 7 -right hand column of table 6 and from 1 to 5000 tape cycles of drives 1, 6 and 7 at the bottom of table of table 6. The stain-to-ferrite separation at the glass region is the height of the stain at the glass region minus the height of the ferrite.

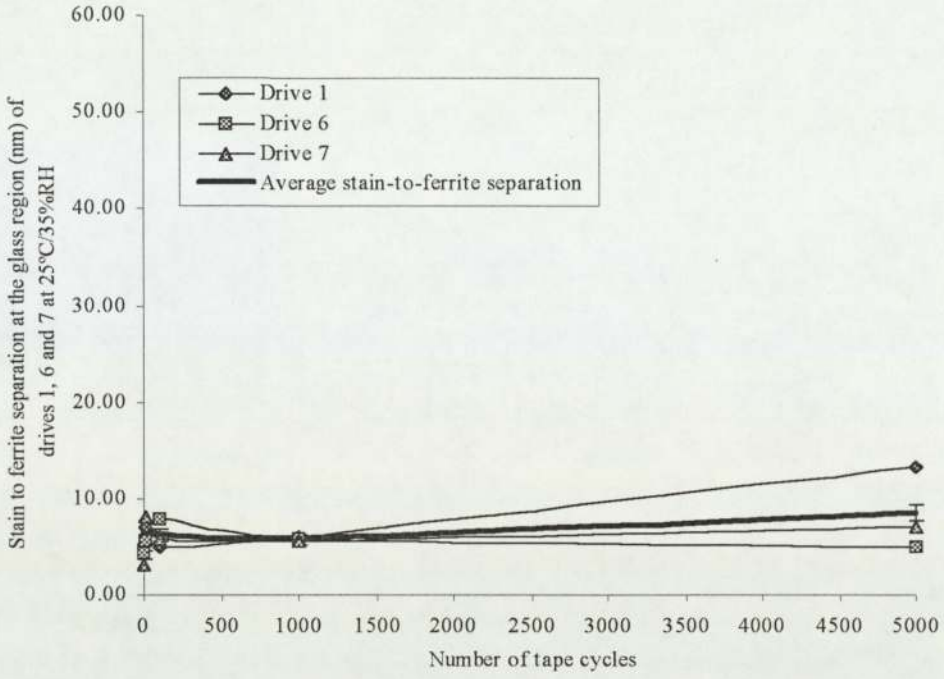

Figure 52 showing a plot of stain-to-ferrite separation at the glass region versus number of tape cycles of drives 1, 6 and 7 at 25°C/35%RH using DDS-2 (M120) tape (1 tape cycle = 2 minutes = 1.8 m). An average stain thickness was calculated at the glass region after 1, 10, 100, 1000 and 5000 tape cycles for drives 1, 6, and 7. The stain-to-ferrite separation at the glass region is the height of the stain at the glass region minus the height of the ferrite.

Figure 51, shows a rapid increase in the average stain thickness at the glass region from 16 nm for one cycle to 25 nm at 10 cycles, and an average stain-to-ferrite separation of 4-8 nm for all cycles. Beyond 10 cycles, there shows an reduction in the average stain thickness from 25 nm to 20 nm for 5000 cycles and average stain-to-ferrite separation remained constant of 6-8 nm and lies above the ferrite.

In all of the AFM images, there was clear evidence of debris (tape debris and/or dust) on the head, an attempt was made to remove this debris using a cotton bud and hexane liquid. This made the situation worse, as the debris was smeared over the ferrite. With this effect, they were no attempt to remove the dust particles. To reduce the accumulation of these particles, the drives need to be examined just after experimentation.

3.1.1.3.2 Stain thickness and stain-to-ferrite separation measurements at 40°C/10%RH

	Stain thickness at the glass and ferrite regions (nm of an inductive read head at 40°C/10%RH							
	Drive 1		Drive 6		Drive 7		Average (nm)	
Number of tape cycles	Glass	Ferrite	Glass	Ferrite	Glass	Ferrite	Glass	Ferrite
1	23.50	0.00	13.00	0.00	16.11	0.00	17.54	0.00
10	20.31	6.70	19.78	5.27	20.15	0.00	20.08	3.99
100	19.73	4.48	26.53	4.74	26.81	3.49	24.36	4.24
1000	17.71	10.35	23.96	15.59	29.77	24.11	23.81	16.68
5000	43.24	11.09	48.17	29.65	44.20	23.68	45.20	21.47
Average stain thickness (nm)	**24.90**	**6.52**	**26.29**	**11.05**	**27.41**	**10.26**	**26.20**	**9.28**

Table 7 showing a table of the results of the stain thickness at the glass region of an inductive read head versus number of tape cycles of drives 1, 6 and 7 at 40°C/10%RH using DDS-2 (M120) tape, (1 tape cycle = 2 minutes = 1.8 m). An average stain thickness was calculated at the glass and ferrite region after 1, 10, 100, 1000 and 5000 tape cycles for drives 1, 6, and 7 -right hand column of table 7 and from 1 to 5000 tape cycles of drives 1, 6 and 7 at the bottom of table of table 7.

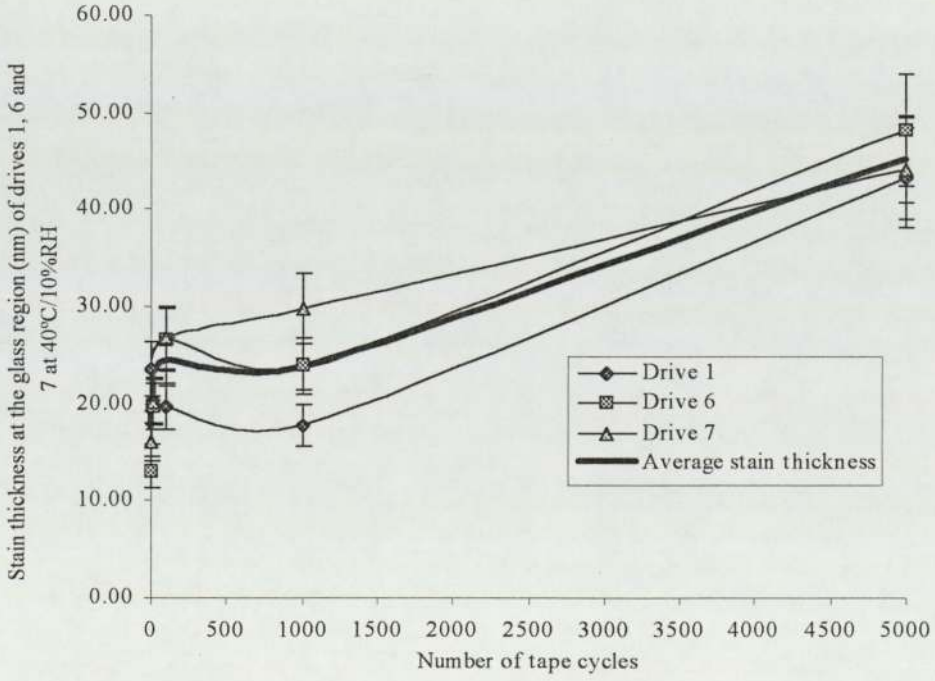

Figure 53 showing a plot of stain thickness at the glass region of an inductive read head versus number of tape cycles of drives 1, 6 and 7 at 40°C/10%RH using DDS-2 (M120) tape, (1 tape cycle = 2 minutes = 1.8 m).

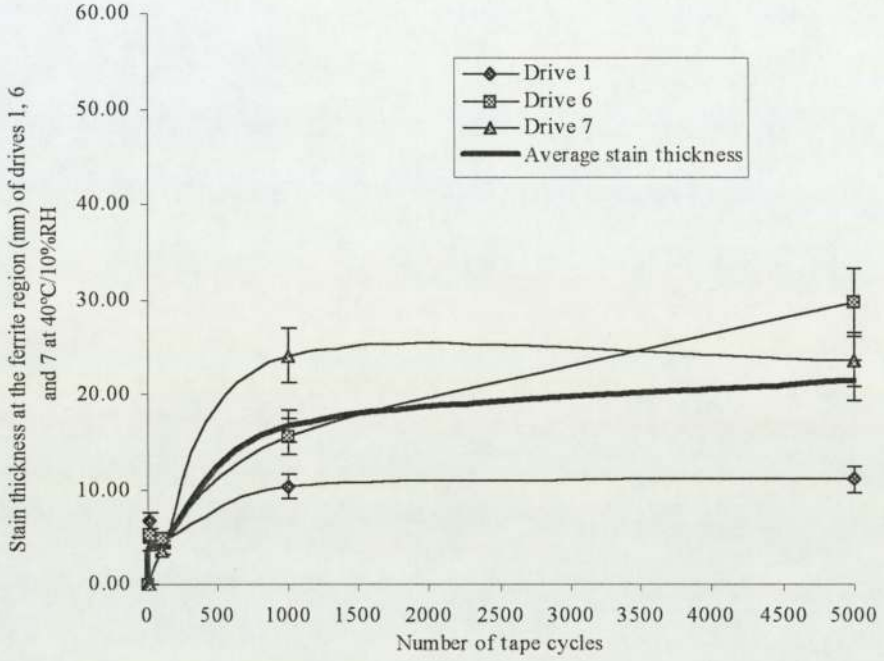

Figure 54 showing a plot of the stain thickness at the ferrite region of an inductive read head versus number of tape cycles of drives 1, 6 and 7 at 40°C/10%RH using DDS-2 (M120) tape, (1 tape cycle = 2 minutes = 1.8 m).

	Stain-to-ferrite separation at the glass and ferrite regions (nm) of an inductive read head at 40°C/10%RH							
Number of	Drive 1		Drive 6		Drive 7		Average (nm)	
Tape cycles	Glass	Ferrite	Glass	Ferrite	Glass	Ferrite	Glass	Ferrite
1	8.01	0.00	7.85	0.00	6.97	0.00	7.61	0.00
10	11.80	0.00	12.94	0.00	12.69	0.00	12.48	0.00
100	17.16	12.55	12.32	0.00	13.82	7.23	14.43	6.59
1000	13.53	10.07	20.45	12.01	13.40	0.00	15.79	7.36
5000	31.08	16.44	30.03	23.39	No result	No result	30.55	19.92
Average stain-to-ferrite separation (nm)	**16.32**	**7.81**	**16.72**	**7.08**	**11.72**	**1.81**	**16.17**	**6.77**

Table 8 showing a results of the stain-to-ferrite separation at the ferrite and glass region of an inductive read head versus number of tape cycles of drives 1, 6 and 7 at 40°C/10%RH using DDS-2 (M120) tape, (1 tape cycle = 2 minutes = 1.8 m). An average stain thickness was calculated at the glass and ferrite region after 1, 10, 100, 1000 and 5000 tape cycles for drives 1, 6, and 7 -right hand column of table 8 and from 1 to 5000 tape cycles of drives 1, 6 and 7 at the bottom of table of table 8. The stain-to-ferrite separation at the glass region is the height of the stain at the glass region minus the height of the ferrite. For stain-to-ferrite separation at the ferrite region is the height of the stain at the ferrite region minus the height of the ferrite. This is equivalent to the stain thickness at the ferrite region.

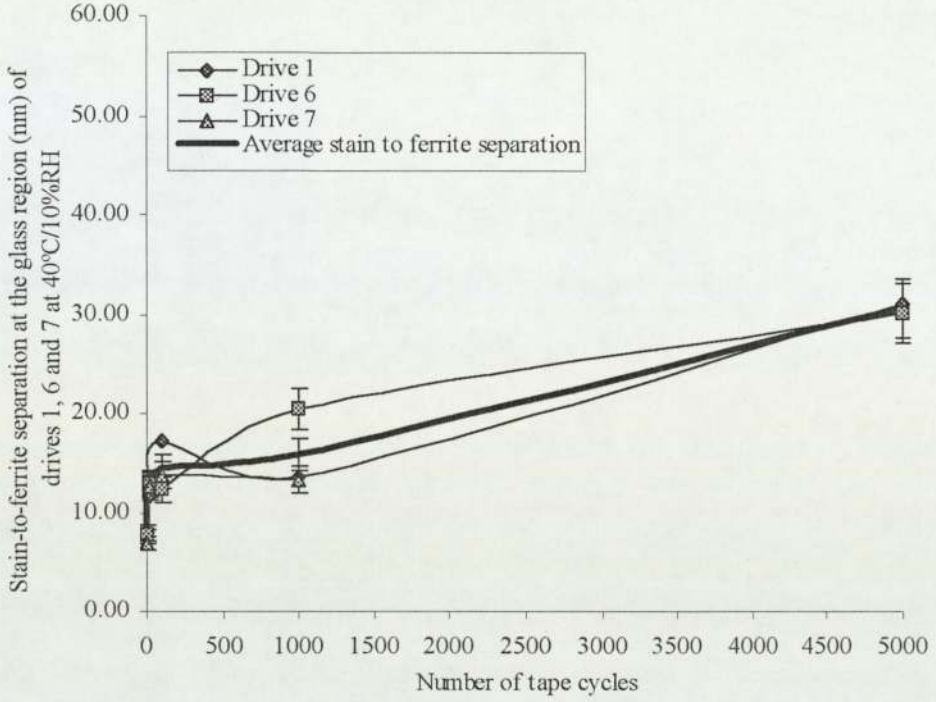

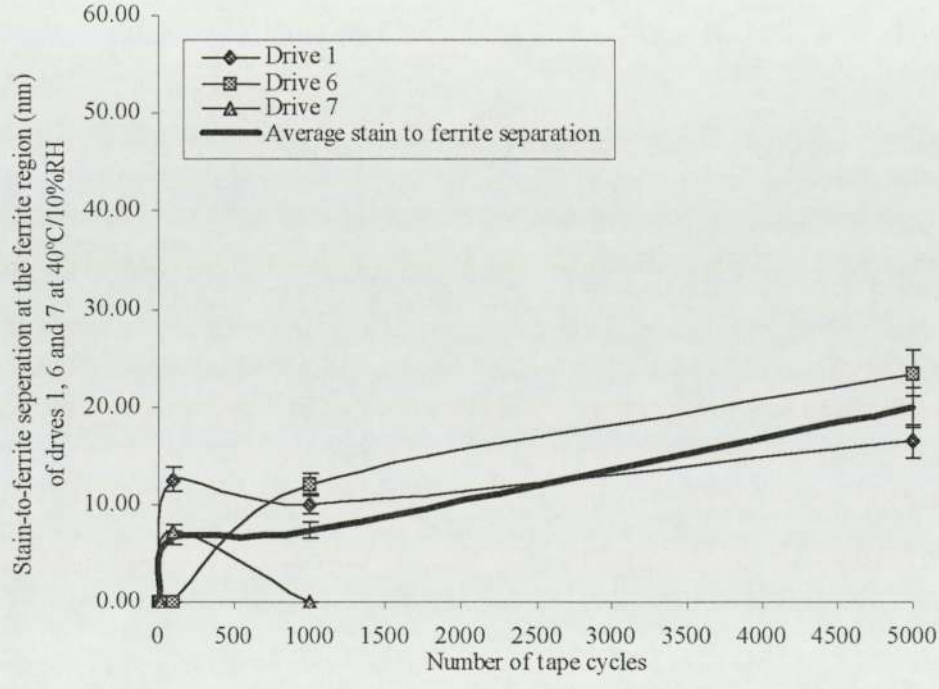

Figures 55 and 56 from top to bottom showing stain-to-ferrite separation at the glass and ferrite regions of an inductive read head versus number of tape cycles at 40°C/10%RH using DDS-2 (M120) tape, (1 tape cycle = 2 minutes = 1.8 m). The stain-to-ferrite separation at the glass region is the height of the stain at the glass region minus the height of the ferrite. For stain-to-ferrite separation at the ferrite region is the height of the stain at the ferrite region minus the height of the ferrite. This is equivalent to the stain thickness at the ferrite region.

At 40°C/10%RH, there was a significant increase in the stain thickness from 17 nm to 45 nm at the glass region from 0 to 5000 tape cycles. Comparing this with the condition of 25°C/35%RH, there was no increase in the stain thickness of 20 nm at the glass region as the tape was cycled. Whereas at the ferrite region the stain thickness increased rapidly from 0 to 16 nm for 0 to 1000 tape cycles then gradually increased to around 21-22 nm.

The stain-to-ferrite separation at 25°C/35%RH and 40°C/10%RH showed similar characteristics shown for the stain thickness measurements.

3.2.2 Error rate measurements at 25°C/35%RH and 40°C/10%RH

The results presented in figures 57 to 62 show the error rates of the drives 1 and 7 at 25°C/35%RH and drives 1, 5, 7 and 9 at 40°C/10%RH.

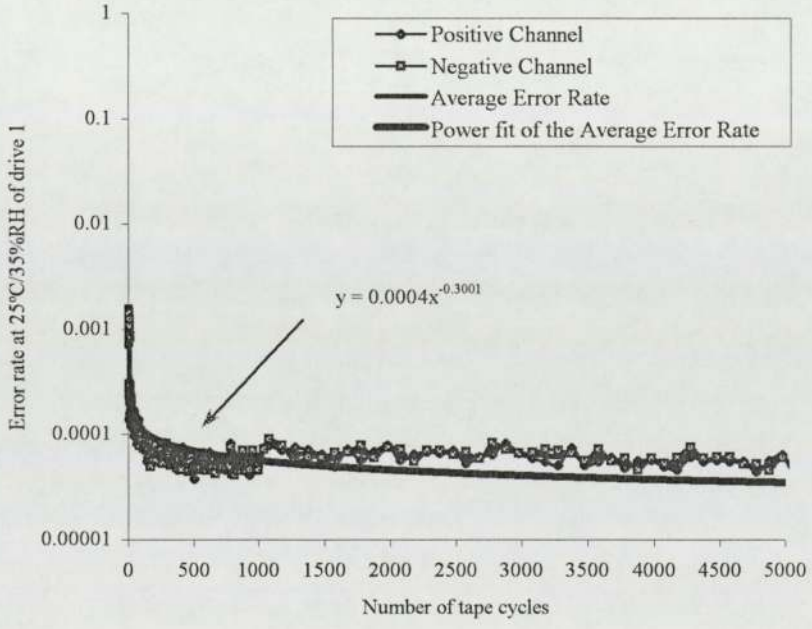

Figure 57 shows the error rate of drive 1 versus number of tape cycles of DDS-2 (M120) tape at 25°C/35%RH, (1 tape cycle = 2 minutes = 1.8 m).

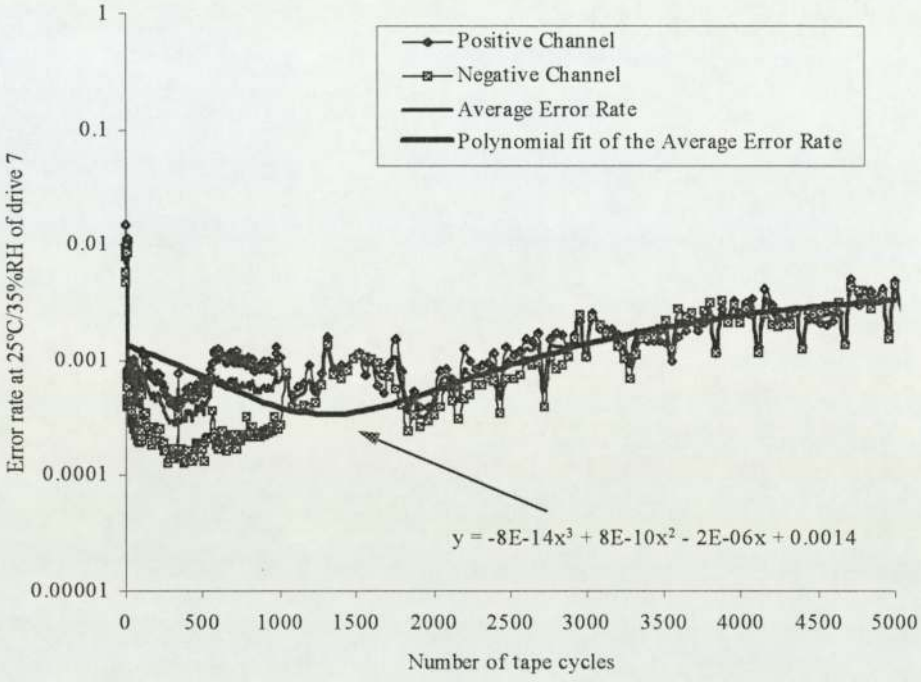

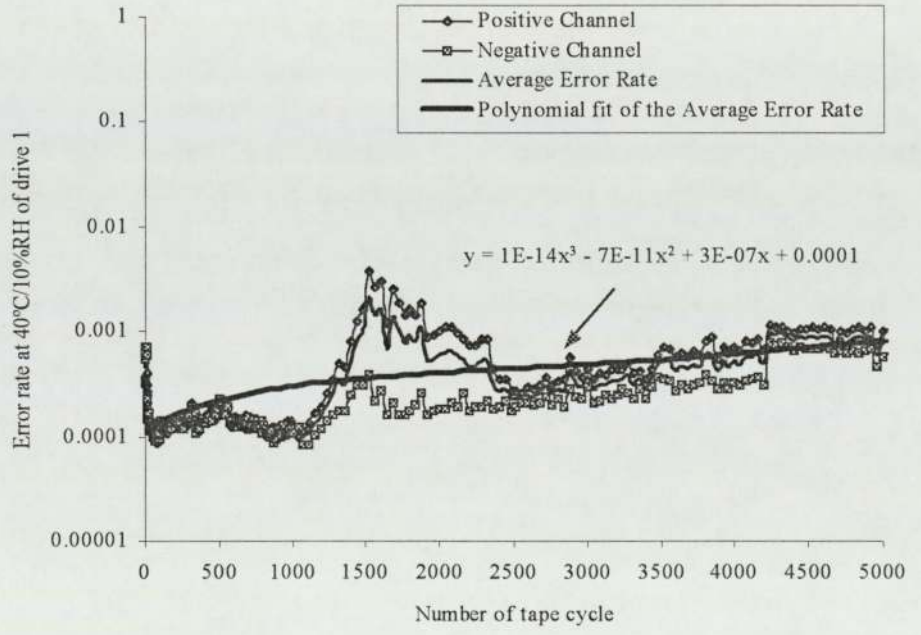

Figures 58 and 59 showing error rates of drive 7 and 1 versus number of tape cycles of DDS-2 (M120) tape at 25°C/35%RH and 40°C/10%RH respectively, (1 tape cycle = 2 minutes = 1.8 m).

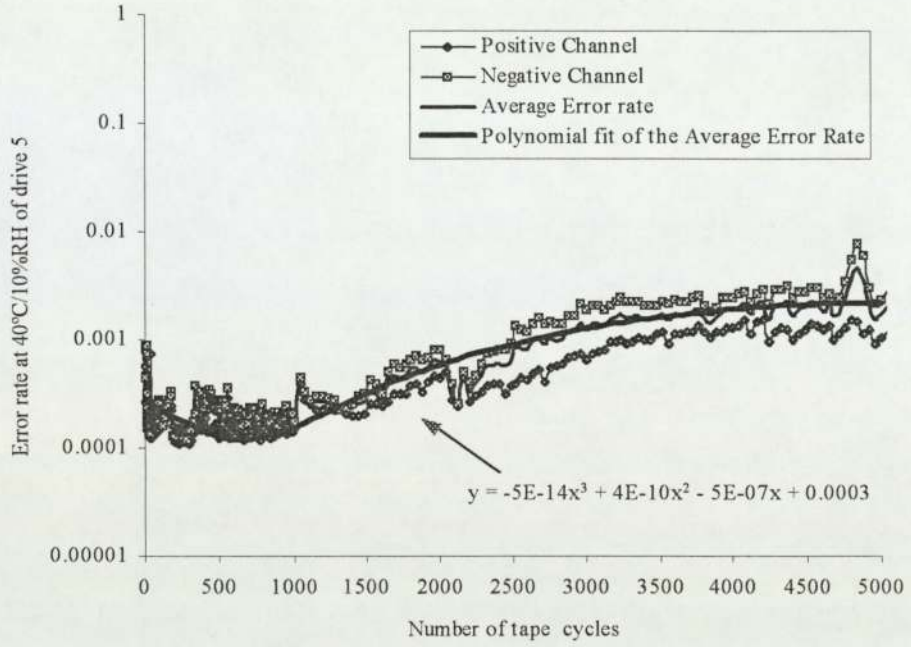

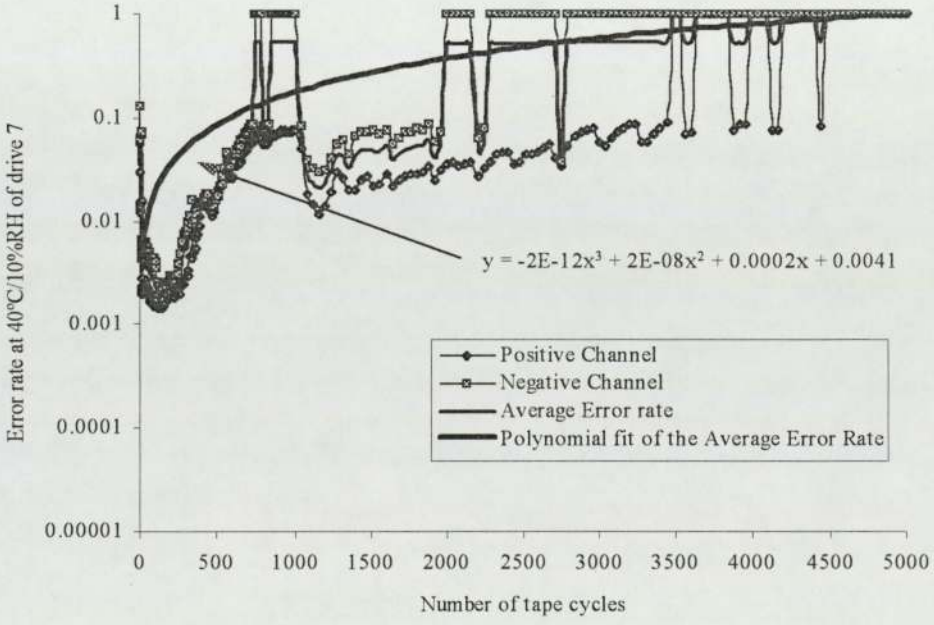

Figures 60 and 61 showing error rates of drives 5 and 7 versus number of tape cycles of DDS-2 (M120) tape at 40°C/10%RH, (1 tape cycle = 2 minutes = 1.8 m).

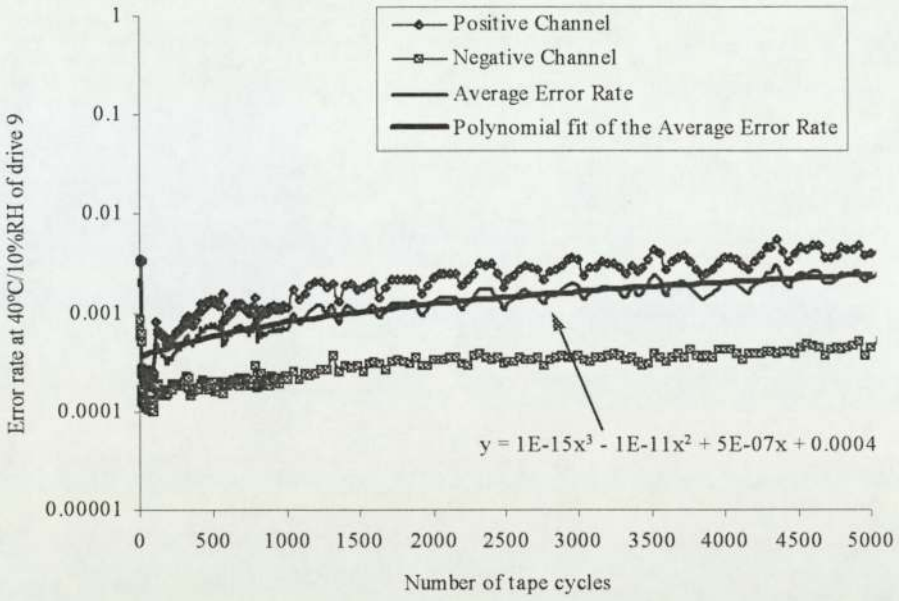

Figures 62 showing error rates of drive 9 versus number of tape cycles of DDS-2 (M120) tape at 40°C/10%RH, (1 tape cycle = 2 minutes = 1.8 m).

Figures 57 and 62 show that when the head assembly was removed from the drive for AFM examination after 10 tape cycles and subsequently reassembled, the error rate was disturbed resulting in a drop in the error rate from 0.01 to 0.001. For 100 cycles, drive 1 showed an improvement in the error rate after removing/reassemble of the drum, whereas drive 7 initially showed an increase in the error rate.

When taking the overall trend of both drives the error rate of drive 1 showed a decrease in the error rate from 0.001 to 0.0001, which stabilised at approximately 500 cycles. Whereas, drive 7 showed greater fluctuations in the error rate, resulting in an average error rate of approximately 0.001. From the measured stain thickness of the AFM scans at 1, 10, 100, and 1000 cycles and the error rates of drive 1, a correlation was made indicating the relationship between the stain thickness and the error rate.

At 40°C/10%RH, figure 59 to 62 shows a gradual increase in the error rate from 0.0001 to 0.001 for both channels as the tape was cycled. AFM results have also shown an increase in the stain build-up on the head. In addition, figure 61 (drive 7) shows a rapid increase in the error rates from 0.001 to 0.1 from 0 to 800 tape cycle range, then drops to 0.01 followed with an gradual increase. Figure 61 shows error rates of 1 from 750 tape cycles indicating that there were head clogging- tape debris adhering between the head gap and tape. It follows from figures 59 to 62 at 40°C/10%RH that when curve fitting to the error rate data presented the error rate follows a polynomial function, that is $E = An^3+Bn^2+Cn+D$, where A,

B, C, D are constants, E is the error rate and n is the number of tape cycles. From the results the value of the constants A, B, C and D appears to be unique to the tape drive. Overall the drives has exhibit an increase in the error rate with an increase in the number of tape cycles, even though each drive showed different error rate characteristics.

3.2.3 Summary of the overall average error rate at 25°C/35%RH and 40°C/10%RH

Presented below, table 9 shows the summary of the average error rate of all drives used at 25°C/35%RH and 40°C/10%RH from 0 to 5000 tape cycles, when using DDS-2 (M120) tape, where each tape cycle = 2 minutes = 1.8 m.

Condition	Drive No	Positive Channel	Negative Channel	Average Error rate
25°C/35%RH	Drive 1	0.0001	0.0001	0.0001
	Drive 7	0.0015	0.0010	0.0013
Average		**0.0008**	**0.0006**	**0.0007**
40°C/10%RH	Drive 1	0.0004	0.0002	0.0003
	Drive 5	0.0004	0.0008	0.0006
	Drive 7	0.1598	0.3653	0.2626
	Drive 9	0.0016	0.0002	0.0009
Average		**0.0406**	**0.0917**	**0.0661**

Table 9 showing the overall average error rate at 25°C/35%RH and 40°C/10%RH of all drives used in experimentation from 0 to 5000 tape cycles, when using DDS-2 (M120) tape (1 tape cycle = 2 minutes = 1.8 m).

The results presented in table 9 show significant differences in the overall average error rate of all the tape drives used at 25°C/35%RH and 40°C/10%RH. The overall average error rate for 25°C/35%RH was shown to be 0.0007, whereas at 40°C/10%RH the average error rate was 0.0661, which is a factor of 100 larger then for 25°C/35%RH. The possible reasons for the large factor are from over-averaging and drive 7 gave a large number of error rates with the value of 1, thus increasing the average error rate for that drive. As expected the error rate for 40°C/10%RH was higher than at 25°C/35%RH due to more staining on the head.

3.2.4 Head wear rate measurements using DDS-2 (M120) tape at 25°C/35%RH and 40°C/10%RH

The results presented in figures 63 to 65 show the head wear rate at the surface of an inductive read head using DDS-2 (M120) tape at 25°C/35%RH and 40°C/10%RH as measured at intervals of 100, 1000 and 5000 tape cycles and a tape cycle = 2 minutes = 1.8

m. Figures 63 and 64 shows head wear rate (nm/m) along the read head (i.e. versus the positions of the indent) after 100, 1000 and 5000 tape cycles at 25°C/35%RH and 40°C/10%RH. Figure 65 shows the average head wear rate versus number of tape cycles at 25°C/35%RH and 40°C/10%RH, where the average head wear rate is calculated using the wear rate measurements along the head. Table 10 shows a summary of the all the wear rate results.

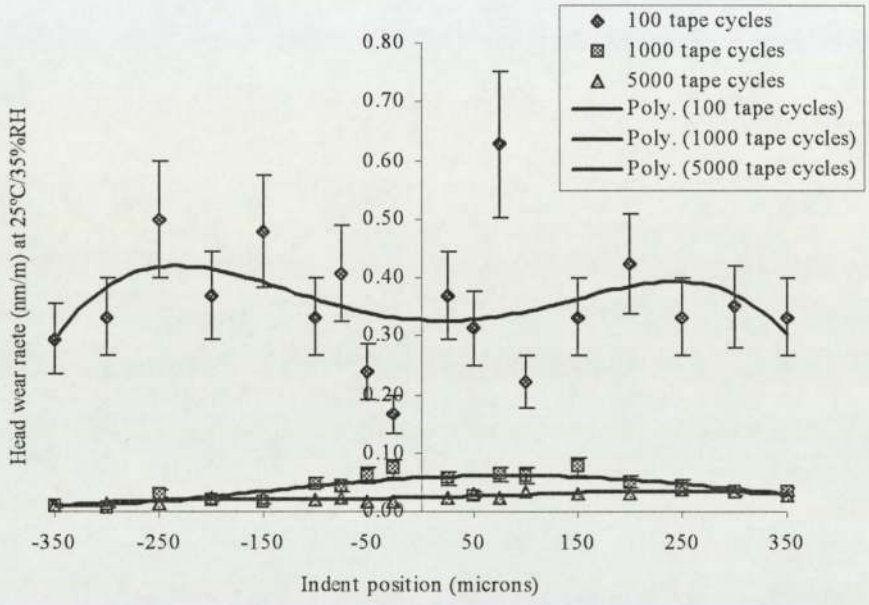

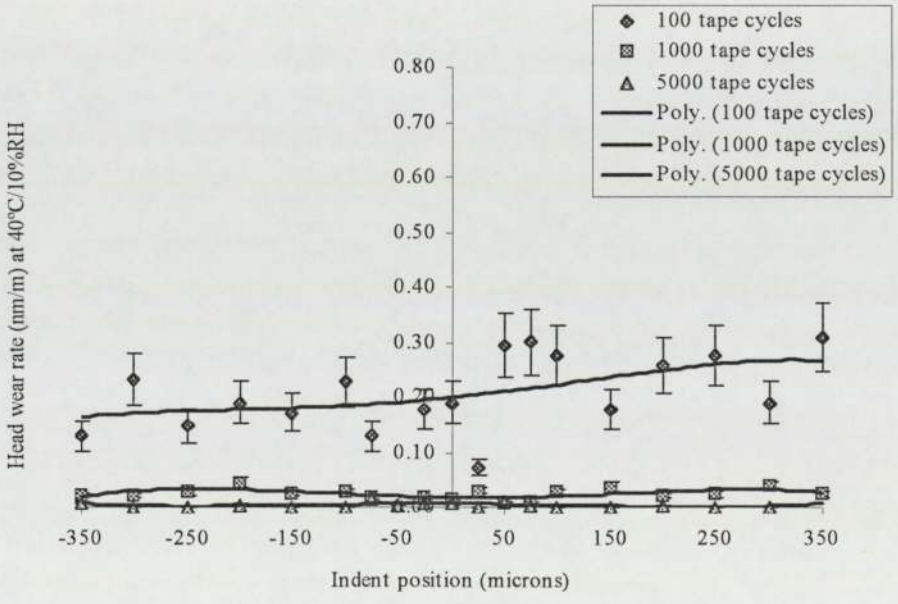

Figures 63 top and 64 bottom showing head wear rate of an inductive read head versus indent position at tape intervals of 100, 1000 and 5000 tape cycles using DDS-2 (M120) tape at 25°C/35%RH and 40°C/10%RH respectively (1 tape cycle = 2 minutes = 1.8 m). The positive indent position (>0) is the trailing edge and the negative indent position (<0) is the leading edge.

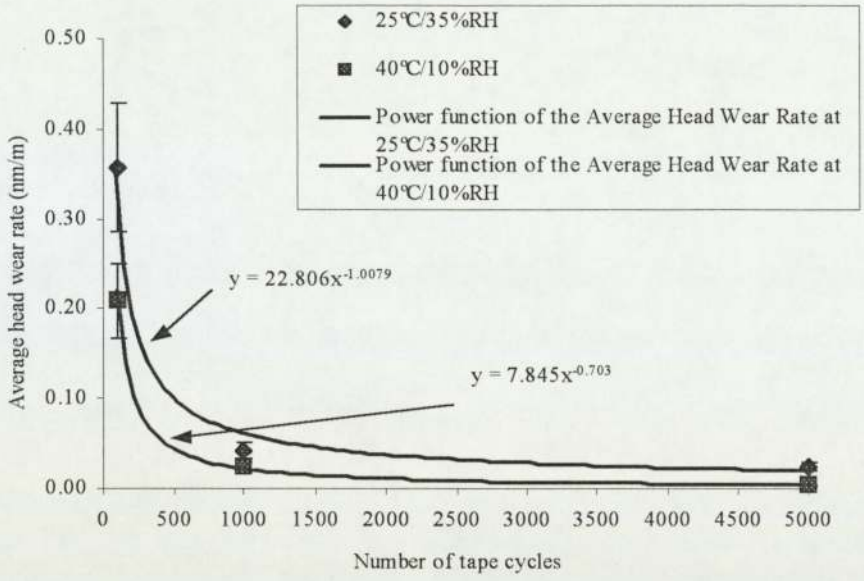

Figure 65 showing average head wear rate of an inductive read head versus number of tape cycles of DDS-2 (M120) tape at 25°C/35%RH and 40°C/10%RH (1 tape cycle = 2 minutes = 1.8 m).

	Head Wear Rate (nm/m) at 25°C/35%RH			Head Wear Rate (nm/m) at 40°C/10%RH		
Indent Position	Number of tape cycles			Number of tape cycles		
(Microns)	100	1000	5000	100	1000	5000
-350	2.95E-01	1.03E-02	1.06E-02	1.29E-01	2.26E-02	7.84E-03
-300	3.32E-01	8.20E-03	1.43E-02	2.34E-01	2.05E-02	9.23E-04
-250	4.98E-01	3.08E-02	1.20E-02	1.48E-01	2.77E-02	1.15E-03
-200	3.69E-01	2.05E-02	2.35E-02	1.91E-01	4.51E-02	5.31E-03
-150	4.80E-01	1.85E-02	2.49E-02	1.72E-01	2.56E-02	6.92E-04
-100	3.32E-01	4.92E-02	1.94E-02	2.28E-01	2.87E-02	1.61E-03
-75	4.06E-01	4.31E-02	2.31E-02	1.29E-01	1.74E-02	1.29E-02
-50	2.40E-01	6.15E-02	1.71E-02	-	1.95E-02	4.15E-03
-25	1.66E-01	7.38E-02	1.85E-02	1.78E-01	1.33E-02	8.54E-03
0	-	-	-	1.91E-01	2.97E-02	6.69E-03
25	3.69E-01	5.74E-02	2.45E-02	7.38E-02	6.15E-03	9.23E-04
50	3.14E-01	2.87E-02	3.18E-02	2.95E-01	9.23E-03	9.69E-03
75	6.28E-01	6.36E-02	2.31E-02	3.01E-01	2.87E-02	3.00E-03
100	2.21E-01	6.15E-02	3.28E-02	2.77E-01	3.79E-02	1.15E-03
150	3.32E-01	7.79E-02	3.00E-02	1.78E-01	2.05E-02	1.15E-03
200	4.25E-01	5.13E-02	3.23E-02	2.58E-01	2.46E-02	3.46E-03
250	3.32E-01	4.51E-02	3.69E-02	2.77E-01	3.90E-02	1.15E-03
300	3.51E-01	3.49E-02	3.55E-02	1.91E-01	2.46E-02	9.23E-04
350	3.32E-01	3.28E-02	2.72E-02	3.08E-01	-	-
Average	**3.57E-01**	**4.27E-02**	**2.43E-02**	**2.09E-01**	**2.45E-02**	**3.96E-03**

Table 10 showing the entire head wear rate of an inductive read head versus position at tape intervals of 100, 1000 and 5000 cycles at 25°C/35%RH and 40°C/10%RH using DDS-2 (M120) tape (1 tape cycle = 2 minutes = 1.8 m). The positive indent position (>0) is the trailing edge and the negative indent position (<0) is the leading edge.

Figures 63 and 64 shows higher wear rate at the leading edge of the head (positive position of the indent) after 100 tape cycles and wear rates were higher for 25°C/35%RH then at 40°C/10%RH as shown in figure 64 after 100, 1000 and 5000 tape cycles of DDS-2 (M120) tape. Figure 63 also shows the highest wear rates occur near the gap region of the read head after 1000 tape cycles and the lowest at the edge of the head-tape contact region.

By curve fitting the experimental data in figure 65, the average wear rate from 1 to 5000 tape cycles at conditions of 25°C/35%RH and 40°C/20%RH show the average head wear rate versus number of tape cycles is an power function. That is the average head wear rate (nm/m), which is a function of the number of tape cycles, temperature and humidity is directly proportional to the power of the number of tapes cycles. In mathematical terms this is

$$\text{Average wear rate } (n, T, H) = A(T, H) * n^{B(T, H)} + C(T, H)$$

Where A, B and C are constants which are functions of temperature T and humidity H and n is the number of tape cycles and the units of A (T, H), B (T, H) and C (T, H) are in (nm/m)/cycle, undefined and nm/m respectively. To determine the constant A, B and C as functions of temperature T and humidity H power regression were correlated with the experimental data. Power regression shows that constants A and B at 25°C/35%RH are A = A (25°C, 35%RH) = 22.806 and B = B (25°C, 35%RH) = -1.009 respectively, whereas at 40°C/10%RH, A = A (40°C, 10%RH) = 7.842 and B = B (40°C, 10%RH) = -0.703. The constant C =C (T, H) = 0 for 25°C/35%RH and 40°C/10%RH. Thus it shows that $A > 0$ and $B < 0$ for these environment conditions.

3.2.5 Surface roughness measurements and characteristics of virgin and cycled DDS-2 (M120) tape at 25°C/35%RH and 40°C/10%RH

Presented in figures 66 and 67 and tables 11 and 12, the surface roughness (measured in nm) and AFM scans of virgin and cycled DDS-2 (M120) tape at 25°C/35%RH and 40°C/10%RH respectively. AFM scans were performed at resolutions of 10 μm^2 and 100 μm^2 with angles of 0° and 270°, where 0° and 270° lies parallel and perpendicular to the plane of tape.

3.2.5.1 Surface roughness measurements and analysis at 25°C/35%RH

Table 11 and figure 66 shows the AFM results of surface roughness analysis of virgin and cycling DDS-2 (M120) tape at 25°C/35%RH respectively.

Tape type	Condition	Number of Tape cycles	Scan area (μm^2)	Direction (degrees)	Average RMS Roughness R_a (nm)	Average Peak-to-valley (nm)
M120	Virgin		10	0	6.44	21.60
M120	Virgin		10	270	8.06	19.62
M120	Virgin		100	0	10.11	15.60
M120	Virgin		100	270	12.34	22.90
M120	25C/35%RH	5000	10	0	4.80	9.01
M120	25C/35%RH	5000	10	270	4.58	7.27
M120	25C/35%RH	5000	100	0	6.95	15.55
M120	25C/35%RH	5000	100	270	7.01	15.67

Table 11 showing a table of average tape surface roughness R_a (rms.) measurements of virgin and cycled DDS-2 (M120) tape at 25°C/35%RH (1 tape cycle = 2 minutes = 1.8m).

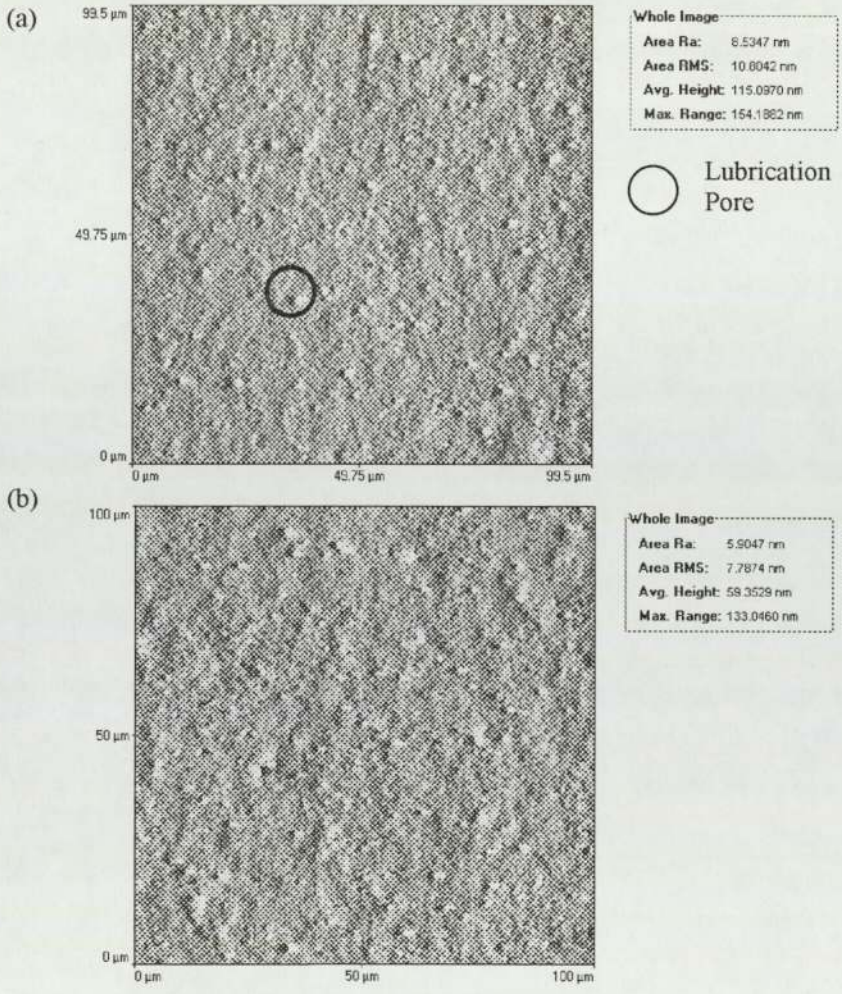

Figure 66 showing two AFM scans at angle of 0° together with surface roughness R_a (rms.) measurements of (a) virgin and (b) after 5000 cycles of DDS-2 (M120) tape at 25°C/35%RH respectively (1 tape cycle = 2 minutes = 1.8 m).

Table 11 shows the average surface roughness has changed considerably after 5000 cycles at 25°C/35RH. The surface roughness R_a of the cycled tape was between 5 and 7 nm and this was considerably smoother than virgin DDS-2 (M120) tape of 6-12 nm. This suggests that the highest of the asperities points of the tape surface were removed as indicated by the peak-valley values at scan area of 10 μm^2 where virgin DDS-2 (M120) tape was approximately 20.61 nm and after 5000 tape cycles was approximately 8.14 nm.

3.2.5.2 Surface roughness measurements and analysis at 40°C/10%RH

Figure 67 and table 12 shows the AFM scans of the surface and the results of the average surface roughness analysis of DDS-2 (M120) tape before (in a virgin state) and after cycling at 40°C/10%RH.

Tape type	Condition	Number of tape cycles	Scan area (μm^2)	Direction (degrees)	Average RMS roughness R_a (nm)	Average Peak-to- valley (nm)
M120	Virgin		10	0	6.44	21.60
M120	Virgin		10	270	8.06	19.62
M120	Virgin		100	0	10.11	15.60
M120	Virgin		100	270	12.34	22.90
M120	40C/10%RH	5000	10	0	3.77	-
M120	40C/10%RH	5000	10	270	4.33	-
M120	40C/10%RH	5000	100	0	6.685	15.79
M120	40C/10%RH	5000	100	270	7.123	-

Table 12 showing a table of average tape surface roughness R_a (rms.) measurements of virgin and cycled DDS-2 (M120) tape at 40°C/10%RH (1 tape cycle = 2 minutes = 1.8 m).

Comparing figures 66(b) and 67(b), lubrication pores were evident on the cycled tape at 25°C/35%RH, then at 40°C/10%RH. The surface roughness R_a (rms.) measurements showed that for an area of 100 μm^2, R_a was 5.905 nm at 25°C/35%RH and 5.106 nm at 40°C/10%RH respectively. Comparing the results of the average RMS roughness R_a for the scan area of 100 μm^2 after 5000 cycles of DDS-2 (M120) tape at 25°C/35%RH (Table 10) and 40°C/10%RH (Table 11) shows similar results for R_a as indicated by 6.95 nm at 25°C/35%RH and 6.685 nm at 40°C/10%RH.

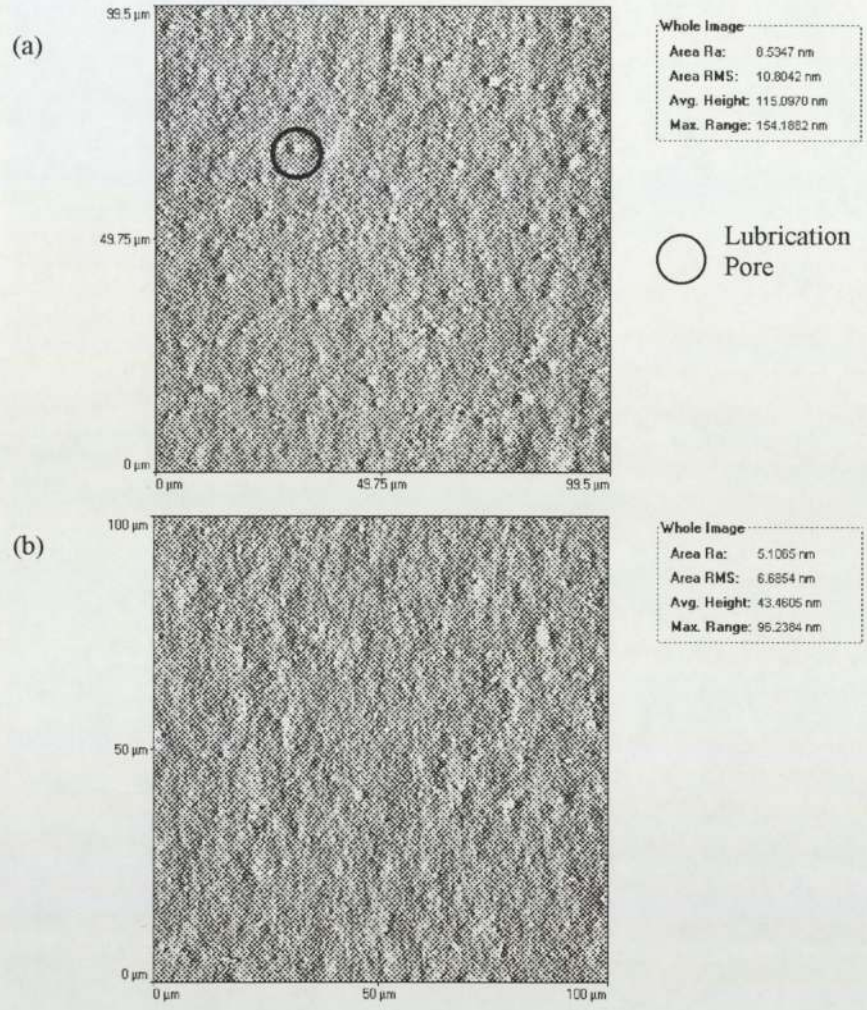

Figure 67 showing two AFM scans at angle 0° together with surface roughness R_a (rms.) measurements of (a) virgin and (b) after 5000 cycles of DDS-2 (M120) tape at 40°C/10%RH respectively (1 tape cycle = 2 minutes = 1.8 m).

3.5.2.3 Atomic Force Microscopy AFM scan of a virgin DDS-2 (M120) tape at area of 10*10 μm^2

Presented in figure 68 is an AFM scan of a virgin DDS-2 (M120) tape at area of 10*10 μm^2. The AFM scan shows a granular effect along the surface of the tape. Some of these granules have a maximum height of 39 nm. These high points may well be the protruding magnetic particles.

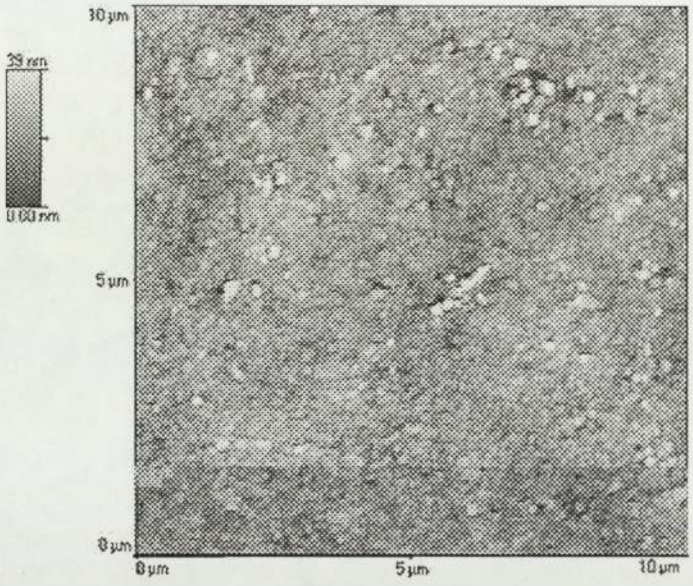

*Figure 68 showing an AFM scan of a virgin DDS-2 (M120) tape at 10*10 μm^2. The AFM scan is without any shading to enhance the surface details.*

The most important feature of the surface of virgin tape as shown in figure 68 is that the surface appears to be rough as measured by the line scans of virgin DDS-2 (M120) tape in table 11 and 12.

3.2.6 Auger Electron Spectroscopy AES survey at the surface of an inductive read head after 5000 cycles of DDS-2 (M120) tape at 25°C/35%RH and 40°C/10%RH

Presented in table 13 are the AES survey results of the average percentage atomic concentrations and elements detected on the glass and ferrite regions of an inductive read head after reconditioning at 25°C/80%RH and 5000 cycles of DDS-2 (M120) tape at 25°C/35%RH and 40°C/10%RH, where 1 cycle is 2 minutes (1.8 m). Both of the read heads have been etched to a point where a iron signal was detected. The AES survey of a reconditioned head is include as comparison to 5000 tape cycles of DDS-2 (M120) at 25°C/35%RH and 40°C/10%RH.

	AES survey results of elements detected and the percentage atomic concentration [AT]% at the surface of an inductive read head after reconditioning at 25°C/80%RH and 5000 cycles of DDS-2 (M120) at 25°C/35%RH and 40°C/10%RH											
	Reconditioned head				25°C/35%RH				40°C/10%RH			
Scan region	C KL1	O KL1	Fe LM2	Si LM1	C KL	O KL1	Fe LM2	Si LM1	C KL1	O KL1	Fe LM2	Si LM1
Glass		76.47		23.53	73.98	24.20	1.82		29.33	62.59	8.08	
		73.78		26.22	63.39	30.94	5.67		37.49	54.38	8.13	
		73.94		26.06	76.87	20.30	2.83		53.34	38.80	7.86	
Average Concentration	**0.00**	**74.73**	**0.00**	**25.27**	**71.41**	**25.15**	**3.44**	**0.00**	**40.05**	**51.93**	**8.02**	**0.00**
Ferrite	13.75	48.74	37.52		63.57	17.96	18.46		44.28	27.10	28.62	
	17.39	46.82	35.86		68.36	18.20	13.44		44.02	27.83	28.15	
	10.69	51.07	38.24		77.27	12.68	10.04		48.47	21.38	30.14	
Average Concentration	**10.69**	**51.07**	**38.24**	**0.00**	**69.74**	**16.28**	**13.98**	**0.00**	**45.59**	**25.44**	**28.97**	**0.00**

Table 13 showing the element detected and their average percentage atomic concentrations at the surface of the glass and ferrite regions of an inductive read head after reconditioning at 25°C/80%RH and 5000 cycles of DDS-2 (M120) tape at 25°C/35%RH and 40°C/10%RH respectively (1 tape cycle = 2 minutes = 1.8 m). The Auger lines C KL1 is carbon, O KL1 is oxygen and Fe LM2 is iron. Silicon Si was not detected at the glass region. The AES survey of a reconditioned head was included as a comparison to the tape cycling at 25°C/35%RH and 40°C/10%RH.

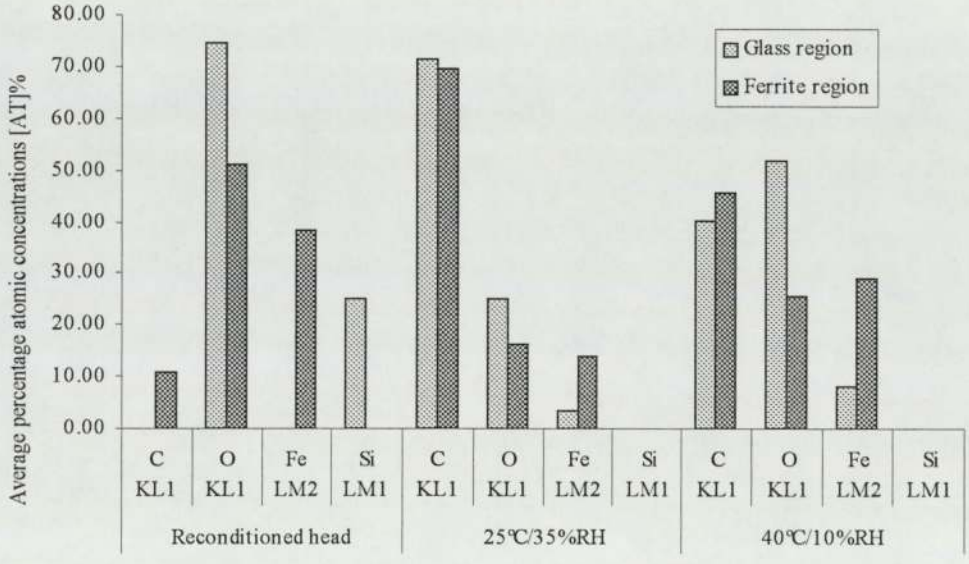

AES survey results of elements detected on the ferrite and glass regions of an inductive read head after reconditioning at 25°C/80%RH and 5000 tape cycles of DDS-2 (M120) tape at 25°C/35%RH and 40°C/10%RH

Figure 69 showing a bar chart of the element detected and their average percentage atomic concentrations at the surface of the glass and ferrite regions of an inductive read head after reconditioning at 25°C/80%RH and 5000 cycles of DDS-2 (M120) tape at 25°C/35%RH and 40°C/10%RH respectively (1 tape cycle = 2 minutes = 1.8 m).

Clearly from figure 69 and table 13, the AES survey have shown staining mainly consists of iron which has been detected on the glass region after 5000 tape cycles and correlates with the AFM results presented in figure 50. Other elements such as the organic and inorganic components: binder and lubricant, aluminium (the head cleaning agent) and silicon at the glass region were not detected. The element silicon Si was not detected by AES at the glass region suggests that there was a complete coverage of stain, which was not expected. Table 13 also shows there was approximately twice as much of iron Fe and carbon C present on the glass and ferrite regions at 40°C/10%RH than at 25°C/35%RH. Note that the total iron Fe signal is the sum of the iron (the magnetic particles) from the tape, which has adhered to the ferrite region of the read head in the form of stain, and the iron oxide Fe_3O_4 from the ferrite region of the read head. Oxygen is always present at the glass and ferrite regions of the head due to the silicon and iron occurring naturally as an oxide. The element carbon C is normally associated with surface contamination, which could mask all other AES signals present at the surface. The high concentrations of carbon C are normally removed by argon Ar etching.

Figure 69 shows large differences in the amount of carbon C, oxygen O and iron Fe detected at 25°C/35%RH and 40°C/10%RH. In particular the amount of carbon C detected on the glass and ferrite regions of the read head for 25°C/35%RH. This gave greater average result of 71.47 [AT]% and 69.74 [AT]% at the glass and ferrite regions of the read head respectively when comparing to the results presented for the equivalent carbon C at 40°C/10%RH. There appears to be more oxygen O detected on the glass and ferrite regions of the read head at 40°C/10%RH and was higher at the glass region than at the ferrite region when comparing the AES results at 25°C/35%RH figure 69.

3.2.7 X-ray Photoelectron Spectroscopy XPS survey of virgin DDS tape

Presented below, table 14 are the XPS survey results of virgin DDS-2 (M120), DDS-3 (F125 and M125) tapes to determine the composition of virgin tape used in these experiments. DDS-3 (F125 and M125) tapes are used as a comparison to the main tape DDS-2 (M120) that is used extensively throughout this project. The results show the average percentage atomic concentration [AT%] of the elements detected at the surface of the tape with take off angle (TOA) of 0° and 70°. The suffix: M120 is Maxell 120 m tape, F125 is Fuji 125 m tape, and M125 is Maxell 125 m tape. Table 15 shows carbon synthesis, where the carbon C total peak is used to identify other chemical states. These chemical states are C-Cl/C-N, which originates from the binder and Carboxyl O=C-O (CAR) is from the binder.

The ratio Fe/N is an indication of the iron (magnetic particle) to binder ratio, which determines the proportion of the binder at the surface of the tape.

			XPS survey of elements detected and the percentage atomic concentrations [AT]% at the surface of virgin DDS-2 (M120), DDS-3 (M125 and F125) tapes									
Tape Type	Condition	TOA	Na	Fe	O	N	Cl	Y	P	Si	Al	C total
DDS-2 (M120)	Virgin	0	4.30	6.86	29.55	1.07	5.76		0.30	2.25	5.48	44.46
DDS-3 (F125)	Virgin	0	3.21	4.22	27.79	1.23	6.46	3.19	0.76		6.39	46.73
DDS-3 (M125)	Virgin	0	1.71	4.74	30.20	1.19	3.24	3.42	0.58		8.08	46.85
DDS-2 (M120)	Virgin	70	4.77	5.52	24.73	1.13	6.60		0.58		5.76	50.91
DDS-3 (F125)	Virgin	70	3.35	3.18	23.08	0.63	5.98	3.21	1.14		6.06	53.35
DDS-3 (M125)	Virgin	70	1.96	2.87	22.45	1.46	4.12	2.85	0.35		6.88	57.05

Table 14 showing the XPS survey of all elements detected and average percentage atomic concentrations [AT%] at the surface of virgin DDS-2 (M120), and DDS-3 (M125 and F125) tapes.

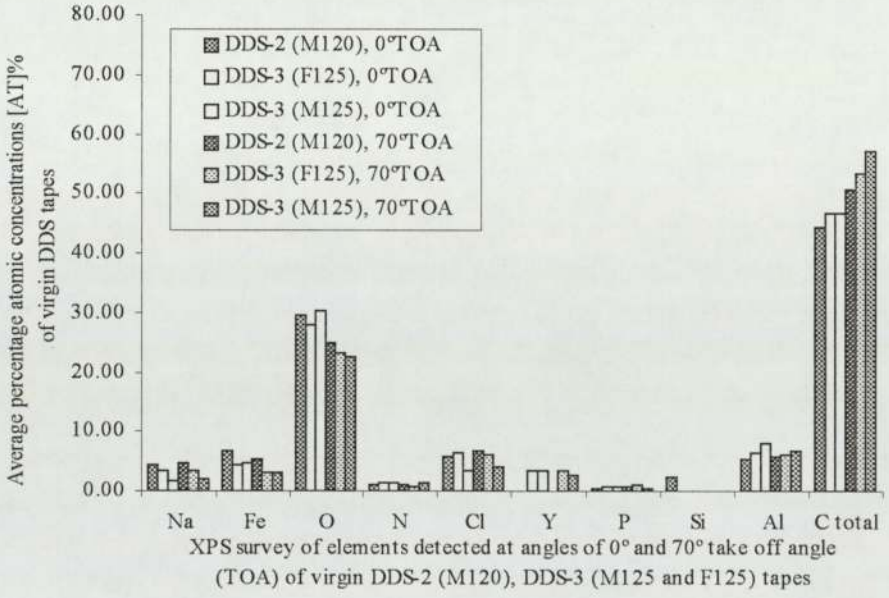

Figure 70 showing a bar chart of the XPS survey of all elements detected and average percentage atomic concentrations [AT%] at the surface of virgin DDS-2 (M120), and DDS-3 (M125 and F125) tapes.

Table 14 shows iron Fe (which normally is in the form of gamma iron oxide γ-Fe_2O_3) is common in the DDS-2 format and the highest iron Fe signal was from DDS-2 (M120) tape at 0° TOA with a value of 6.9 [AT%]. Whereas for DDS-3 the iron oxide detected is lower then for DDS-2 suggesting that smaller magnetic particles were used, which is in this case was metal particle (MP). The element aluminium Al, normally in the form of Al_2O_3 is identified as the head-cleaning agent (HCA), which is used primarily as a bearing surface as

well as for removing stain of tape debris. This element is common to all tape types. This result is approximately the same for all tape types. C total is referred to the total amount of carbon C detected, which is shown to be the highest of all the signals detected in the XPS survey of all the tape types. The element oxygen O is normally associated with the oxide components of iron Fe and aluminium Al, and possibly with the binder and/or lubricant. The elements nitrogen N and sodium Na are mainly associated with the durable (hard wearing) polyurethane component of the binder whereas chlorine Cl is associated with the poly-vinyl-chloride PVC that gives the tape binder flexibility.

			Carbon synthesis [AT]% of virgin DDS-2 (M120), DDS-3 (M125 and F125) tapes						
Tape Type	Condition	TOA	CAR	C-Cl	C-O	C-Cl/N	C-C	Fe/N	C total
DDS-2 (M120)	Virgin	0	1.97	2.89	4.67	3.94	30.99	6.43	44.46
DDS-3 (F125)	Virgin	0	1.15	3.39	2.53	4.66	35.00	3.43	46.73
DDS-3 (M125)	Virgin	0	1.61	1.61	2.94	2.86	37.84	3.97	46.85
DDS-2 (M120)	Virgin	70	1.98	3.29	4.01	4.60	36.99	4.90	50.91
DDS-3 (F125)	Virgin	70	2.12	3.02	3.66	3.66	40.89	5.03	53.35
DDS-3 (M125)	Virgin	70	1.51	2.08	1.63	3.54	48.29	1.96	57.05

Table 15 showing the carbon synthesis calculated in average percentage atomic concentrations [AT%] of virgin DDS-2 (M120) tape, DDS-3 (M125 and F125) tape. CAR is Carboxyl O=C-O molecule which originates from the binder, whereas C-Cl and C-N is from the binder. C total is the total amount of Carbon C detected in XPS survey. The ratio Fe/N is the iron (magnetic particles)/binder ratio and C-C is the total amount of carbon, which is independent to the rest of the tape system. C Total – (C-C) is the carbon difference, which is distributed between the binder and lubricant. TOA is the take off angle that is the angle where the auger electrons are collected relative to the normal to the sample surface.

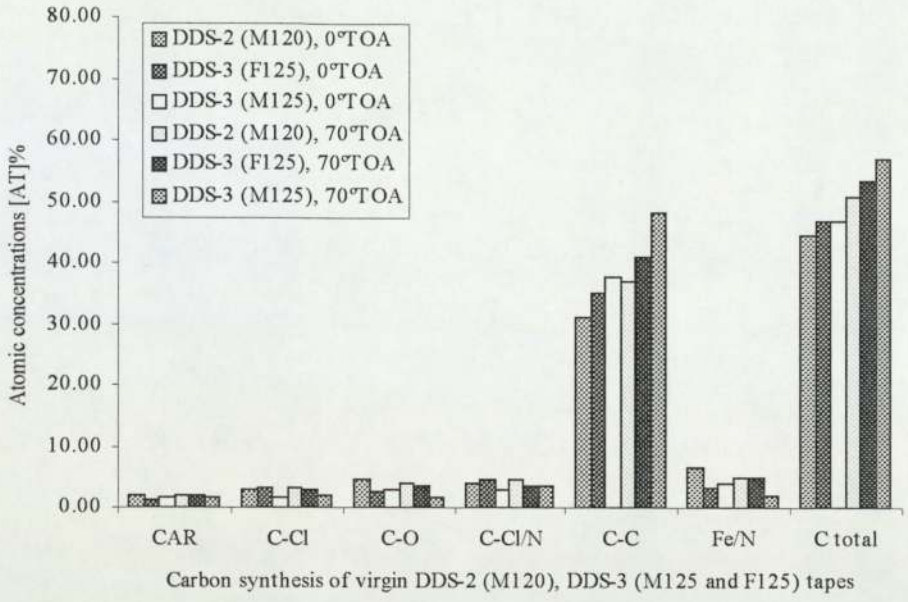

Figure 71 showing a bar chart of the carbon synthesis calculated in average percentage atomic concentrations [AT%] of virgin DDS-2 (M120) tape, DDS-3 (M125 and F125) tape.

Both of these elements are again common with all of the tape types shown in table14. XPS survey as revealed a further two elements; firstly yttrium Y has been detected with the DDS-3 format (M125 and F125) which is a double layered tape; and secondly silicon Si was detected with the DDS-2 (M120) format only which is a single layered tape. The origins and functions of yttrium Y and silicon Si are at unknown. The element phosphorus P was detected in all tape types as shown in table 14 and is used as a wetting agent.

Carbon synthesis of virgin DDS-2 (M120) and DDS-3 (M125 and F125) tapes, table 15, shows major differences in the DDS-2 and DDS-3 formats. The carboxyl molecule, which is the binder and lubricant, shows DDS-2 (M120) having considerable more binder/lubricant of 2.0 [AT%] at the surface of the tape than for the two DDS-3 (M125 and F125) tapes with 1.6 and 1.2 [AT%] respectively. The ratio Fe/N that is the iron (magnetic particles) to binder ratio shows that virgin DDS-2 (M120) tape has more iron (magnetic particles) at the surface of the tape then binder material and for the rest of the other tapes in table 15. The quantity of C-Cl/C-N, which is the binder to lubricant ratio for all tape types are shown to range from 2.9 [AT%] for DDS-3 (M125) at 0°TOA to the highest of 4.7 [AT%] for DDS-3 (F125) at 0°TOA. This shows there is more lubricant in DDS-3 tapes then for DDS-2.

3.2.8 The Stain thickness versus error rate with DDS tape type interchanging at 25°C/10%RH

The aim of these experiments were to determine the relationship between stain thickness and error rate with the effects of tape type interchanging at 25°C/10%RH using 10 seconds of DDS tape. Presented below is figures 72 to 75 show the error rate versus tape type interchange: M120-F125-M125-M120 at 25°C/10%RH. The suffixes: M120 is 120m of Maxell DDS-2, F125 is 125 m of Fuji DDS-3 and M125 is 125 m of Maxell DDS-2 tapes.

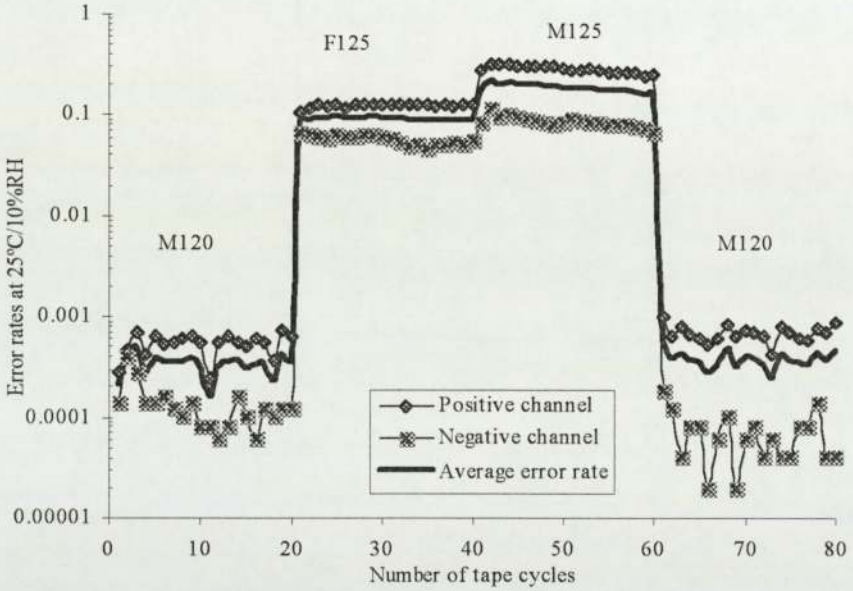

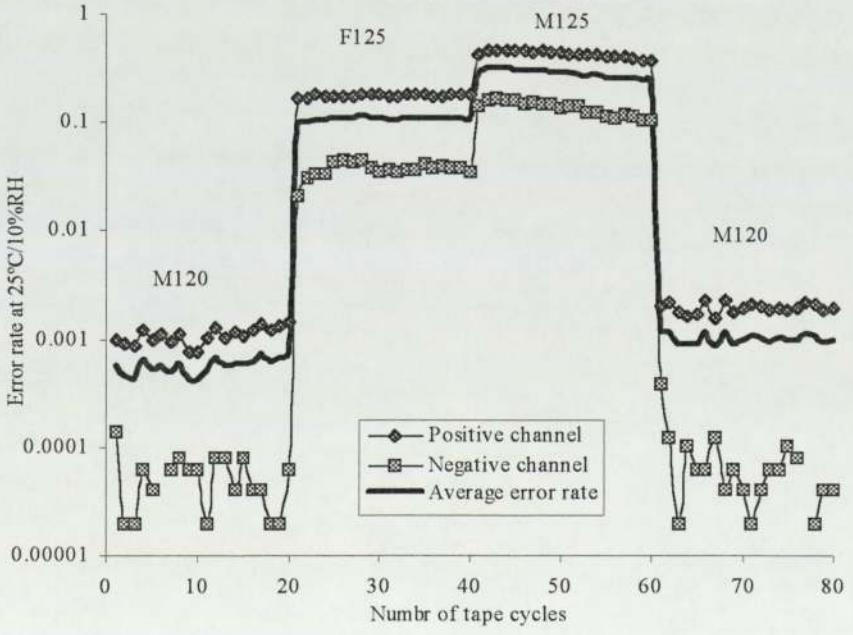

Figures 72 top and 73 bottom showing the error rate (Test 1 and 2) of tape type interchange cycling of M120-F125-M125-M120 at 25°C/10%RH respectively (1 tape cycle = 10 seconds = 0.15m).

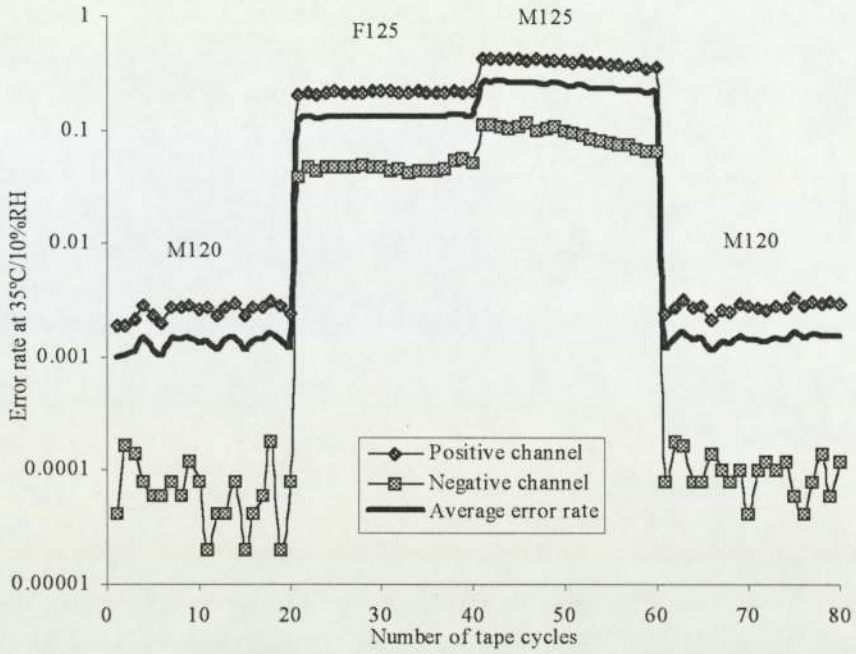

Figure 74 showing the error rate (Test 3) of tape type interchange cycling of M120-F125-M125-M120 at 25°C/10%RH respectively (1 tape cycle = 10 seconds = 0.15 m).

These results presented in figures 72-74 show a 'step' effect where a low error rate rapidly increases to a high value then after x number of tape cycles rapidly decreases again to a new lower error rate. The highest of the average error rates at 0.1 are the DDS-3 tapes: M125 and F125 and the lowest is the DDS-2 tape: M120 of 0.001, that is a factor of 100. This shows that the DDS-3 tapes are prone to higher error rates at low humidity which may suggest that they well of been considerable more stain on the head. The DDS-2 (M120) tapes on either side of the DDS-3 tapes show similar results but a slight increase in the error rate results was observed. Figures 72-74 also shows scattered error rate behaviour for the negative channel of DDS-2 (M120), whereas DDS-3 (F125 and M125) show a consistent stable and downward error rate result respectively for both channels.

Possible reasons for the differences in the error rate for the tape types are the differences in the thickness/formulation of the magnetic/binder layer system and the magnetic flux densities of the magnetic particles used in the magnetic/binder layer. Looking at the DDS-2 (M120) tape has a thick single magnetic/binder layer and large magnetic particles (γ-Fe_2O_3) with weaker magnetic flux densities of around 300 Oe was used but the error rates were lower then for the two DDS-3 tapes. Whereas a DDS-3 (M125) tape is a simple dual layer system consisting of a thinner magnetic/binder layer with smaller magnetic particles (metal particle) and stronger magnetic flux densities of around 1000 Oe resulting in lower

error rates but this was not observed due to the possible staining from the previous DDS-2 (M120) tape. The second layer which lies under the magnetic or binder layer of the DDS-3 (M125) tape system is for tape lubrication, Overall the dual layer DDS-3 tape system is considerably thinner and more flexible then the singular layered DDS-2 tape.

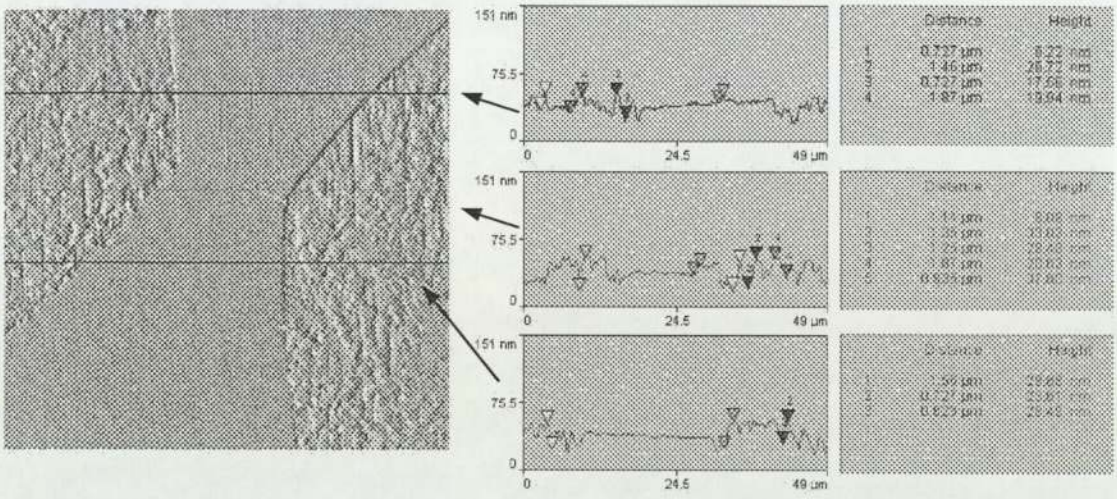

Figure 75 showing AFM scan and associated line scan of an inductive read head after tape type interchange cycling M120-F125-M125-M120 tape at 25°C/10%RH. (1 cycle = 10 seconds = 0.15 m). Any evidence of head curvature was removed by second order levelling before AFM analysis.

Figure 75 shows what it appear to be large amounts of staining on the glass region of the inductive head and at the trailing edge (the top section of the AFM scan). Staining in the form of straight line that is parallel to the direction of the tape was also evident at the top section of the AFM scan. To confirm staining on the head shown in figure 75, AES is required. The line scans of the head at the glass region; figure 75 has shown stain thickness was 17.56-37.60 nm, whereas at the ferrite region the stain thickness was 6.22 nm. When taking into account the curvature of head the stain seems to protrude above the ferrite resulting in a head-to-tape spacing and the increase in the error rate. The rippling effects evident in figure 75 were artefacts due to the stray laser light reflecting from the surface of the read head since the ferrite was highly polished and no staining was present.

To study the effects of error rate and the changes to the surface of the head a tape type interchange of two different DDS formats: DDS-2 and DDS-3 from the same manufacture: Maxell at 25°C/10%RH (dry atmosphere) was implemented. The error rate results presented in figures 76-77 show a similar 'step' effect as in figures 72-74. For DDS-2 (M120) tape an error rate scattering for both channels was evident, which averaged at around 0.0001 and DDS-3 (M125) tape showed a decrease in the error rate. Again the average error

rate of 0.05 for DDS-3 (M125) tape was higher then for DDS-2 (M120) tape due to previous tape and head staining.

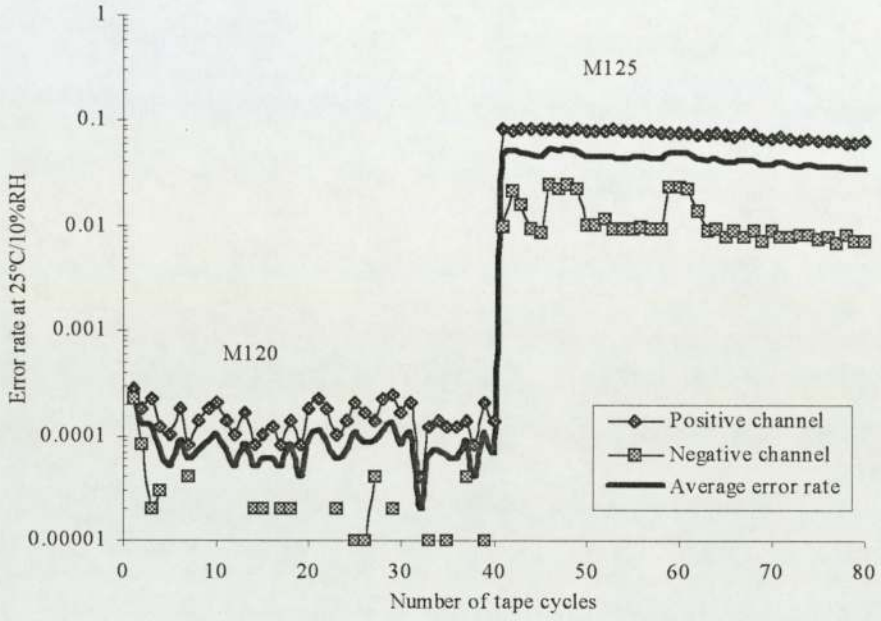

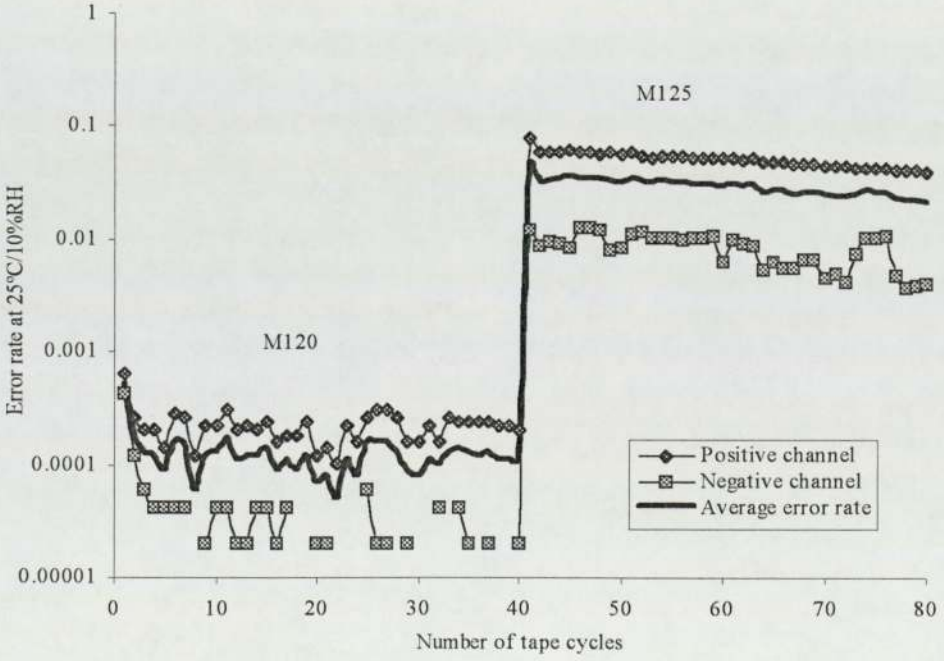

Figures 76 top and 77 bottom showing the error rate (Test 1 and 2) of tape type interchange cycling of M120- M125 at 25°C/10%RH (1 tape cycle = 10 seconds = 0.15 m)

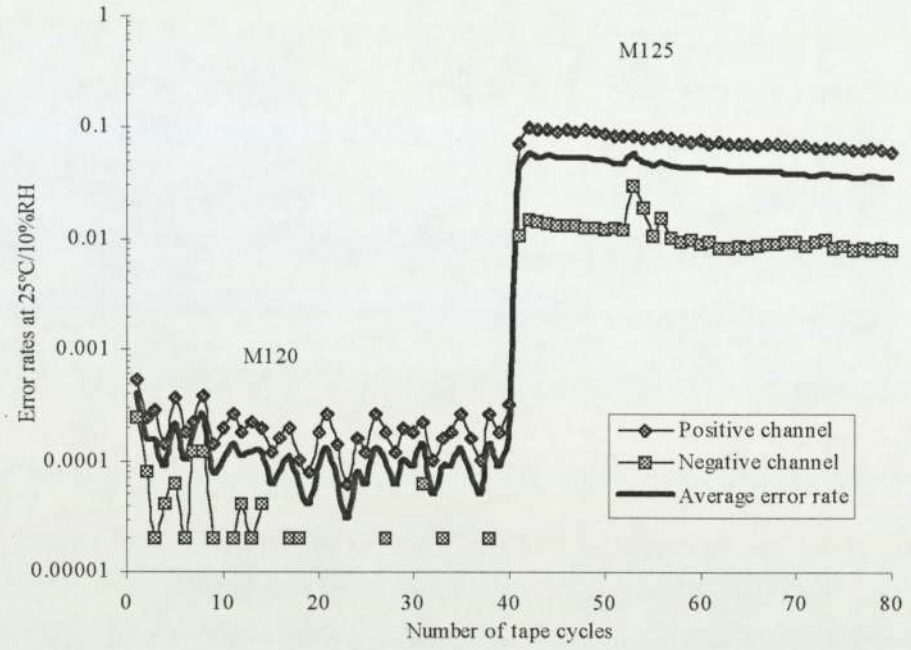

Figure 78 showing the error rate (Test 3) of tape type interchange cycling of M120- M125 at 25°C/10%RH (1 tape cycle = 10 seconds = 0.15 m)

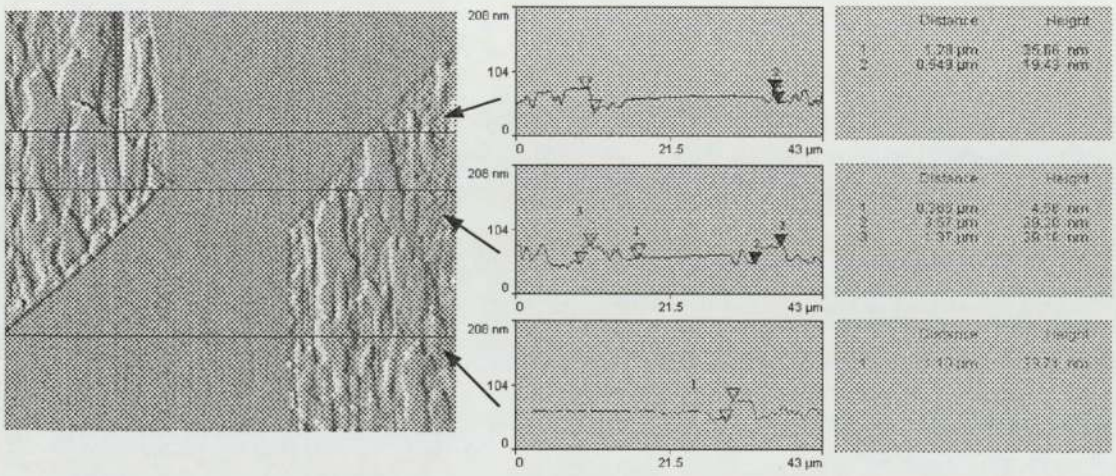

Figure 79 showing an AFM scan of an inductive read head after cycling DDS-2 (M120) to DDS-3 (M125) tape at 25°C/10%RH (1 cycle = 10 seconds = 0.15 m). Any evidence of head curvature was removed by second order levelling before AFM analysis.

AFM scan of the inductive read head shown in figure 79 has revealed even larger stain deposits and abrasion marks at the glass region of the read head only. Staining in the form of a 'stepping stone' was evident at the gap, which measured at around 5 nm in thickness (a 0.5 dB spacing, where 1 dB = 10 nm). Again, to confirm staining on the head shown in figure 75, AES is required. The 'stepping stone' is where pieces of tape debris have

adhered to the glass material within the head gap. Some of this stain will have broken away from the gap and created a stepping-stone.

At the glass region of the head, stain was again more apparent with complete coverage, which probably projected above the ferrite. The thickness of this stain was from 19.43-33.71 nm at glass region of the head. Figure 78 shows abrasive marks on the ferrite region that are parallel to the direction of the tape but no stain was evident. The AFM scan of the read head figure 75 showed smaller stain deposits on the glass region than for figure 79.

Figure 80 shows error rate of an additional experiment to determine the behaviour of DDS-3 (M125) tape when subjected to a 400 tape cycle, where each error rate measurements was made every 10^{th} tape cycle and each tape cycle = 10 seconds = 0.15 m as before. The results presented in figure 80 show a constant average error rate of 0.01 and this error rate follows a polynomial function to the power of 2.

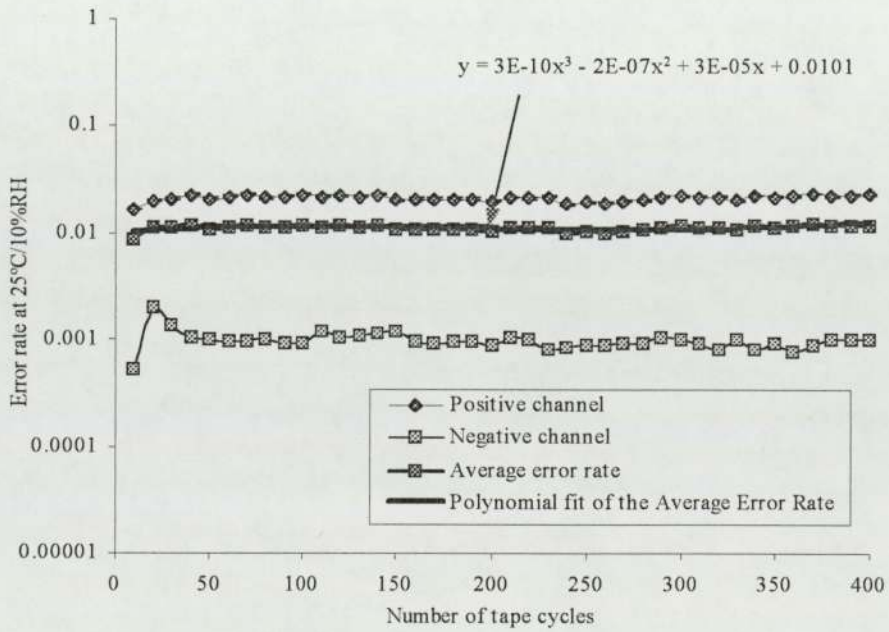

Figure 80 showing the error rate of DDS-3 (M125) tape after 400 cycles at 25°C/10%RH (1 cycle = 10 seconds = 0.15 m). Error rate recorded every 10^{th} tape cycle

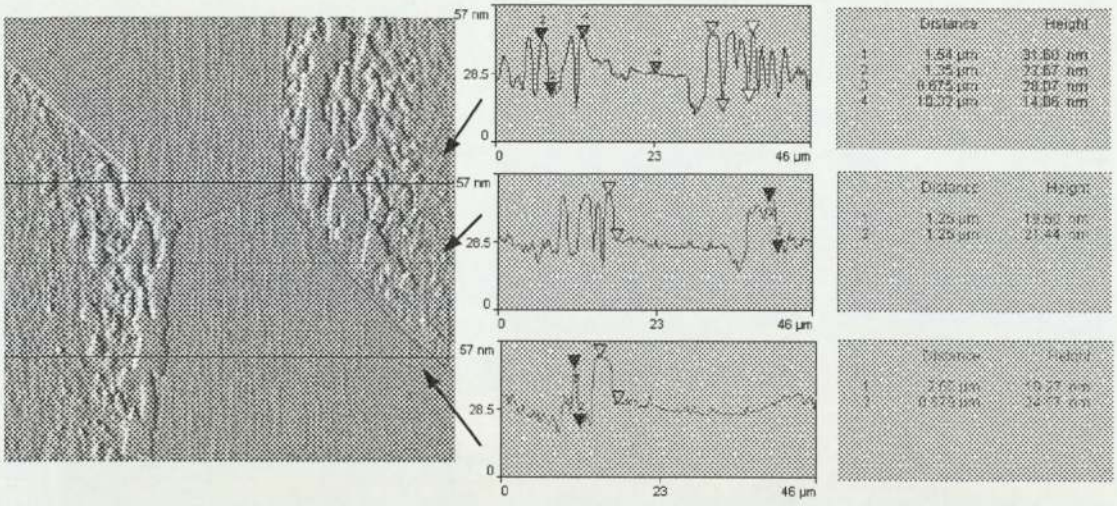

Figure 81 showing an AFM scan of and inductive read head after 400 cycles of DDS-3 (M125) tape at 25°C/10%RH (1 cycle = 10 seconds = 0.15 m). Any evidence of head curvature was removed by second order levelling before AFM analysis.

Figure 80 showed no increase in the error rate, whereas the AFM scan of head, figure 81 showed greater areal coverage of stain at the ferrite and glass region of the head. The stain thickness at the glass region was from 14.86-31.60 nm, which appears to protrude above the ferrite at around 15 nm as indicated by the associated line scans when taking into account of any curvature. Staining was the most dominant at the trailing edge of the read head, where stain was shown to radiate from the gap and in the direction parallel to the tape. Accumulation of stain was observed at the glass and ferrite interface, which peaked to around 32 nm.

Chapter 4 The Discussion

The repeatability testing conducted at 25°C/35%RH, gave consistent error rates for the most of the drives examined. One drive in particular, figures 30 to 32, shows on an error rate of around 0.01 to 0.0001 for both channels (negative and positive). Initially from 0-10 tape cycles, the error rate for the negative channel showed a decrease from 0.001 to 0.0001 followed with a gradual increased to 0.001 after 60 tape cycles. This suggests that the head contour or head shape has changed according to the tape type used and the environmental condition the tape was operated at, in this case the tape type DDS-3 (M125) at 25°C/35%RH. The AFM scans of the read heads of three DDS-3 tape drives after repeatability testing (60 tape cycles at 25°C/35%RH), figure 33 shows patchy deposits on the glass region and abrasion marks on the ferrite region. These abrasion marks were due to the head-cleaning agent (HCA) and the magnetic particles used in the magnetic/binder layer.

Initially, staining experiments conducted where virgin DDS-2 (M120) tape was cycled a few times (1 cycle = 20 seconds = 0.15m) at 25°C/35%RH to determine whether staining does occur after a few short tape cycles. The AFM scans figures 34 to 36, show some changes to the surface topography of the read head after few tape cycles, such as staining and deep abrasion marks on the glass region due to the head-cleaning agent (HCA) and magnetic particles from the tape. These abrasion marks were mostly observed on the glass region then on the ferrite, since the glass region is softer then the harder ferrite region. This results in deep abrasion marks on the glass region and smaller marks on the ferrite region. These abrasion marks come primarily from the reconditioning process at 25°C/80%RH, where the whole of the tape (120 m = 1 tape cycle) was used. Thus after a few tape cycles (where 20 seconds = 1 cycle = 0.15m), the tape used has little effect on the surface contours of the read head. The AFM line scans of the average stain thickness at the glass region has revealed a small difference of 2.72 nm after 4 tape cycles, where a reconditioned head was 21.72 nm and after 4 tape cycles was 24.44 nm.

To confirm staining on the glass region of the head after a few tape cycles, Auger Electron Spectroscopy AES survey was conducted to detect any elements present on the head. Table 4 shows iron Fe was detected at the glass region, which confirms the presence of staining and correlates with the research of Chandler [1], Stahle [4] and Talke [5]. The AES survey shows that staining is primarily made of gamma iron oxide γ-Fe_2O_3 (magnetic particles) deposited from the surface of the tape onto the glass and ferrite regions of the head and occurs after a few tape cycles. The atomic concentration of iron Fe at the ferrite region is

higher then the glass region due the total sum of the ferrite in the form of iron oxide Fe_3O_4 at the surface of the head and the stain. Silicon Si was also detected at the glass region since this region is mainly composed of silicon oxide. Table 4, shows that there were large amounts of carbon C and oxygen O detected on the glass and ferrite regions of the head. Carbon C may be due to surface contamination from the atmosphere and oxygen O was identified from the oxide component of silicon Si at the glass region and iron Fe at the ferrite region. The element aluminium Al (in the form of aluminium oxide Al_2O_3, which is commonly known as the head-cleaning agent HCA) was not detected as part of the stain as to the findings of Chandler [13], Stahle [14] and Talke [17] who has reported small amounts of Al within the stain. The possible reason for not detecting any aluminium Al as part of the stain is that the tape manufactures have introduces only small amount of around 5% within the binder, thus reducing the chances of any aluminium Al deposits detected as part of the stain. The main purpose of the head-cleaning agent was to remove stain by reducing the prosperity of staining and to act as a bearing surface. Consequently, Bhushan [4] has reported that as you increase the amount of aluminium oxide (HCA) within the tape binder, signal reproduction was improved with the removal of stain at the expense of higher abrasive head wear. However, there seems to be a limit to improving the signal quality by increasing the HCA or tape roughness. Therefore, a compromise was to reduce stain prosperity and head wear with good signal reproducibility. The elements: nitrogen N and chlorine Cl associated with the binder was not detected due to the limitations of AES used in this chemical analysis.

Increasing the number of tape cycles to 5000 of DDS-2 (M120) tape at 25°C/35%RH at tape intervals of 1, 10, 100, 1000 and 5000 have shown a progressive increase in the stain areal coverage at the glass region of the read head only. As the stain areal coverage increases significant changes to the structure and texture of the stain with the increase in tape cycling was observed. The greatest increase in the stain areal coverage at the glass region was observed from 10 to 100 tapes cycles, where the whole of the glass region was covered. After 100 tape cycles the stain texture changed from a few large lumpy deposits to many small particles at 5000 tape cycles.

Abrasive wear in the form of thick lines lying parallel to the direction of the tape at intervals of 1, 10, 100, 1000 and 5000 tape cycles at 25°C/35%RH was evident on the ferrite and more so on the glass region of the read head. The abrasive wear – can be referring to as the 'ploughing effect', where significant at the glass region due to the harder particles such as the head cleaning agent and the magnetic particles used in the magnetic tape removing the softer glass material from this region.

Comparing an AFM scan of a reconditioned read head figure 39 with figure 40, staining in the form of large 'lumpy' deposits at the glass region after 1 tape cycle at 25°C/35%RH was evident. AFM line scans analysis of the stain thickness at the glass region after 1 tape cycle in figure 40 was measured at around 17-30 nm. Further tape cycling at intervals of 10, 100, 1000 and 5000 tape cycles, show no significant change in the stain thickness. After 5000 tape cycles figure 44 shows tape debris deposited along the direction of the tape and staining occurred mainly at the glass region of the head. This suggests that the surface adhesion forces at the surface of the glass and tape interface are considerably higher then at the surface of the ferrite and tape interface. At the ferrite region of the head, the surface adhesion forces between the head and tape appears to be very weak, so any staining occurring at this region is easily removed by the tapes head cleaning agent. The nature of these adhesion forces is unclear, but is related to the surface intermolecular forces of the tape and surface of the read head at the ferrite and glass regions.

Lets assume that humidity and temperature can affect the surface adhesion force (that is the intermolecular forces) between the head and tape interface, so that at higher humidity (25°C/35%RH) the surface adhesion force decreases so probability of finding stain on the head decreases which correlates with the results. At low humidity (40°C/10%RH) the surface adhesion increases resulting in the increase in the probability of finding stain on the head, which again correlates with the results. This shows that the surface adhesion forces between the polymeric binder (the tape surface) and the glass and ferrite regions of the read head is influenced by humidity (water vapour). It appears that the water molecules within the water vapour saturate the surface bonds of the tape and head resulting in the reduction of the adhesion forces between the tape and head. Further research needs to be conducted to determine how the humidity effects staining.

The line scans of figures 40 and 41 show a curved surface at the ferrite region of the read head even after AFM second order levelling. This is where the AFM 'second order' levelling routine has failed in levelling the head curvature, due to the physical nature of the head. That is the head is curved in two directions: this being parallel and perpendicular to the direction of the tape along the head. With this dual curvature the AFM tip scanning along the head curvature on large area of 100 μm^2 problems occurred when keeping the tip at a constant distance away from the surface of the head resulting in the AFM tip missing surface features. This problem made it difficult in obtaining good AFM scans of the head. On an occasion, several attempts were made in reaching an optimum position of the AFM tip with the head curvature in a given area so that a good AFM scan can be produced.

The AFM scans at 40°C/10%RH (at low humidity) after 5000 tape cycles using DDS-2 (M120) tape, figure 49, shows considerable more stain on the glass and ferrite region of the read head when compared with the equivalent number of tape cycles at 25°C/35%RH (at ambient humidity). Comparing figure 42 with figure 48 at 100 tape cycles, large lumpy stain with a thickness from 15-23 nm as shown by the line scans was observed on the glass region of the read head. As the tape was cycled from 100 to 1000 tape cycles, staining occurred on both the glass and ferrite region of the read head with an approximately 100% areal coverage as shown in figure 49. The thickness of this stain was measured from 30-50 nm at the glass and ferrite regions as indicated by the line scans and a significant increase in the stain thickness was measured. After 5000 tape cycles, figure 50, again there was no change in the stain areal coverage but an increase in the measured stain thickness from 40-90 nm. The highest of the stain thickness measurement was 95 nm at the glass region of the head. At 25°C/35%RH for the equivalent number of tape cycles and at higher humidity (that is higher concentration of moisture or water vapour), staining was observed at the glass region of the head only and no significant increase in the thickness of the stain.

Taking these measurements an average stain thickness was calculated for tape intervals of 1, 10, 100, 1000 and 5000 cycles (1 tape cycle = 2 minutes = 1.8 m) on the glass and ferrite regions of the head for 25°C/35%RH and 40°C/10%RH (low humidity). For the average stain thickness at 25°C/35%RH as its shown in table 5 an increase from 16.5 nm at 1 tape cycle, which peaked to 25.0 nm after 10 tape cycles. After 10 tape cycles (from 100 to 5000 tape cycles) the average stain thickness decreased to 18.7-20.1 nm, which shows that the stain thickness remains constant throughout the history of the head. Table 5 shows all the three drives tested that the stain thickness at the glass region was 21.5-21.3 nm after 1 tape cycle then increased of 23.2-26.2 nm at 10 tape cycles. Further tape cycling showed a small decrease to 19.1-20.0 nm after 100 tape cycles. These results show an increase in the average stain thickness of around 10 nm at intervals of 1 to 10 tape cycles that most of the staining at 25°C/35%RH occurs at the start of tape cycling. This is the point where most of the tape debris was produced with the removal of surface asperities of virgin DDS tape at the point of contact resulting in the tape smoothing. After 10 tape cycles this initial staining is removed by the tapes head-cleaning agent since the surface adhesion force between the tape and glass region of the head may be weak at 25°C/35%RH. Overall results presented in figure 50 show an average stain thickness of 20.0 nm with a fluctuation of 16-25 nm at 25°C/35%RH from 1-5000 tape cycles of DDS-2 (M120) tape. This showed no significant change to the stain thickness at 25°C/35%RH. On the other hand the average stain-to-ferrite separation measurements at 25°C/35%RH, table 6, the results show an average stain-to-ferrite separation of 6.3 nm from 1-5000 tape cycles, which fluctuates from 4-8 nm. This translates to a spacing

of < 1 dB (where 10 nm = 1 dB spacing). With a spacing loss of < 1 dB, a low error rate measurements is expected.

The average stain thickness at 40°C/10%RH table 7 and figure 53 shows a progressive increase in the stain thickness on the glass and ferrite regions of the read head as the tape was cycled. The greatest increase in the average stain thickness occurred at the glass region, which peaked to 45.2 nm after 5000 tape cycles, whereas at the ferrite the stain thickness peaked to 21.5 nm, which is less than half at the glass region. Two possible reasons for the greater stain thickness at the glass region may be (1) due to the physical dimensions of the head, which is curved in a parallel and perpendicular direction to the tape; and (2) the head protrusion from the surface of the rotating drum.

At the glass region of the read head at 40°C/10%RH after 1 tape cycle of DDS-2 (M120), figure 53 and table 7, staining occurred only on the glass region with an average thickness of 17.5 nm. Further tape cycling showed average stain thickness at the glass region continued to increase from 20.0 nm for 10 tape cycles to 23.81nm for 1000 tape cycles. The biggest increase in the average stain thickness was from 23.8 nm after 1000 tape cycles to 45.2 nm after 5000 tape cycles at the glass region. Since the stain thickness continues to increase further cycling may be required to determine whether the average stain thickness reaches an equilibrium state. That is the rate of stain removal is equal to the rate of stain deposition so no increase in the stain thickness. It appears that the rate of stain removal is lower than the rate of stain deposition, resulting in the increase in the average stain thickness. This increase in the average stain thickness, may suggest that the adhesion force between the stain and the surface of the tape are strong indicating that the stain may also contain binder and/or lubricant material (which are the organic components of the tape) as well as the iron oxide (the magnetic particles from the tape) as detected by the AES survey. Possibly, this binder material initiates the staining process so that the stain can easily adhere to the surface of the head. Subsequently, this initial thin layer of stain increases the adhesion force between the surface of the tape and the stain, resulting in the further removal of a thin layer of tape. This thin layer of tape is deposited on top of the previous layer of stain, thus increasing the average stain thickness as the tape is cycled over the same length of tape.

At the ferrite region, 40°C/10%RH, figure 54 and table 7 showed a situation where the rate of stain removal is approximately equal to the rate of stain deposition at the ferrite region of the inductive head. At this point the average stain thickness reached 16.7 nm after 1000 tape cycles of DDS-2 (M120) tape. Further tape cycling, that is after 1000 tape cycles the rate of stain removal is approximately equal to the rate of stain deposition, resulting in a

gradual increase in the average stain thickness from 16.7 nm to 21.5 nm at 5000 tape cycles. Tape cycling beyond 5000 tape cycles say to 10000 tape cycles may be justified in determining whether an equilibrium point could be reached. Tape cycling beyond 5000 tape cycles may increase the chance of tape breakage due to the thinning of the tape and is beyond the predicted lifetime of the tape.

Clearly from the results of the average stain thickness versus number of tape cycles at 25°C/35%RH and 40°C/10%RH that the average stain thickness is a function of (or dependent on) the humidity, temperature, number of tape cycles and the tapes abrasivity (= head wear rate). At 25°C/35%RH (medium humidity) no change in the stain thickness was measured at the glass region as the tape was cycled and no stain was found on the ferrite and gap regions of the head due high head wear rate. Thus the average stain thickness is independent of the number of tape cycles. Whereas at 40°C/10%RH (low humidity), an increase in the stain thickness at the glass and ferrite regions of the head was measured as the tape was cycled and the tapes abrasivity (= head wear rate) has decreased indicating that the average stain thickness is dependent on the humidity, temperature, and the tapes roughness or abrasivity.

Using the average stain thickness results at 25°C/35%RH and 40°C/10%RH a relationship between the average stain thickness and the error rate can be determined if any. The results presented for 25°C/35%RH show no increase in the error rate for drive 1, whereas a gradual increase in the stain thickness was observed. Figure 58; drive 7 shows a gradual increase in the error rate after 500 tape cycles and no increase in the stain thickness were measured. In the case for 25°C/35%RH there appears to be no relationship between error rate and average stain thickness. Possible reason for this is that only the head contours have changed which influences the error rate since only small amount of stain was found only on the glass region of the head.

In contrast at 40°C/10%RH, the error rate gradually increases as the tape is cycled, figures 59-62, which corresponds to the increase in the stain thickness at the glass and ferrite region of the head. Chandler [13] has shown similar results where the increase in the stain thickness results in the increase in the error rate at low humidity and as the tape was cycled. Figure 59 shows a rapid increase in the error rate to around 0.05 from 1000 to 1500 tape cycles for the positive channel, and decays slowly from 1500 to 2500 tape cycles. This error rate increase suggests that tape debris build-up between the head and tape may be the culprit. This tape debris build-up is then removed again to a point where the error rate for the positive channel catches up with the negative channel after 2500 tape cycles and then each channel

follows the same error rate trend. The negative channel has also suffered from similar behaviour but a smaller increase in the error rate from 1000 to 1500 tape cycles was measured. One drive in particular in this testing, figure 61 showed an error rate trend similar to the average stain thickness at the ferrite region of the head at 40°C/10%RH, but recorded numerous maximum error rate of 1.000 from 600 to 5000 tape cycles. This may suggest that tape debris as well as some staining between the head and tape may be the cause, since tape debris attaches itself to the head temporary then is easily removed after a few tape cycles.

At the start of tape cycling a high initial error rate of 0.001 and 0.01 respectively was measured, which decays to 0.001-0.0001 after a few hundred-tape cycles at 25°C/35%RH. This appears to correlate with the high initial stain thickness that decays rapidly as the tape was cycled. At high temperature and low humidity, 40°C/10%RH, figures 59, 60 and 62, the initial error rate and stain thickness decay was smaller for 25°C/35%RH after a few hundred-tape cycles. Possible reason for this may be the change in the shape of the head as the tape was cycled.

With averaging of all the error rate measurements from 1 to 5000 tape cycles for the positive and the negative channels at 25°C/35%RH and 40°C/10%RH, table 9, an overall average error rate for 25°C/35%RH was 0.0007 and 40°C/10%RH was 0.0661, which is around 100 times larger than the error rate results for 25°C/35%RH. This was mainly due to the large number of recorded error rates with the value of 1. The average error rates results for 25°C/35%RH and 40°C/10%RH show a correlation with the AFM results for the average stain thickness. At 25°C/35%RH stain deposits was found on the glass region only with an average stain thickness of 6.33 nm. Taking into account the geometry of the head and no stain was seen on the ferrite region intimate contact between the ferrite/gap regions and tape was achieved at 25°C/35%RH resulting in smaller average error rate. Whereas for 40°C/10%RH, considerable more stain was found on the glass and ferrite regions of the head including the head gap. The average stain thickness at these regions was measured at 26.2 nm and 9.3 nm (approximately 1dB spacing) respectively; so higher the spacing between the ferrite/glass/gap regions of the head and the tape, resulting in a higher average error rate of 0.0661.

The head wear rate (measured nm/m) is an important factor that relates to the tape abrasivity (depending on tape type) which controls the amount of staining on the head, where the distribution and the thickness of the stain depends on the operating conditions: humidity and temperature. The results presented for 25°C/35%RH and 40°C/10%RH, show large differences in the head wear rate at the ferrite region. For example at 100 tape cycles at 25°/35%RH, figure 63, shows the average head wear rate of $3.57*10^{-1}$ nm/m was

considerably higher then $2.09*10^{-1}$ nm/m at 40°C/10%RH for the equivalent number of tape cycles. The results presented for 25°C/35%RH is expected since the AFM has shown no stain on the ferrite, so higher the average head wear rate that correlates with the observed abrasion marks. For 40°C/10%RH staining was present on the ferrite region, suggesting that the layer of staining on the ferrite is acting as a protective layer so reducing head wear and prolonging the operating lifetime of the head.

Further tape cycling to 1000 tape cycles has shown that the average head wear rate distribution has decreased at the leading and trailing edge of the head for 25°C/35%RH and 40°C/10%RH. Figure 63 has shown higher wear rate at the gap region and at the leading edge of the head for 25°C/35%RH, resulting in a higher calculated average wear rate of $2.27*10^{-2}$ nm/m. Whereas, at 40°C/10%RH the head wear rate was evenly distributed along the head as shown in figure 64 and was calculated at an average wear rate of $2.45*10^{-2}$ nm/m. Comparing the average wear rates for 25°C/35%RH and 40°C/10%RH at 1000 tapes, table 9, showed a negligible difference (of $0.18*10^{-2}$ nm/m) in the head wear rates. The AFM scans of the two heads at 1000 tape cycles, 25°C/35%RH and 40°C/10%RH, figures 43 and 49 which used the same tape type have shown no stain on the ferrite at 25°C/35%RH, whereas at 40°C/10%RH stain was found on the ferrite with an average thickness of 16.7 nm.

Increasing the tape cycling to 5000 tape cycles, the average head wear rates for 25°C/35%RH and 40°C/20%RH, were calculated as $2.43*10^{-2}$ nm/m and $3.96*10^{-3}$ nm/m ($0.396*10^{-2}$ nm/m) respectively resulting in a difference of the order of $2.394*10^{-2}$ nm/m. The average wear rate appears to be greatly influenced by the amount of staining deposited and the humidity/temperature combination. So for 40°C/10%RH, a thick layer of stain (of thickness of 21.47 nm at the ferrite region, table 7), which covered the whole of the ferrite and glass regions of the head as shown in figure 50, has greatly reduced the head wear rate. At 25°C/35%RH, no stain was detected (0 nm) on the ferrite after 5000 tape cycles, figure 44 so a substantial increase in the average head wear rate of $2.43*10^{-2}$ nm/m was measured.

By calculating of the average head wear rate at intervals of 100, 1000 and 5000 tape cycles the results presented in figure 65, shows curve fitting of the experimental obeys a power function. That is the average head wear rate, which is a function of the number of tape cycles, temperature and humidity is directly proportional to the power of the number of tape cycles. In mathematical terms this is can be expressed as:

$$\text{Average wear rate } (n, T, H) = A(T, H) * n^{B(T, H)} + C(T, H)$$

Where n is the number of tape cycles and A, B and C are constants which are a function of temperature T and humidity H. Power regression have shown that these constants A and B at 25°C/35%RH was A = A (25°C, 35%RH) = 22.806 and B = B (25°C, 35%RH) = -1.009 respectively, whereas at 40°C/10%RH, A = A (40°C, 10%RH) = 7.842 and B = B (40°C, 10%RH) = -0.703. The constant C =C (T, H) = 0 for 25°C/35%RH and 40°C/10%RH. The results shows that the constants $A > 0$, $B < 0$ and $C = 0$. In addition as the tape operating conditions were set at 40°C/10%RH less water vapour (or low humidity) was present in the tape drives operating environment, resulting in a decrease in the constants A and B and the average head wear rate per tape cycle. For the operating condition of 25°C/35%RH an increase in the water vapour (or higher the humidity) was evident, resulting in an increase in the value of these constants A and B since the average wear rate has increased per tape cycle. Further environmental conditions are required to determine whether this power function relationship is valid.

The results presented in figures 66 and 67 are used to determine whether there is a relationship between tape surface roughness and the average head wear rate at 25°C/35%RH and 40°C/10%RH during tape cycling. AFM scans of virgin and cycled DDS-2 (M120) tape were analysed and any physical changes that occur at the surface of the tape before and after tape cycling were noted. Firstly at 25°C/35%RH, the average RMS roughness measured after 5000 tape cycles at a scan area of 100 μm^2 are similar to the results for 40°C/10%RH. Secondly, both tables 10 and 11 have shown that virgin DDS-2 (M120) tape becomes smoother as the tape was cycled. For example at 25°C/35%RH area scans of 100 μm^2 at an angle of 0°, table 10 has shown an average RMS surface roughness R_a of 10.1 nm for virgin tape which decreases to a slightly smoother 7.0 nm after 5000 tape cycles. This suggests that highest of the tape asperities has been removed when the same length of tape is cycled repeatedly. Lastly, the surface roughness R_a measurements after 5000 tape cycles at 25°C/35%RH and 40°C/10%RH have shown similar surface roughness R_a when measured in either directions 0° and 270° at scan areas of 10 μm^2 and 100 μm^2. Overall these results show that the surface roughness is independent to the tape-operating environment since the surface roughness R_a results are similar. In addition as the tape becomes smoother the average head wear rate decreases during tape cycling confirming that tape roughness and head wear rate are linked.

The AFM scans of virgin and cycled DDS-2 (M120) tape at 25°C/35%RH and 40°C/10%RH figures 66 and 67 respectively have shown two distinct surfaces. At

25°C/35%RH, the tape surface after 5000 tape cycles figure 66(b) show a large number of dark circles spread randomly at the surface of the DDS tape. These dark spots are identified as lubrication pores. The main function of the lubrication pores is to act as a thin low friction layer between the tape and the surface of the head resulting in the reduction of head wear. To reduce the effect of spacing between the head and tape in addition to any staining deposited on to the head, the lubrication layer has to be as thin as possible. In addition there is a requirement where the lubrication layer needs to be replenished on a regular basis since the old lubrication layer is easily removed during tape cycling. To do this the lubrication diffuses through the binder via these pores thus replenishing the thin lubrication layer with a new one. This lubrication diffusion process is help by applying mechanical pressure, which is normally performed by high tape tension during tape-head contact.

At 40°C/10%RH, figure 67(b) shows fewer identified lubrication pores in comparison to figure 66(b), even though the results indicate that the average surface roughness R_a of cycled DDS tape at 25°C/35%RH and 40°C/10%RH were similar. The surface of AFM scan figure 67(b) also show that the surface is smoother than at 25°C/35%RH of the equivalent number of tape cycles since there were small number of lubrication pores present in this scan. Many surface scans of the tape are required to determine whether this AFM scan is a true representation. Assume that there was less lubrication pores present in this AFM scan this may indicate that there was less lubricant expelled to the surface of the tape.

AFM results was confirmed by Auger electron spectroscopy AES that staining occurred at the glass and ferrite regions of the read head after 5000 tape cycles of DDS-2 (M120) tape at 25°C/35%RH and 40°C/10%RH. The AES survey, table 13 has confirmed the AFM results with the iron Fe detected at the glass and ferrite regions of the read head, where stain is mainly composed of magnetic particles in the form of gamma iron oxide γ-Fe_2O_3 from the tape. At the glass region of the read head the AES survey for 25°C/35%RH and 40°C/10%RH has shown no silicon Si present. The main reason for this is that there were 100% areal coverage of staining on the glass region as confirmed by the AFM results so reducing the chances of detecting any silicon Si. Referring to table 13 again larger amounts of carbon C contamination was detected at 25°C/35%RH than at 40°C/10%RH even though an increase in the Argon etching time was required at 40°C/10%RH. The purpose of removing carbon contamination is to increases the element detection rate at the surface of the head. The differences in the amount of iron appears to correlate with the AFM results for instance at 40°C/10%RH the head was completely covered with stain after 5000 tape cycles resulting higher levels of iron Fe detected. Whereas at 25°C/35%RH AFM have shown small amounts

of stain at the glass region only which correlates with the smaller amount of iron Fe detected by AES. The element chlorine Cl normally associated with the binder was not detected with the AES survey. At 40°C/10%RH the AES survey, figure 69 have shown (1) there was more oxygen present at the glass and ferrite regions of the head then at 25°C/35%RH; (2) the amount of oxygen detected is higher at the glass region then at the ferrite region; (3) there was reduction in the amount of oxygen detected from head reconditioning at 25°C/80%RH to the head after 5000 cycles of DDS-2 (M120) tape at 25°C/35%RH and 40°C/10%RH. The possible reasons for more oxygen detected at 40°C/10%RH than at 25°C/35%RH is firstly more stain was present which is mostly made of iron oxide γ-Fe_2O_3. These deposits were detected on the ferrite and glass regions of the read head. Secondly a large proportion of the total oxygen detected by AES at the glass and ferrite regions is the oxide components of the ferrite and the glass regions. The remainder of the total amount of oxygen detected at the glass and ferrite regions of the head may be linked to the content of the polymeric binder and/or the lubricant used in the tape. Possibly this may be an indirect way in determining whether the binder is an integral component of the stain deposit. Thirdly, AES survey have shown a reduction in the amount of oxygen detected from a head reconditioning to a cycled head at 25°C/35%RH and 40°C/10%RH. Further investigation is required to understand the reason for the reduction in the amount of oxygen detected.

To correlate the elements detected at the surface of the head by Auger electron spectroscopy AES survey with x-ray photoelectron spectroscopy XPS surveys of various virgin DDS tape were conducted. It has been shown, table 14 that iron Fe is common in all tape types examined and the highest of iron detected was from DDS-2 (M120) tape at 0° TOA with a value of 6.9 [AT%], which is γ-Fe_2O_3 and is the most common magnetic particles used in this project. This correlates with the iron detected by the AES survey of the glass region of the inductive read head after 5000 tape cycles of DDS-2 (M120) tape at 25°C/35%RH and 40°C/10%RH. For DDS-3 tapes, the iron detected (4.2-4.7 [AT]%) was less than for DDS-2 tapes due to smaller magnetic particles (metal particles) was used in the binder. Aluminium in the form of aluminium oxide Al_2O_3 is common in all the tape types and is identified as the head-cleaning agent (HCA). The main functions of the head-cleaning agent HCA was to act as a bearing surface that offers greater tape durability (harder wearing) and to remove any staining/tape debris if any on the head. The AES survey has shown no evidence of aluminium oxide at the surface of the head due to low percentage atomic concentrations from 5-8 [AT]% for all tape types. The lowest amount of aluminium Al detected was 5.5-5.8 [AT]% for a DDS-2 (M120) tape suggesting that the chances of detecting aluminium Al of the read head after tape cycling were very small. The oxygen O is

normally associated with the oxide component of iron and aluminium, and possibly the binder and/or the lubricant, which are the organic or polymeric components of the tape. A proportion of the total oxygen detected with XPS at the surface of tape may be transferred to the head during tape cycling via the oxide component of the magnetic particles and the rest detected may indicate the transferral of binder and/or lubricant to the surface the head as part of the staining process. Nitrogen N is mainly related to the durable (hard wearing) polyurethane component of the binder. Chlorine Cl is a component of the flexible poly-vinyl-chloride PVC of the binder that allows the tape to conform to the shape of the inductive read head during tape cycling. Sodium Na is again part of the binder whose function is unknown. These elements are common to all of tape types analysed with XPS. XPS survey as detected a further two elements; firstly yttrium Y associated with the DDS-3 format (M125 and F125) which is a double layered tape; and secondly silicon Si associated with the DDS-2 (M120) format only which is a single layered tape. The function of yttrium Y and silicon Si are at unknown since the tape manufactures are unwilling to divulge such information. Lastly the element phosphorus P was detected in all tape types and is identified as the wetting agent.

Carbon synthesis of virgin DDS-2 (M120) and DDS-3 (M125 and F125) tapes, table 15, shows major differences in the two DDS-2 and DDS-3 formats. The carboxyl molecule, which is a component of the binder, shows DDS-2 (M120) having slightly higher concentration of 2 [AT%] at the surface of the tape than for the two DDS-3 (M125 and F125) tapes with 1.6 and 1.1 [AT%] respectively. The ratio Fe/N that is the iron (magnetic particles) to binder ratio shows that virgin DDS-2 (M120) tape has more iron (magnetic particles) at the surface of the tape than binder material and is the highest of the rest of the other tapes as shown in table 15. The reason for these results may be due to DDS-2 tape using larger magnetic particles then for the two DDS-3 tapes.

The relationship of stain thickness versus error rate with tape type interchanging at 25°C/10%RH figures 72-74 show a similar error rate stepping where a low error rate of 0.001 from a DDS-2 (M120) tape rapidly increases to a high error rate of 0.01 when changing from a DDS-2 (M120) tape to a DDS-3 (F125) tape. This was followed with another tape change to DDS-3 (M125) that resulted in a further increase in the overall error rate. It is clearly shown that the initial staining from the DDS-2 tape has increased the error rate for the DDS-3 tapes since no long head reconditioning was performed between tape types. The error rates for the DDS-2 tape have shown a gradual increase at the start and end of the tape type interchange experiment. The repeatability testing for the drives used in these experiments have shown a high degree of success where each successive test has produced similar results. These results also show that the tape structure and composition may be a factor that affects

the overall error rate. For example a DDS-2 tape has a thick singular magnetic/binder layer, which uses large magnetic particles with weak magnetic flux densities but lower error rates were measured at low humidity. This suggests that there were intimate contact between the head gap and the tape even though stain may be present. Whereas for the thinner double-layered DDS-3 tape system smaller magnetic particles with larger magnetic flux densities were used to increase the data recording density. Higher error rates were measured when cycling DDS-3 tape at 25°C/10%RH (low humidity) suggesting that the staining from the previous tape type interchange may be to blame. The AFM scan of the inductive read head figure 75 showed staining on the glass and ferrite region, but more stain was observed on the glass region. At this point there is a need to confirm by AES that was stain on the glass region of the inductive read head. The thickness of this stain was measured at 17.6-37.6 nm at the glass region and 6.2-9.1 nm (approximately 0.6 - 1dB spacing) at the ferrite region.

For a two-tape type interchange using the same manufacture such as Maxell DDS-2 (M120) and DDS-3 (M125) and under the same conditions as before. Figures 76-78 shows the same error rate step effect, but the AFM results figure 79 showed an abundance of stain on the glass and gap regions and none on the ferrite. The AFM results have revealed large stain deposits then the stain in figure 75 and abrasive marks are also evident at the ferrite region. The thickness of this stain was measured at 19.4-35.7 nm and was similar to the AFM results figure 75.

A single tape type interchange such as DDS-3 (M125) tape and an increase in tape cycling to 400 under the same conditions as before figure 80 shows an average stable error rate of around 0.01. This result did not correlate with the average error rate of around 0.1 figures 72-74 owing to the additional staining from the previous tape type interchange (DDS-2 (M120)) resulting in the increase in the overall error rate for the DDS-3 tapes. In addition, the drive was long reconditioned before the single tape type interchange for the purpose of the removal of any staining and to return the heads to its previous stable condition ready for the next batch of experiments. The AFM results, figure 81 shows staining on the glass and ferrite regions of the head. Mostly the stain was found in large lumps at the ferrite-glass boundary, close to and within the gap. At the ferrite region staining occurred as stripes, which are parallel to the direction of the tape. The thickness of this stain at the glass region was measured at 19.5-31.6 nm. This increase in the stain thickness and an increase in the error rate are expected as the tape was cycled. In this case as the tape was cycled staining has increased, no change in the error rate was evident.

Chapter 5 The Conclusions

The AES survey results show head stain consists mainly of magnetic particles, which are gamma iron oxide particles (γ-Fe_2O_3) transferred from the surface of a DDS-2 tape the deposited on top of an inductive read head. Organic components of the stain such as the polymeric binder and lubricant were not detected but the polymeric binder is believed to be the initiators of head stain.

The results presented show that head staining occurs after a few tape cycles and stain deposits are observed at the glass region for 25°C/35%RH and 40°C/10%RH. This shows that the surface adhesion forces between the tape/glass region and tape/ferrite are different in magnitude that is the surface adhesion forces between the tape and glass interface are stronger then at the tape and ferrite interface. At 25°C/35%RH (medium humidity), stain was easily removed from the ferrite region after further tape cycling due to weaker adhesion forces between the surface of the binder of the tape and the ferrite. At 40°C/10%RH (low humidity) more stain was deposited on the ferrite after further tape cycling and was harder to remove indicating an increase in the adhesion force between the surface of the tape and head.

Increasing the humidity or water vapour from 40°C/10%RH to 25°C/35%RH shows the adhesion forces between the surface of the binder of the tape and the glass and ferrite regions of the read head have decreased so no stain was found on the ferrite region and a reduction in the amount of stain found was on the glass region only. This gives the idea that the rate of stain deposition is less than rate of stain removal (depending on the abrasivity or surface roughness of the tape) at the ferrite region. Also it appears that by increasing the humidity or the amount of water vapour, the surface bonds of the binder of the tape becomes saturated with water molecules resulting in the reduction in the adhesion force between the surface of the head and tape. The opposite also occurs when the humidity (or water vapour) is decreased resulting in the tape surface adhesion forces increasing and less surface bond saturation of the tapes polymeric binder thus more stain was deposited on the head.

The results show that the error rate is approximately directly proportional to the average stain thickness at 25°C/35%RH and 40°C/10%RH. For 25°C/35%RH (medium humidity), the stain thickness at the glass region was constant and no stain was measured at the ferrite region as the tape was cycled resulting in a constant but small error rate. This indicates that the average stain thickness is independent on the number of tape cycles at 25°C/35%RH. Whereas for 40°C/10%RH (low humidity), the average stain thickness

increases at the glass and ferrite regions as the tape was cycled resulting in the increase in the error rate. The increase in the stain thickness at the glass region for 40°C/10%RH shows the rate of stain deposition is greater then the rate of stain removal. At the ferrite region, 40°C/10%RH, the stain thickness increases to a point where small changes in the thickness of the stain (an equilibrium point) were measured. At this point the rate of stain deposition is approximately equal to the rate of stain removal, so the measured stain thickness was approximately constant at the ferrite region. This condition also applies for 25°C/35%RH at the glass region but the stain thickness equilibrium point was reached earlier in the tape cycling then at 40°C/10%RH. Clearly from these results that the average stain thickness is dependent on the humidity, temperature, the number of tape cycles and the abrasivity of the tape (head wear rate).

Since the rate of stain removal is equivalent to the average head wear rate or tape abrasivity. Thus for 40°C/10%RH (high temperature/low humidity = low water vapour content), the average head wear rate per tape cycle is lower then at 25°C/35%RH (medium temperature/medium humidity = higher water vapour content) for the equivalent number of tape cycles. Possible reason for this is that head staining is acting as a protective layer at the ferrite region reducing head wear even though the results for tape roughness or abrasivity are similar for 25°C/35%RH and 40°C/10%RH. The results suggest that at 25°C/35%RH and 40°C/10%RH the average head wear is directly proportional to the power of number of tape cycles. The constants A, B and C which exists in the power function relationship are dependant on the humidity and temperature, whereas average head wear rate is a function of the number of tape cycles, humidity and temperature.

The tape surface roughness for 25°C/35%RH and 40°C/10%RH before tape cycling and after (5000 tape cycles) show there is relationship between tape surface roughness and head wear during tape cycling. At the start of tape cycling the tape surface roughness of virgin tape was very high which correlates with a high average head wear rate. As the tape was cycled the tape surface roughness decreases (smoother the tape becomes) and the resultant average head rate decreases. In addition the tape roughness or abrasivity are independent to the temperature and humidity after 5000 tapes cycles at 25°C/35%RH and 40°C/10%RH.

It was found that in most of the drives tested the error rate for 40°C/10%RH is directly proportional to cubic root of the number of tape cycles, whereas for 25°C/35%RH the error rate is directly proportional to power of the number of tape cycles. The constant A, B

and C used in these relationships are dependent on the temperature, humidity and the individual characteristics of the drives under test.

Chapter 6 Further Research

Further research in staining includes repeating these experiments by extending the range of humidity and temperatures such as 5°C/35%RH, 5°C/10%RH, 25°C/80%RH, 40°C/35%RH, 40°C/80%RH and 10°C/10%RH to understand how these conditions influences staining if any. The purposes of this proposal are to have a clear and wider picture on how the humidity, temperature, tape cycling and the length of tape used influences or effects staining on an inductive read head. Secondly to develop a predictive model based on the probability of finding stain on the head, the average thickness (related to head wear rate), and average error rate after a preset number of tape cycles at any humidity and temperature.

An accurate method of measuring the stain areal coverage could be devised to determine whether there is a relationship of stain areal coverage with average stain thickness and tape cycling.

Additional x-ray photoelectron spectroscopy XPS work is required to the study the chemical changes that occur from virgin to cycled tape at various humidities and temperatures. A correlation between the surface of the head and the chemical changes that occurs after cycling virgin tape could be used.

To develop a technique where you could measure directly the magnitude of the adhesion forces at the surface of the glass and ferrite regions of a read head before and after tape cycling, at surface of the stain and the surface of the tape. This technique must also be used to determine the nature of the adhesion forces involved (possibly ionic, covalent and physical) at the surface of the glass and ferrite regions of a read head and the tape. One possible technique could involve modifying an atomic force microscopy AFM so that it can measure the adhesion forces instead of mapping the surface of the sample (the surface topography) via silicon AFM tips and a series of cantilevers. This may be a direct way of determining whether the stain also includes polymeric material such as binder that probably initialises staining by acting as a sticking agent. This technique could be used to understand how the humidity and temperature effects the adhesion forces between the head and tape during tape cycling

To employ an electron scanning or an optical microscope to study the colour of the stain and the changes that occur as the tape is cycled.

Chapter 7 The References

1. Y.Kaneda, "Tribology of metal evaporated tape for high density magnetic recording", IEEE Transactions of Magnetics, March 1997, Vol. 33, No. 2.
2. B.L.Weick and B.Bhushan, "Characteristic of magnetic tapes and substrates", IEEE Transactions of magnetics, Vol.32, No.4, July 1996
3. Y.Nishida, Y.Hisamichi, H.Kondo, "Behaviour of perfuoropolyether in particulate magnetic recording media", IEE Transactions on magnetics, Sept. 1996, Vol.32, No.5, pp.2738-3740
4. B.Bhushan and D.V.Khataukar, "Role of tape abrasivity on friction, wear, staining, and signal degradation in audio tapes", Wear (190), No.1, Nov. 1995, pp.16
5. M.S.Hempstock and J.L.Sullivan, "The durability and signal performance of M.E. and M.P. tapes", IEE Transactions on magnetic, Sept. 1996, Vol. 32, No. 5
6. J.Archard, Journal of Applied Physics, Vol. 24, 1953, pp.981
7. B.Bhushan, Journal of Tribology-Transactions of ASME, 106(1984), pp.26
8. J.A.Greenwood, J.B.P.Williamson, Proc. Roy. Soc. Ap292 (1996) 3006
9. B.Bhushan and D.V.Khatavkar, "Role of water vapour on the wear of Mn-Zn ferrite heads sliding against magnetic tapes", Wear 202 (1996), pp.30-34
10. S.T.Pattan and B.Bhushan, "Friction and Wear of metal particle, barium ferrite and M.E. tapes in rotary head recorders", Transactions of ASME- Journal of Tribology, Vol. 118, Jan. 1996, pp.21-31
11. J.L.Sullivan, "Tribology of flexible magnetic recording media", Journal of magnetism and magnetic materials, 155(1996), pp.312-317
12. B.Bhushan, "Stains on tape heads", Wear 184(1995), pp.193-202
13. S.Chandler, B.Tucker, P.Turner, and P.Heard, "Case study: An investigation into the cause of Error Rate Drift", Tribology International 1998, Vol. 31, No. 8. Pp.443-448
14. C.M.Stahle, T.D.Lee, "Characterisation of the deposits on helical scan heads", Advanced Info. Storage System, Vol. 4, 1992.
15. V.Prabhakaran S.K.Kim, F.E.Talke, "Tribology of helical scan head tape interface", Wear, 215(1998), pp.91-97
16. B.K.Gupta and B.Bhushan, "Chemical analysis of stains formed on Co-Nb-Zr metal-in-gap heads sliding against oxide and metal particle magnetic tapes", Journal of material Research, Vol.10, No. 7, July 1995, pp.1795-1809
17. Y.F.Liow, J.C.Lauer, and F.E.Talke, "Analysis of deposits from friction at head-tape interfaces by Raman Spectroscopy", Tribology Transactions, 38(1995), No.3, pp.728-732

18. S.Kim, V.Pkalhokaran, and F.E.Talke, "Investigation of head wear and contamination in helical scan tape systems", IEE Transactions of magnetics, Vol.32, No.5, 1996, pp.3741-3743
19. T.Tsuchiya and B.Bhushan, "Metal core recession and head stain studies of MIG heads sliding against cobalt-doped gamma iron oxide and metal particle tape", Tribology Transactions, Vol. 38 (1995), No.4, pp.941-949
20. T.Kamei, N.Kishii, K.Kurihara, "Removal of Brown Stain on magnetic Head by A chelting Agent on Magnetic Tapes", TP2-4, 1998
21. W.W.Scott, B.Bhushan, "Generations of magnetic tape debris and head stain in a linear tape drive", Proceedings of the Institute of Mechanical Engineers Part J- Journal of Engineering Tribology, Vol. 213 (1999), No. J2, pp.127-138
22. H.Osaki, J.Kurihara and T.Kanou, " Mechanism of Head-Clogging by Particulate Magnetic Tapes in Helical Scan Video tape Recorder", IEEE Transactions on Magnetic, Vol. 30, No.4, July 1994, pp. 1491-1498
23. H.Ota, K.Namura and N.Ohmae, " Brown stain on VCR Head Surface Through Contact with magnetic tape", Advanced Information Storage System, Vol.2, 1991
24. B.Bhushan and J.A.Lowry, "Friction and Wear studies of various head materials and magnetic tapes in a linear mode accelerated test using a new nano-scratch wear measurement test", Wear190 (1995), pp.1-15
25. P.J.Sharma, "Factors affecting the durability of 5.25 inch floppy diskettes and its mechanism of wear", 1989, Ph.D. Thesis, Aston University, Surface Science Group.
26. P.H.Clifton, " An investigation into the physical properties of the head tape interface in the Hewlett Packard Digital Data Storage (DDS) Helical Tape Drives", EEAP, Aston University, 1998.
27. H.Kron, M.H.Wahl, F.E.Talke, "Finite Element simulation of a helical scanner with head/tape contacts", IEE Transactions on magnetics, Vol. 32, No. 5, 1996, pp.3735-3737
28. Y.Wu and F.Talke, "The effect of surface roughness on the head-tape interface", Transactions of ASME- Journal of Tribology, Vol. 18, 1996, pp.376-381
29. P.I.Oden, A.Mayumada, B.Bhushan, A.Pudmanabha, and J.J.Graham, "AFM Imaging, roughness analysis, and contact mechanics of magnetic tape and head surfaces", Transactions of ASME- Journal of Tribology, Vol. 14, 1992, pp.666-674
30. E.Baugh and F.E.Talke, "The head/tape interface: A critical review and recent results", Tribology transactions, Vol. 36 (1996), No.2, pp.306-313
31. C.Lacey and F.E.Talke, "The effect of head wear and tape shear on the head/tape interface", Tribology Transactions, Vol.36 (1993), No.3, pp.387-392

30 M.Brendle, P.Turgis, S.Lamouri, "A general approach to Discontinuous Transfer Films: The General Role of Mechanical and Physico-chemical Interactions", Tribology Tranactions Vol.39 (1996), No. 1, pp.157-165

31 V.L.Vakula, L.M.Pritykin, "Polymer Adhesion: basic physico-chemical principles", Ellis Horwood series in polymer science and technology 1991 ISBN 0-13-662990-3

32 J.Hirschfelder, "Intermolecular Forces", John Wiley and sons, 1967, 58-9935

33 M.L.Miller, " Structure of polymers", Polymer Science and engineering series, Reinhold Publishing Corporation 1966 66-24452.

34 W.D.Harkins, "The Physical Chemistry of Surface Films", Reinhold Publishing Corporation 1952

35 D.T.Clark, W.J.Feast, "Polymer Surfaces", Wiley-Interscience Pub., 1978 ISBN 0-471-99614-9

36 M.Prutton, "Surface Physics", Oxford Physics Series, 1975 ISBN 0-19-851819-6

37 J.M.Blakely, "Surface Physics of Materials Vol. II", Material Science Series, 1975, ISBN 0-12-103802-5

38 R.Vanselow, "Chemistry and Physics of solid Surfaces Vol. 2", 1979, ISBN

39 John.F.Watts, "An introduction to surface analysis by electron spectroscopy"

40 C.Mee and E.Daniel, "Magnetic recording handbook – Technology and Application"

41 Kentaro Odaka, Eng.T.Tan, and Bert Vermeulen, "Designing a data storage format for DAT" revision B Oct 1988 (Digital Storage)

42 "Digital Audio Tape for Data Storage", IEEE Spectrum, Vol. 26, No. 10, Oct 1989, pp.34-38

43 L.Reeves, "The mechanism of wear of the video head", 1990 Ph.D. Thesis Aston University Surface Science Group

44 B.Bhushan, " Tribology and mechanics of magnetic storage devices", Springer-Verlag, New York Inc.

45 C.Martin, "MTC Firmware Specifications", Rev. A.03, November 1996, H.P Computer Peripherals Bristol.

46 B.L.Weick and B.Bhushan, "Relationship between dynamic mechanical behaviour, transverse curvature and wear of magnetic tape", Wear 202(1996), pp17-29

47 R.M.Anderson and B.Bhushan, "Concurrent measurements of in situ friction force and head signal amplitude during dropouts in rotary head tape drives", Wear 202(1996), pp.17-29

48 Y.Xie and B.Bhushan, "Fundamental wear studies with magnetic particles and head cleaning agents used in magnetic tapes", Wear 202(1996), pp.3-16

49 M.S.Hempstock and J.L.Sullivan, "Study of the mechanical and magnetic performance of M.E tapes", Journal of Magnetism and magnetic materials 155(1996), pp.323-328

50 "Computer Systems Europe", Vol. 10, No. 7, July 1990, p12-22

51 H.Kron, M.H.Wahl, F.E.Talke, "Finite Element simulation of a helical scanner with head/tape contacts", IEE Transactions on magnetics, Sept. 1996, Vol. 32, No. 5, pp.3735-3737

52 B.Bhushan and D.V.Khataukar, "Role of tape abrasivity on friction, wear, staining, and signal degradation in audio tapes", Wear (190), No.1, Nov. 1995, pp.16-

53 F.Talke, "A review of contact recording technology", Wear 207(1997), pp.118-121

54 B.Bhushan and S.T.Pattan, "Friction and wear of ultrahigh-density magnetic tape", Journal of Applied Physics 75(10), 15th May 1994

55 T.Tsuehija and B.Bhushan, "Running characteristics of MIG heads against M.P, Barium ferrite, and M.E. tape", IEEE Transactions of magnetics, Vol. 30, No.6, July 1995

56 B.Bhushan and J.A.Lowry, "Frictions and wear of particulate and M.E magnetic tapes sliding against a Mn-Zn ferrite head in a linear mode", IEEE Transactions of magnetics, Vol.30, NO.6, Nov 1994

57 K.C.Ludema, "Mechanism based modelling of friction and wear", Wear 200(1996), p1-7

58 C.Nadimpalli, F.Talke, M.Smallen, J.J.K.Lee, "Pole tip recession: Investigation of factors affecting its measurement and its variation with constant start-stop and contact speed drag test", Transactions of ASME- Journal of Tribology, Vol. 117, Oct. 1995, pp.580-587

59 Y.Wu and Frank Talke, "The effect of surface roughness on the head-tape interface", Transactions of ASME- Journal of Tribology, Vol. 18, April 1996, pp.376-381

60 C.Lacey and F.E.Talke, "Measurement and simulation of partial contact at head and tape interface", Transactions of ASME- Journal of Tribology, Vol.14, Oct. 1992, pp.646-652

61 B.Bhushan and J.A.Lowry, "Friction and wear of particulate and M.E magnetic tapes sliding against a Mn-Zn ferrite head in a linear mode", IEEE Transactions on magnetics, Vol. 30, No.6, Nov. 1994, pp.4176-4178

62 K.Sakai, Y.Nagaia, H.Okuyama, and T.Terayama, "Thin spacing analysis for head-tape interface", Transactions of ASME- Journal of Tribology, Vol. 118, Oct. 1996, pp.800-806

63 B.Bhushan and J.A.Monahan, "Accelerated friction and wear studies of various particulate and tin-film magnetic tapes against tape path materials in pure sliding and rotary/sliding modes", Tribology Transactions, Vol. 38(1995), No.2, pp.329-341

64 H.L.Bestram, "Fundamentals of the magnetic recording process", Proceeding of the IEE, Vol. 74, No.11, Nov. 1986

65 B.Bhushan, ASME Transactions, Vol. 28, 1985, pp.181

66 B.Bhushan and M.F.J.Boerer, Tribology Transactions of ASME, Vol. 111, 1989, pp.453.

Chapter 8 The Appendix

8.0 The mtcl scripts used in these experiments

8.0.1 The Long reconditioning script

```
/*****************************************************************************
* File: Long_recondDDS3_FFEOFF.mtcl
* Description:  Reconditions the drives in DDS3 mode at 80%RH 25C by
*           - write ERT measurement for 2000h frames (2 MINS)
*           - move forward at *1 speed
*           - write ERT measurement for 2000h frames (2 MINS)
*           - move forward at *1 speed
*           - write ERT measurement for 2000h frames (2 MINS)
*           Then repeat the following 16 times
*           - rewind for 15 mins at *12 speed.
*           - write ERT measurement for 3000h frames (2 MINS)
*           - move forward at *1 speed
*           - write ERT measurement for 3000h frames (2 MINS)
*           - move forward at *1 speed
*           - write ERT measurement for 2000h frames (2 MINS)
*           The same stretch of media is used 16 times. The script
*           ends with the tape positioned at the end of this
*           reused section of media. If the script is rerun on
*           this drive it will start on virgin media.
*           Will take 2 days.
*
*           Version:    1.0
*
*           This version DOES NOT deal with need to download headbonk
*           for Caliban.  Could have problems if using old Othello boards.
*
*           This version does not actually do any headbonking/slapping
*
*           This version has the capability to turn the FFE off (for Lear
*           or Andronicus units) with the code for doing this
*           selectable from a #define line (1st in program). This
*           avoids need to change a whole set of lines when loading
*           into different drives.
*
* Author:      Christopher Skidmore
*
* Created:     16/2/98
* Machine:     Jungfrau
* Language:    MTCL
* Status:      Experimental (Do Not Distribute)
*/
/*****************************************************************************/
/* Configuration options...                                                  */
/*****************************************************************************/

/* Is this MACBETH, OTHELLO, LEAR or ANDRONICUS? */
/* Note: this change requires new, non-standard .h header files */
#Define LEAR

/*****************************************************************************/
/* Includes...                                                               */
/*****************************************************************************/

#include "servo.h"
```

```
#include "mtcl.h"
#include "genmtcl.h"
#include "headbonk.h"
#include "leds.h"
#include "turn_ffe_off.h"

/*****************************************************************************/
/* Misc...                                                                   */
/*****************************************************************************/

#define WRITE_ERT_LENGTH  1D,E2 /* 3000h frames = 12288d, about 70Mb       */
#define FILL_WRITE_LENGTH FF,FF /* FFFFh frames = 65535d, about 370Mb      */
#define WRITE_ERT_LIMIT   FF,FF,FF,FF /* We don't want it to fail...       */

#define NO_OUTER_LOOPS    10   /* 10h = 16 passes or runs */

/* We want to define our own LED patterns, so forget those from genmtcl.h */

#undef TESTING
#undef FAIL
#undef PASS
#undef PASS1
#undef PASS2

#define REWINDING       GREEN_YELLOW
#define RECOVERING      GREEN_YELLOW

#define WRITING         GREEN_OFF
#define FILLING         OFF_OFF

#define FAIL            OFF_YELLOW
#define PASS            GREEN_OFF

/* Note about use of registers:                                          */
/* Register 2: used for counting outer loops of the Mloop routine.       */
/* Register 4: used to 'map' progress of script and decide where to
   return to after routines etc.                                         */
/* Register 6: used for controlling the FFE unit on Lear.                */
/* Register 8: used in the rewinding process.                            */

#define ZERO            0,0   /* for register comparisons                */
#define TEN_SECONDS     64    /* 64h = 100d = 10s                        */
#define TWENTY_SECONDS  C8    /* 20s                                     */

/* if drive is an Othello then prevent attempts to turn off the FFE -
   since there isn't one */

#ifdef OTHELLO
#undef TURN_FFE_OFF
#define TURN_FFE_OFF    NOP
#endif

/*****************************************************************************/
/* This is the main program.                                                 */
/*****************************************************************************/

/* Script revision */

        LOG     EVERYTHING
        URD     64,66,74,43         /* "dftC" */
        URD     76,31,2E, 30        /* "v1.0" */
        LOG     ERRORS_ONLY
        BOE:    Error_handler

/* Initialise the drive */

        SERVO_CMD (RESET)
```

```
        SERVO_CMD (IGNORE_LURK)
        SERVO_CMD (EJECT)

/* This ONLY works in DDS3 mode, since the times are wrong for DDS1  */

        TURN_FFE_OFF

        LDR     REGISTER6, IMMEDIATE, 00,00,00
        SRB     REGISTER6, 41,5E, 8B
        LDT     ONE25_METRE_TAPE

        CAL

        LED     RECOVERING
        SERVO_CMD (CAPS_FWD_LO)
        WAI     TIME_DELAY, 64

/* Eject and reload tape to zero the tape counter                       */

        SERVO_CMD (EJECT)
        SERVO_CMD (STOP)

/* The next series of commands are causing a routine to be called from a      */
/* label number. After finishing, the routine will check to see where it was  */
/* called from and jump to another label corresponding to that place.         */

        LDR     REGISTER4, IMMEDIATE, 00,00,01   /* initialise 'map' register */

        BRA:    Drift
: Return1d LOG     EVERYTHING
        LED     PASS
        SERVO_CMD (EJECT)
        BRA:    End

/************* Drift routine **************/

: Drift LED     WRITING
        LOG     EVERYTHING
        SRS
        WER     DATA_RANDOM,    START_HERE,     FAIL_IF_EXCEED,     WRITE_ERT_LENGTH,
WRITE_ERT_LIMIT
        SRS
        LOG     ERRORS_ONLY

        LED     RECOVERING
        SERVO_CMD (CAPS_FWD_LO)
        WAI     LONG_TIME_DELAY, AE

        LED     WRITING
        LOG     EVERYTHING
        SRS
        WER             DATA_RANDOM,    START_HERE,     FAIL_IF_EXCEED,     WRITE_ERT_LENGTH,
WRITE_ERT_LIMIT
        SRS
        LOG     ERRORS_ONLY

        LED     RECOVERING
        SERVO_CMD (CAPS_FWD_LO)
        WAI     LONG_TIME_DELAY, AE

        LED     WRITING
        LOG     EVERYTHING
        SRS
        WER             DATA_RANDOM,    START_HERE,     FAIL_IF_EXCEED,     WRITE_ERT_LENGTH,
WRITE_ERT_LIMIT
        SRS
        LOG     ERRORS_ONLY
```

```
      LDR    REGISTER2, IMMEDIATE, 00, 00, 01

: Rpt01   LED    REWINDING

/*Rewind to just after start of new data. First use time to get
  to approx area, then use tape counter                    */

      SERVO_CMD (CAPS_REV_HI)
      WAI    LONG_TIME_DELAY, 1E

: Rewd03  LDR    REGISTER8, SERVO_REP_2_3
      BLT    REGISTER8, F0, 00,:Rewd03
      SERVO_CMD (CAPS_FWD_NOM)
: Fwd03   LDR    REGISTER8, SERVO_REP_2_3
      BGT    REGISTER8, 10,00,:Fwd03

      LOG    EVERYTHING
      LED    WRITING
      SRS
      WER            DATA_RANDOM,   START_HERE,   FAIL_IF_EXCEED,   WRITE_ERT_LENGTH,
WRITE_ERT_LIMIT
      SRS
      LOG    ERRORS_ONLY

      LED    RECOVERING
      SERVO_CMD (CAPS_FWD_LO)
      WAI    LONG_TIME_DELAY, AE

      LED    WRITING
      LOG    EVERYTHING
      SRS
      WER            DATA_RANDOM,   START_HERE,   FAIL_IF_EXCEED,   WRITE_ERT_LENGTH,
WRITE_ERT_LIMIT
      SRS
      LOG    ERRORS_ONLY

      LED    RECOVERING
      SERVO_CMD (CAPS_FWD_LO)
      WAI    LONG_TIME_DELAY, AE

      LED    WRITING
      LOG    EVERYTHING
      SRS
      WER            DATA_RANDOM,   START_HERE,   FAIL_IF_EXCEED,   WRITE_ERT_LENGTH,
WRITE_ERT_LIMIT
      SRS
      LOG    ERRORS_ONLY

      INC    REGISTER2
      BLT    REGISTER2, 00,NO_OUTER_LOOPS,:Rpt01

      BEQ    REGISTER4, 00,01,:Return1d

/* Should never get this far but if so then handle error */

: Error_handler CBE
      SRS
      SERVO_CMD (EJECT)
      LOG    EVERYTHING
      URD    46,61,69,6C   /* write "Fail" to show didn't finish */
      LED    FAIL

      BRA:    End

: End  EOT
      . End
```

8.02 The repeatability testing mtcl script

```
/*
*****************************************************************************
* File: CharacterDDS3.mtcl
* Description:  Characterises the drives in DDS3 mode at 35%RH 25C by
*           - write ERT measurement for 3000h frames ( 3 MINS)
*           - move forward for 2*5508h frames ( 12 MINS)
*           Then repeat the following 58 times
*           - rewind
*           - write ERT measurement for 3000h frames
*           - move forward for 2*5508h frames
*           The same stretch of media is used 59 times. The script
*           ends with the tape positioned at the end of this
*           reused section of media. If the script is rerun on
*           this drive it will start on virgin media.
*           Will take 36 hours.
*
*           Version:    1.0
*
*           This version DOES NOT deal with need to download headbonk
*           for Caliban.  Could have problems if using old Othello boards.
*
*           This version does not actually do any headbonking/slapping
*
*           This version has the capability to turn the FFE off (for Lear
*           or Andronicus units) with the code for doing this
*           selectable from a #define line (1st in program). This
*           avoids need to change a whole set of lines when loading
*           into different drives.
*
* Author:   Modified by Christopher Skidmore
*
* Created:     30/10/97
* Machine:     ee-hypo
* Language:    MTCL
* Status:      Experimental (Do Not Distribute)
*
*/
/*****************************************************************************/
/* Configuration options...                                                  */
/*****************************************************************************/

/* Is this MACBETH, OTHELLO, LEAR or ANDRONICUS ? */
/* Note: this change requires new, non standard .h header files */
#define LEAR

/*****************************************************************************/
/* Includes...                                                               */
/*****************************************************************************/

#include "servo.h"
#include "mtcl.h"
#include "genmtcl.h"
#include "headbonk.h"
#include "leds.h"
#include "turn_ffe_off.h"

/*****************************************************************************/
/* Misc.                                                                     */
/*****************************************************************************/

#define WRITE_ERT_LENGTH  30,00 /* 3000h frames = 12288d, about 70Mb       */
#define FILL_WRITE_LENGTH 55,08 /* FFFFh frames = 65535d, about 370Mb      */
#define WRITE_ERT_LIMIT   FF,FF,FF,FF /* We don't want it to fail...       */
```

```
#define NO_OUTER_LOOPS    3A    /* 3Ah = 58 loops */

#define RECOVERY_TIME    04    /* 04, in units of 30 seconds */

/* We want to define our own LED patterns, so forget those from genmtcl.h */

#undef TESTING
#undef FAIL
#undef PASS
#undef PASS1
#undef PASS2

#define REWINDING        GREEN_YELLOW
#define RECOVERING       GREEN_YELLOW

#define WRITING          GREEN_OFF
#define FILLING          OFF_OFF

#define FAIL             OFF_YELLOW
#define PASS             GREEN_OFF

/* Note about use of registers:                                          */
/* Register 2 : used for counting outer loops of the Mloop routine.      */
/* Register 4 : used to 'map' progress of script and decide where to
        return to after routines etc.                                    */
/* Register 6 : used for controlling the FFE unit on Lear.               */
/* Register 8 : used in the rewinding process.                           */

#define ZERO             0,0   /* for register comparisons               */
#define TEN_SECONDS      64    /* 64h = 100d = 10s                       */
#define TWENTY_SECONDS   C8    /* 20s                                    */

/* if drive is an Othello then prevent attempts to turn off the FFE -
  since there isn't one */

#ifdef OTHELLO
#undef TURN_FFE_OFF
#define TURN_FFE_OFF    NOP
#endif

/*****************************************************************************/
/* This is the main program.                                                 */
/*****************************************************************************/

/* Script revision */

        LOG     EVERYTHING
        URD     64,66,74,43          /* "dftC" */
        URD     76,31,2E, 30         /* "v1.0" */
        LOG     ERRORS_ONLY
        BOE:    Error_handler

/* Initialise the drive */

        SERVO_CMD (RESET)
        SERVO_CMD (IGNORE_LURK)
        SERVO_CMD (EJECT)

/* This ONLY works in DDS2 mode, since the times are wrong for DDS1  */
/* First load the 120m cleaning tape */

        LDT     ONE25_METRE_TAPE
        CAL
        TURN_FFE_OFF

/* Should already be there, but just in case ... */
/* Move to EOD */
```

```
      WER   DATA_RANDOM, START_EOD, FAIL_IF_EXCEED, 00,00,WRITE_ERT_LIMIT

/* Eject and reload tape to zero the tape counter                    */

      SERVO_CMD (EJECT)
      SERVO_CMD (STOP)

/* The next series of commands are causing a routine to be called from a    */
/* label number. After finishing, the routine will check to see where it was */
/* called from and jump to another label corresponding to that place.       */

      LDR   REGISTER4, IMMEDIATE, 00,00,01  /* initialise 'map' register */

      BRA:  Drift
: Return1d LOG   EVERYTHING
      LED   PASS
      SERVO_CMD (EJECT)
      BRA:  End


/************ Drift routine **************/

: Drift  LED   WRITING
      LOG   EVERYTHING
      SRS
      WER           DATA_RANDOM,  START_HERE,  FAIL_IF_EXCEED,  WRITE_ERT_LENGTH,
WRITE_ERT_LIMIT
      SRS
      LOG   ERRORS_ONLY

/* Perform additional non-logged write error rate to make up total required  */

      LED   FILLING
      WER           DATA_RANDOM,  START_HERE,  FAIL_IF_EXCEED,  FILL_WRITE_LENGTH,
WRITE_ERT_LIMIT
      WER           DATA_RANDOM,  START_HERE,  FAIL_IF_EXCEED,  FILL_WRITE_LENGTH,
WRITE_ERT_LIMIT
      LDR   REGISTER2, IMMEDIATE, 00,00,01

: Rpt01  LED   REWINDING

/* Rewind to just after start of new data. First use time to get
   to approx area, then use tape counter                          */

      SERVO_CMD (CAPS_REV_LO)     /* REWINDS FOR 15 MINS */
      WAI   LONG_TIME_DELAY, 1E

: Rewd03  LDR   REGISTER8, SERVO_REP_2_3
      BLT   REGISTER8, F0, 00,:Rewd03
      SERVO_CMD (CAPS_FWD_NOM)
: Fwd03  LDR   REGISTER8, SERVO_REP_2_3
      BGT   REGISTER8, 10,00,:Fwd03

      LOG   EVERYTHING
      LED   WRITING
      SRS
      WER           DATA_RANDOM,  START_HERE,  FAIL_IF_EXCEED,  WRITE_ERT_LENGTH,
WRITE_ERT_LIMIT
      SRS
      LOG   ERRORS_ONLY

/* Perform additional non-logged write error rate to make up total required  */

      LED   FILLING
      WER           DATA_RANDOM,  START_HERE,  FAIL_IF_EXCEED,  FILL_WRITE_LENGTH,
WRITE_ERT_LIMIT
```

```
        WER          DATA_RANDOM,  START_HERE,  FAIL_IF_EXCEED,  FILL_WRITE_LENGTH,
WRITE_ERT_LIMIT
      INC    REGISTER2
      BLT    REGISTER2, 00,NO_OUTER_LOOPS,:Rpt01

      BEQ    REGISTER4, 00,01,:Return1d

/* Should never get this far but if so then handle error */

: Error_handler CBE
      SRS
      SERVO_CMD (EJECT)
      LOG    EVERYTHING
      URD    46,61,69,6C   /* write "Fail" to show didn't finish */
      LED    FAIL

      BRA:    End

: End  EOT
      . End
```

8.03 The ShortDriftDDS3.mtcl script

```
/*
*******************************************************************************
* File: ShortDriftDDS3.mtcl

* Description:  Stains the drives in DDS3 mode at 10% RH 25C by
*           - moves forward at *4 for 10 secs
*           - ejects, then reloads
*           - *1 for 10 secs
*           - ERT for 5 secs
*           Then repeat the following 39 times
*           - rewind
*           - *1 speed for 5 secs
*           - ERT for 5 secs
*           The same stretch of media is used 40 times. The script
*           ends with the tape positioned at the end of this
*           reused section of media. If the script is rerun on
*           this drive it will start on virgin media.
*           Will take 13 mins.
*
*           Version:     1.0
*
*           This version DOES NOT deal with need to download headbonk
*           for Caliban.  Could have problems if using old Othello boards.
*
*           This version does not actually do any headbonking/slapping
*
*           This version has the capability to turn the FFE off (for Lear
*           or Andronicus units) with the code for doing this
*           selectable from a #define line (1st in program). This
*           avoids need to change a whole set of lines when loading
*           into different drives.
*
* Author:       Modified by Christopher Skidmore
*
* Created:      22/1/98
* Machine:      ee-hypo
* Language:     MTCL
* Status:       Experimental (Do Not Distribute)
*
*/
/*****************************************************************************/
```

```
/* Configuration options...                                                    */
/*****************************************************************************/

/* Is this MACBETH, OTHELLO, LEAR or ANDRONICUS ? */
/* Note: this change requires new, non standard .h header files */
#define LEAR

/*****************************************************************************/
/* Includes...                                                                 */
/*****************************************************************************/

#include "servo.h"
#include "mtcl.h"
#include "genmtcl.h"
#include "headbonk.h"
#include "leds.h"
#include "turn_ffe_off.h"

/*****************************************************************************/
/* Misc.                                                                       */
/*****************************************************************************/

#define WRITE_ERT_LENGTH 01,3B
#define FILL_WRITE_LENGTH 55,08
#define WRITE_ERT_LIMIT  FF,FF,FF,FF /* We don't want it to fail...      */

#define NO_OUTER_LOOPS   28  /* 28h = 40 loops */

#define RECOVERY_TIME   04   /* 04, in units of 30 seconds */

/* We want to define our own LED patterns, so forget those from genmtcl.h */

#undef TESTING
#undef FAIL
#undef PASS
#undef PASS1
#undef PASS2

#define REWINDING       GREEN_YELLOW
#define RECOVERING      GREEN_YELLOW

#define WRITING         GREEN_OFF
#define FILLING         OFF_OFF

#define FAIL            OFF_YELLOW
#define PASS            GREEN_OFF

/* Note about use of registers:                                    */
/* Register 2 : used for counting outer loops of the Mloop routine.      */
/* Register 4 : used to 'map' progress of script and decide where to return to after routines etc. */
/* Register 6 : used for controlling the FFE unit on Lear.               */
/* Register 8 : used in the rewinding process.                     */

#define ZERO                    0,0     /* for register comparisons          */
#define TEN_SECONDS             64      /* 64h = 100d = 10s                  */
#define TWENTY_SECONDS  C8      /* 20s                               */

/* if drive is an Othello then prevent attempts to turn off the FFE -
   since there isn't one */

#ifdef OTHELLO
#undef TURN_FFE_OFF
#define TURN_FFE_OFF    NOP
#endif
```

```
/*****************************************************************************/
/* This is the main program.                                                 */
/*****************************************************************************/

/* Script revision */

        LOG     EVERYTHING
        URD     64,66,74,43         /* "dftC" */
        URD     76,31,2E,30         /* "v1.0" */
        LOG     ERRORS_ONLY
        BOE:    Error_handler

/* Initialise the drive */

        SERVO_CMD (RESET)
        SERVO_CMD (IGNORE_LURK)
        SERVO_CMD (EJECT)

/* This ONLY works in DDS2 mode, since the times are wrong for DDS1  */
/* First load the 120m cleaning tape */

        LDT     ONE25_METRE_TAPE

        LED     RECOVERING
        SERVO_CMD (CAPS_FWD_MID)  /* forwarding at *4 speed for 30 seconds */
        WAI     LONG_TIME_DELAY, 1

/* Eject and reload tape to zero the tape counter                            */

        SERVO_CMD (EJECT)
        SERVO_CMD (STOP)

        CAL

/* The next series of commands are causing a routine to be called from a     */
/* label number. After finishing, the routine will check to see where it was */
/* called from and jump to another label corresponding to that place.        */

        LDR     REGISTER4, IMMEDIATE, 00,00,01   /* initialise 'map' register */

        BRA:    Drift
: Return1d LOG    EVERYTHING
        LED     PASS
        SERVO_CMD (EJECT)
        BRA:    End


/************* Drift routine **************/

: Drift LED     RECOVERING
        SERVO_CMD (CAPS_FWD_LO)
        WAI     TIME_DELAY, 64

        LED     WRITING
        LOG     EVERYTHING
        SRS
        WER             DATA_RANDOM,   START_HERE,   FAIL_IF_EXCEED,   WRITE_ERT_LENGTH,
WRITE_ERT_LIMIT
        SRS
        LOG     ERRORS_ONLY

        LDR     REGISTER2, IMMEDIATE, 00,00,01

: Rpt01   LED     REWINDING

/* Rewind to just after start of new data. First use time to get
   to approx area, then use tape counter                                    */
```

```
        SERVO_CMD (CAPS_REV_MID)        /* REWINDS */

: Rewd03   LDR     REGISTER8, SERVO_REP_2_3
        BLT     REGISTER8, F0, 00,:Rewd03
        SERVO_CMD (CAPS_FWD_NOM)
: Fwd03    LDR     REGISTER8, SERVO_REP_2_3
        BGT     REGISTER8, 10,00,:Fwd03


        LED     RECOVERING
        SERVO_CMD (CAPS_FWD_LO)
        WAI     TIME_DELAY, 64

        LOG     EVERYTHING
        LED     WRITING
        SRS
        WER             DATA_RANDOM,    START_HERE,    FAIL_IF_EXCEED,    WRITE_ERT_LENGTH,
WRITE_ERT_LIMIT
        SRS
        LOG     ERRORS_ONLY

        INC     REGISTER2
        BLT     REGISTER2, 00,NO_OUTER_LOOPS,:Rpt01

        BEQ     REGISTER4, 00,01,:Return1d

/* Should never get this far but if so then handle error */

: Error_handler CBE
        SRS
        SERVO_CMD (EJECT)
        LOG     EVERYTHING
        URD     46,61,69,6C   /* write "Fail" to show didn't finish */
        LED     FAIL

        BRA:    End

: End   EOT
        . End
```

8.04 The SSS.mtcl script

```
/*
*****************************************************************************
*
* File:         sss.mtcl, based on demo.mtcl
*
* Description:  Repeated strips of random data are written, with a 'recovery routine' *.
*               between each one
* Version:  1.2
*           This version DOES NOT deal with need to download headbonk
*           for Caliban.  Could have problems if using old Othello boards.
*
*           This version does not actually do any headbonking/slapping
*
*           This version has the capability to turn the FFE off (for Lear
*           or Andronicus units) with the code for doing this selectable from
*           a #define line (1st in program). This avoids need to change a whole
*           set of lines when loading into different drives.
*
* Author:       Simon Chandler
*
* Created:      26/2/98
```

```
* Machine:     Pix
* Language:    MTCL
* Status:      Experimental (Do Not Distribute)
*
*/
/*****************************************************************************/
/* Configuration options...                                                  */
/*****************************************************************************/

/* Is this MACBETH, OTHELLO, LEAR or ANDRONICUS ? */
/* Note: this change requires new .h header files */
#define LEAR
! #define OTHELLO

/*****************************************************************************/
/* Includes...                                                               */
/*****************************************************************************/

#include "servo.h"
#include "mtcl.h"
#include "genmtcl.h"
#include "headbonk.h"
#include "leds.h"
#include "turn_ffe_off.h"

/*****************************************************************************/
/* Misc...                                                                   */
/*****************************************************************************/

/* Following lengths chosen to make the WER about 10 seconds long.          */
/* This makes each stain loop about 13 seconds long,                        */
/* so each drift is about 8 minutes long.                                   */
#define WRITE_ERT_LENGTH_S  03,00  /* should be 03,00 */

#define NO_DRIFTS       04
#define NO_PASSES       28   /* 28h = 40d loops, 14h = 20d */
#define LOG_N           02   /* record WER only on every Nth pass */

#define RECOVERY_TIME   0A   /* in units of 30 seconds 0A = 10 mins */

/* We want to define our own LED patterns, so forget those from genmtcl.h */
#undef TESTING
#undef FAIL
#undef PASS
#undef PASS1
#undef PASS2

#define REWINDING       GREEN_YELLOW
#define RECOVERING      GREEN_YELLOW

#define WRITING         GREEN_OFF
#define READING         OFF_YELLOW

#define FAIL            OFF_YELLOW
#define PASS            GREEN_OFF

/* Note about use of registers:                                             */

/* Register 1: used for counting number of drifts done in experiment
   i.e., decide whether to do another drift or stop.  */

/* Register 2: used for counting number of passes done in each drift
   i.e., decide whether to do another WER pass.  */

/* Register 3: used for counting inner loops of the Drift routine. i.e.,
   decide if ERT is to be recorded.                                         */
```

```
/* Register 6: used for controlling the FFE unit on Lear.              */
/* Register 8: used as counter monitor in the rewinding process.       */


#define ZERO                    0,0  /* for register comparisons          */
#define TEN_SECONDS             64   /* 64h = 100d = 10s                  */
#define TWENTY_SECONDS          C8   /* 20s                               */

#define WRITE_ERT_LIMIT  FF,FF,FF,FF /* We don't want it to fail...       */

/* if drive is an Othello then prevent attempts to turn off the FFE -
   since there isn't one */

#ifdef OTHELLO
#undef TURN_FFE_OFF
#define TURN_FFE_OFF    NOP
#endif


/*****************************************************************************/
/*  This is the main program.                                                */
/*****************************************************************************/

/* Script revision */
        LOG     EVERYTHING
        URD     73,73,73,20         /* "sss " */
        URD     76,31,2E, 30         /* "v1.0" */
        LOG     NOTHING
        BOE:    Error_handler

/* Initialise the drive */
        SERVO_CMD (RESET)
        SERVO_CMD (IGNORE_LURK)
        SERVO_CMD (EJECT)

: Start    SERVO_CMD (CLEAN_HEADS)

/* THE WHOLE EXPERIMENT WILL BE DONE IN DDS-2 MODE */
/* First load the calibration tape */

        TURN_FFE_OFF

        LDT     ONE20_METRE_TAPE
        CAL
        SERVO_CMD (EJECT)           /* eject the calibration tape */

/* The next series of commands are causing a routine to be called from a
   label number. After finishing, the routine will check to see where it was
   called from and jump to another label corresponding to that place.
   This checking is actually done in a separate routine "Returnable"
*/

        LDR     REGISTER1, IMMEDIATE, 00,00,00   /* initialise drift count */

: Loopstart BRA: Recover                 /* recover  */
: Returnr   BRA: Drift                  /* drift */

: Returnd   INC     REGISTER1

        BGE     REGISTER1, 00,NO_DRIFTS,:Endexpt

        BRA:    Loopstart

: Endexpt  LOG     NOTHING
        LED     PASS
        SERVO_CMD (EJECT)
        BRA:    End
```

```
/********** Recover ************/
/* This is the recovery routine */


: Recover    LDT    ONE20_METRE_TAPE  /* load the recovery tape */
        SERVO_CMD (CLEAN_HEADS)

        LED    RECOVERING

        SERVO_CMD (CAPS_FWD_MID)  /* Move forward at mid speed */
        WAI    LONG_TIME_DELAY, RECOVERY_TIME  /* wait for recovery time */
        SERVO_CMD (EJECT)        /* eject the recovery tape */

        BRA:    Returnr


/**************** Drift *****************/
/* This is the multi-pass drift routine */

: Drift   LDT    ANY_TAPE  /* Now load the measurement tape */
      SERVO_CMD (CLEAN_HEADS)

! These lines need to be added in next version
! Move away from BOM
      SERVO_CMD (CAPS_FWD_MID)    /* Move forward at mid speed */
      WAI TIME_DELAY, TEN_SECONDS  /* for 10 seconds */

      LDR    REGISTER2, IMMEDIATE, 00,00,00
      LDR    REGISTER3, IMMEDIATE, 00,00,00

: Dopass  LED    WRITING

      BNE    REGISTER3, 00,00,:Dower
      LOG    EVERYTHING

: Dower      WER        DATA_RANDOM, START_HERE, FAIL_IF_EXCEED, WRITE_ERT_LENGTH_S,
WRITE_ERT_LIMIT
      LOG    NOTHING

      INC    REGISTER3
      INC    REGISTER2
      BLT    REGISTER3, 00,LOG_N,:Skipreset
      LDR    REGISTER3, IMMEDIATE, 00,00,00
: Skipreset BGE    REGISTER2, 00, NO_PASSES,:Enddrift

      LED    REWINDING
      SERVO_CMD (CAPS_REV_HI)
: Rewd03  LDR    REGISTER8, SERVO_REP_2_3
      BLT    REGISTER8, F0, 00,:Rewd03
      SERVO_CMD (CAPS_FWD_NOM)
: Fwd03   LDR    REGISTER8, SERVO_REP_2_3
      BGT    REGISTER8, 10,00,:Fwd03

      BRA:    Dopass

: Enddrift SERVO_CMD (EJECT)        /* eject the measurement tape */
      BRA:    Returnd


/**************** Error_handler *****************/
: Error_handler CBE
      SSC    CLEAR_ERROR
      SERVO_CMD (EJECT)
      LOG    NOTHING
      URD    46,61,69,6C  /* write "Fail" to show didn't finish */
      LED    FAIL
```

```
    BRA:   End

/*************** End ****************/
: End  LOG    EVERYTHING
       URD    50,41,53,53  /* write "PASS " */
       EOT
       . End
```

8.1 The Initial and final error rate values for each drive after repeatability testing at 25°C/35%RH

Presented below are the initial and final error rates of the positive and negative channels of all the drives in repeatability testing at 25°C/35%RH including long reconditioning error rates at 80°C/25%RH. ERT is referred to error rate testing and Recon is long reconditioning.

	Condition	Positive Channel	Negative Channel
Drive 1	ERT1	No	Data
	Recon1: Start	0.002744	0.001808
	End	0.00119	0.000836
	ERT2: Start	0.002067	0.000824
	End	0.001623	0.000649
	Recon2: Start	0.004641	0.001397
	End		
	ERT3: Start	0.000695	0.000349
	ERT3: End	0.001171	0.000796
Drive 2	ERT1	No	Data
	Recon1: Start	0.000029	0.003255
	End		
	ERT2: Start	0.001794	0.000624
	End	0.002317	0.002469
	Recon2: Start	0.661072	0.663871
	End		
	ERT3: Start	0.000317	0.000256
	ERT3: End	0.00054	0.00049
Drive 3	ERT1b: Start	0.00131	0.009203
	End	0.000506	0.003275
	Recon1b: Start	0.000751	0.009039
	End	0.002485	0.005729
	ERT2: Start	0.001041	0.002549
	End	0.00042	0.002993

	Condition	Positive Channel	Negative Channel
Drive 3	Recon2: Start	0.000304	0.002675
	End	0.001751	0.004633
	ERT3: Start	0.000513	0.00344
	End	0.000231	0.007829
Drive 4	ERT1	No	Data
	Recon1: Start	0.001146	0.000382
	End	0.00121	0.001194
	ERT2: Start	0.00078	0.000658
	End	0.000587	0.000521
	Recon2: Start	0.001517	0.000306
	End	0.00735	0.006245
	ERT3: Start	0.000756	0.000495
	End	0.000598	0.000371
Drive 5	No ERT1		
	Recon1: Start	1	1
	ERT2: Start	No	Data
	Recon2: Start	0.000256	0.000306
	End	0.003754	0.003557
Drive 6	ERT1b: Start	0.000884	0.00332
	End	0.000269	0.001233
	Recon1: Start	0.000284	0.000726
	End	0.000323	0.000585
	ERT2: Start	0.000426	0.001494
	End	0.000206	0.001252
	Recon2: Start	0.000294	0.000679
	End	0.000514	0.000656
	ERT3: Start	0.000353	0.001468
	End	0.000256	0.001444
Drive 7	ERT1b: Start	0.003505	0.006408
	End	0.002252	0.003188
	Recon1	0.002344	0.00218
	End	0.002022	0.001918
	ERT2: Start	1	1
	End		
	Recon2: Start	0.000412	0.00078
	End	0.001148	0.000913
	ERT3: Start	0.000548	0.000701
	ERT3: End	0.001169	0.000699

	Condition	Positive Channel	Negative Channel
Drive 8	ERT1	No	Data
	Recon1: Start	0.001274	0.007744
	End	0.000615	0.00226
	ERT2: Start	0.000862	0.003045
	End	0.001072	0.004765
	Recon2: Start	0.00102	0.007
	End	0.000412	0.002293
Drive 8	ERT3: Start	0.000796	0.0063
	End	0.001554	0.020233
Drive 9	ERT1b: Start	1	0
	End		
	Recon1	1	1
	ERT2: Start	0.000792	0.000248
	End	0.001088	0.000303
	Recon2: Start	0.001777	0.000412
	End	0.001402	0.000291
	ERT3: Start	0.001002	0.000356
	End	0.004778	0.001345
Drive 10	ERT1b: Start	0.004173	0.000762
	End	0.001898	0.000315
	Recon1b: Start	0.002144	0.000412
	End	0.003439	0.001742
	ERT2: Start	0.006738	0.005151
	End	0.002274	0.000435
	Recon2: Start	0.001905	0.000164
	End	0.003029	0.001128
	ERT3: Start	0.001469	0.000214
	End	0.001983	0.0005